

Parameter optimization of CNT production using Sri Lankan graphite by arc discharge method

Rathnayake Mudiyanseelage Sunanda Jayalath Gunasekara
(R. M. S. J. Gunasekara)

(09/8110)

Degree of Master of Philosophy



University of Moratuwa, Sri Lanka
Electronic Theses & Dissertations
www.lib.mrt.ac.lk

Department of Electrical Engineering

University of Moratuwa

Sri Lanka

December 2012

**Parameter optimization of multi wall carbon nano tube
production (MWCNT) using Sri Lankan graphite by electric
arc discharge method**

Rathnayake Mudiyanseelage Sunanda Jayalath Gunasekara
(R. M. S. J. Gunasekara)

(09/8110)

Degree of Master of Philosophy



University of Moratuwa, Sri Lanka.
Electronic Theses & Dissertations
www.lib.mrt.ac.lk

Department of Electrical Engineering

University of Moratuwa

Sri Lanka

December 2012

DECLARATION

I declare that this is my own work and this thesis does not contain any material previously submitted for a Degree or Diploma in any other University or published elsewhere, without acknowledgement to the best of my knowledge.

Also, I hereby grant to University of Moratuwa the non-exclusive right to reproduce and distribute my thesis, in whole or in part in print, electronic or any other medium. I retain the right to use this content in whole or part in future works (such as articles or books).

.....

R. M. S. J. Gunasekara

Date:

The above candidate has carried out research for the M. Phil thesis under our supervision.



University of Moratuwa, Sri Lanka
Electronic Theses & Dissertations
www.lib.mrt.ac.lk

.....

Prof. J. P. Karunadasa

Date:

Supervisor

.....

Prof. Ajith de Alwis

Date:

Supervisor

.....

Dr. Lilantha Samaranayake

Date:

Supervisor

ACKNOWLEDGEMENT

I acknowledge with gratitude the Sri Lanka Institute of Nanotechnology (SLINTEC) for giving me the opportunity to conduct this project with full financial support along with National Science Foundation while providing the access for its valuable high end equipment facilities.

I am grateful to Prof. J.P. Karunadsa, Prof. Ajith de Alwis and Dr. Lilantha Samaranayake, my supervisors who very generously spent their precious time to provide necessary guidance and assistance to carry out this task.

I also extend my gratitude and thank to Prof. Veranja Karuinanayake, Science Team Leader, Sri Lanka Institute of Nanotechnology and Prof. Gehan Amarathunge, Department of Electrical Engineering, University of Cambridge and Head of Research and Innovations at SLINTEC, providing me with all necessary guidance in carrying out this project.

Further I wish to sincerely thank Dr. Nilwala Kottegoda, Dr. Gamini Kumarasinghe and Dr. Jeewantha Premachandra at SLINTEC who helped me in numerous ways to complete my project successfully.

I am also thankful to all my colleagues at SLINTEC for encouragement and assistance extended to me, especially to Mr. Neil who has assisted me in preparation of arc discharge set up.

R. M. Sunanda Jayalath Gunasekara

ABSTRACT

Since their discovery in 1991 by Iijima, carbon nanotubes have been of great interest. The key advantages of these structures are their electronic, mechanical, optical and chemical characteristics, which open a way to a variety of applications. These properties can even be measured on single nanotubes. For commercial application, large quantities of purified nanotubes are needed.

Different types of carbon nanotubes can be produced in various ways. The most common techniques used nowadays are: arc discharge, laser ablation, chemical vapor deposition and flame synthesis.

Fundamental and practical nanotube researches have shown possible applications in the fields of energy storage, molecular electronics, nano-mechanical devices, and composite materials. Real applications are still under development.

This project is basically focused on arc discharge method of CNT production using Sri Lankan vein graphite. Sri Lankan graphite is unique due to its perfect crystalline structure and the higher as mined purity compared with that of commonly available flake graphite. This type of natural resource is found mainly in Sri Lanka. Detailed study on flake and vein graphite was carried out in this study as one of its objectives. Also SEM and TGA analysis of the multiwall carbon nanotubes are discussed. Special technique for comparing diameters of multiwall wall carbon nanotube was developed by using TGA. Further, the cross section analysis was carried out for the arc sputter to analyze the formation of the nanotubes on the cathode. Another objective here was to identify the optimum parameters for the production of CNT using the arc discharge method. Arcing time, current, chamber inert gas, chamber pressure and the type of the electrode were the variables. Arcing current around 100 A, pressure around 700~900Torr and arcing duration around 60s with helium as the inert gas were the optimize conditions.

Key words: Vein Graphite, CNT, MWCNT, Arc discharge, Nanotube

TABLE OF CONTENTS

| | |
|---|-----|
| DECLARATION | i |
| ACKNOWLEDGEMENT | ii |
| ABSTRACT..... | iii |
| TABLE OF CONTENTS..... | iv |
| TABLE OF FIGURES | vii |
| LIST OF TABLES | xi |
| LIST OF ABBREVIATIONS | xii |
| Chapter 1 : INTRODUCTION..... | 1 |
| 1.1 Background | 1 |
| 1.1 Structure of CNT..... | 2 |
| 1.2 Research objectives..... | 3 |
| Chapter 2 : LITERATURE STUDY | 4 |
| 2.1 Different Structures of Carbon Nanotubes..... | 4 |
| 2.1.1 Single Wall Carbon Nano Tubes (SWCNT)..... | 4 |
| 2.1.2 Multi Wall Carbon Nanotube (MWCNT)..... | 6 |
| 2.2 Physical Properties of CNT..... | 8 |
| 2.2.1 Strength | 8 |
| 2.2.2 Hardness..... | 9 |
| 2.2.3 Kinetic..... | 9 |
| 2.2.4 Electrical | 10 |
| 2.2.1 Thermal | 11 |
| 2.3 Applications of carbon nanotubes | 11 |
| 2.3 Manufacturing of carbon nanotubes..... | 12 |
| 2.4 Global trend for carbon nanotube..... | 14 |
| 2.7 Introduction to graphite..... | 18 |

| | |
|---|----|
| 2.7.1 Application of natural graphite | 21 |
| Chapter 3 : MATERIALS AND METHODS | 23 |
| 3.1 Characterization techniques | 23 |
| 3.1.1 Thermo gravimetric analysis (TGA)..... | 23 |
| 3.1.2 Scanning electron microscopy (SEM) | 25 |
| 3.1.3. Atomic force microscopy (AFM) | 27 |
| 3.1.4 Elemental analysis | 28 |
| 3.2. Other equipment used | 28 |
| 3.2.1 Vacuum pump | 28 |
| 3.2.2 High current DC power supply | 28 |
| 3.2.3 High voltage generator | 29 |
| 3.2.4 Stop watch..... | 29 |
| 3.2.5 Glove box | 29 |
| 3.3 Methodologies..... | 29 |
| 3.3.1 Characterization of raw materials | 29 |
| 3.3.2 Characterization of standard CNT samples | 32 |
| 3.2.3 Experiments with commercial grade CNT..... | 32 |
| 3.2.4 Setting up of the arc discharge apparatus | 33 |
| 3.2.5 Cross section analysis of the arc soot | 38 |
| 3.2.6 Testing with different arcing times | 38 |
| 3.2.7 Testing with different arcing current | 39 |
| 3.2.8 Testing with different arcing environment pressure | 40 |
| 3.2.9 Testing with different arcing environment..... | 40 |
| 3.2.10 Testing with an external electrical field..... | 42 |
| 3.2.11 Testing with different shapes and materials of anode/cathode | 43 |
| 3.2.12 Testing with Flake graphite anode and cathode..... | 43 |
| Chapter 4 : RESULTS AND DISCUSSIONS | 44 |
| 4.1 Characterization of raw materials | 44 |
| 4.2 Characterization of standard CNT samples | 47 |
| 4.3 Experiments with commercial grade CNT | 50 |

| | |
|---|----|
| 4.4 Setting up the arc discharge apparatus | 53 |
| 4.5 Cross section analysis of the arc soot..... | 53 |
| 4.6 Testing with different arcing time..... | 55 |
| 4.7 Testing with different arcing currents | 58 |
| 4.8 Testing with different arcing environment pressures..... | 64 |
| 4.9 Testing under different arcing environments | 68 |
| 4.10 Testing with an external electric field..... | 74 |
| 4.11 Testing with different shapes and materials of anode/cathode | 75 |
| Chapter 5 : CONCLUSIONS | 78 |
| 5.1 Future works | 79 |
| References | 80 |



University of Moratuwa, Sri Lanka
Electronic Theses & Dissertations
www.lib.mrt.ac.lk

TABLE OF FIGURES

| | |
|--|----|
| Figure 1-1 Schematic illustration of the basal and edge planes in graphite (7) | 3 |
| Figure 2-1 SWCNT (Original is in colour) | 4 |
| Figure 2-2 SWNTs with different chiralities. | 4 |
| Figure 2-3 Chiral Vectors of SWCNT (10) original is in colour | 6 |
| Figure 2-4: MWCNT(Original is in colour)- Generated from NINITHI software | 6 |
| Figure 2-5: Different structures of MWCNT- TEM images..... | 7 |
| Figure 2-6 Chiral notation of SWCNT (10)- original is in colour | 10 |
| Figure 2-7 Application of MWCNT | 12 |
| Figure 2-8 Schematic drawings of the laser ablation apparatus (8)..... | 13 |
| Figure 2-9 Schematic diagram of synthesis of CNT by CVD technique..... | 13 |
| Figure 2-10 Comparison of CNT, Graphene and Fullerene (Original is in colour) publication [20]..... | 14 |
| Figure 2-11 Productivity of Nanotubes..... | 16 |
| Figure 2-12 commercial scale CNT manufactures (Original is in colour) | 17 |
| Figure-2-13 Different form so Carbon (Original is in colour)..... | 18 |
| Figure 2-14 sp ³ -hybrid orbital | 19 |
| Figure 2-15 sp ² Hybridization | 19 |
| Figure 2-16 Band structure of graphite | 20 |
| Figure 2-17 Lattice Structure of Graphite..... | 21 |
| Figure 3-1 Schematic diagram of TGA (Original is in colour) (www.tainstruments.com)..... | 23 |
| Figure 3-2 Typical Schematic diagram of a SEM set-up..... | 26 |
| Figure 3-3 An AFM probe scans over a sample surface (Original is in colour)..... | 27 |
| Figure 3-4 TGA Analysis example | 31 |
| Figure 3-5 Weight % calculation from DTG curve (Sample: CNT produced with arc discharge) | 32 |
| Figure 3-6 First generation arcing setup in open air(Original is in colour) | 34 |
| Figure 3-7 schematic view of the arc-discharge apparatus (26) | 34 |
| Figure 3-8 Second generation arc discharge set up (Original is in colour)..... | 35 |

| | |
|--|----|
| Figure 3-9 Third generation arc discharge setup(Original is in colour) | 36 |
| Figure 3-10 Final Arc discharge set up(Original is in colour)..... | 37 |
| Figure 3-11 Arcing inside de ionized water. (Original is in colour)..... | 41 |
| Figure 3-12 Schematic diagram of set up with external electric field | 42 |
| Figure 4-1 - SEM images of (A) Flake graphite, (B) Vein Graphite | 44 |
| Figure 4-2 XRD Analysis of Vein and Flake graphite | 44 |
| Figure 4-3 TGA results of Vein graphite (solid line) and Flake graphite (Dotted line) (Original is in colour) | 46 |
| Figure 4-4 SEM image of Standard MWCNT from Sigma with 13000 magnification..... | 47 |
| Figure 4-5 SEM image of Standard MWCNT from Sigma with 60000 magnification..... | 48 |
| Figure 4-6 TGA Analysis of Sigma MWCNT (solid line) and Sigma SWCNT (dash line) (Original is in colour)..... | 49 |
| Figure 4-7 AFM analysis of MWCNT(Original is in colour)..... | 50 |
| Figure 4-8 TGA analysis of commercial MWCNT samples (Original is in colour) | 50 |
| Figure 4-9 Repeat TGA analysis of commercial grade MWCNT samples (Original is in colour)..... | 52 |
| Figure 4-10 Temperature at maximum decomposition rate or the maximum heat flow while decomposing of the CNT Vs CNT Diameter for commercial samples (Original is in colour) | 52 |
| Figure 4-11 SEM image of Cross section of the Arc soot (Original is in colour) | 53 |
| Figure 4-12 SEM image of the arc soot A) view from the top B) image of the middle structure c) image of the formed CNT layer D) view of the bottom surface | 54 |
| Figure 4-13 SEM images of the cathode deposit for arc time of 10s, 15s, 20s and 25s | 55 |
| Figure 4-14 SEM images of the cathode deposit for arc time of 30s, 40s, 45s and 50s | 55 |
| Figure 4-15 SEM images of the cathode deposit for arc time of 55 s, 60s, 90s and 120 s | 56 |

| | |
|---|----|
| Figure 4-16 Temperature at the maximum decomposition of the samples with different arcing time (Original is in colour)..... | 57 |
| Figure 4-17 CNT yield of the samples with different arcing times (Original is in colour) | 58 |
| Figure 4-18 Temperature at the maximum decomposition rate vs arcing time | 59 |
| Figure 4-19 CNT yield vs. arcing current (Original is in colour)..... | 60 |
| Figure 4-20 CNT yield % vs. arcing current (Repeat experiment) (Original is in colour) | 61 |
| Figure 4-21 CNT yield vs. arcing current (Repeat test) (Original is in colour)..... | 61 |
| Figure 4-22 Temperature at the maximum decomposition rate vs .arcing current (Repeat experiment) (Original is in colour)..... | 62 |
| Figure 4-23 SEM images of CNTs produced with different arcing current (60A, 88 A, 92 A, 100A) | 63 |
| Figure 4-24 SEM images of CNTs produced with different arcing current (100A and 110A)..... | 63 |
| Figure 4-25 SEM images of CNTs produced with different arcing current (100A and 118A)..... | 64 |
| Figure 4-26 CNT yield Vs. Arcing pressure (Original is in colour)..... | 66 |
| Figure 4-27 temperature at the maximum decomposition rate vs. arcing environment pressure (Original is in colour) | 66 |
| Figure 4-28 SEM images of produced CNT for different arcing pressure | 67 |
| Figure 4-29 SEM images of produced CNT for different arcing pressure | 67 |
| Figure 4-30 TGA analysis of the sample with N2 at 1 atm, 100 A (Original is in colour) | 68 |
| Figure 4-31 TGA analysis of the sample with N2 at 900Torr, 100 A | 69 |
| Figure 4-32 TGA results of the test with He gas (Solid line: 900Torr, 100A, 60s Dash line : 1 atm, 100A, 60s) (Original is in colour) | 69 |
| Figure 4-33 CNT Yield with different gases | 70 |
| Figure 4-34 SEM images of the CNT produced with Nitrogen as the inert gas | 70 |
| Figure 4-35 SEM images of the CNT produced with Argon as the inert gas | 71 |
| Figure 4-36 SEM images of the CNT produced with Helium as the inert gas | 71 |
| Figure 4-37 Comparison of SEM images of arc with He (left) and N2 (Right) | 72 |

| | |
|---|----|
| Figure 4-38 Carbon onion formation on the CNT produced with nitrogen gas as the inert media..... | 72 |
| Figure 4-39 Clean CNT formation with He | 73 |
| Figure 4-40 SEM images of the samples from arcing inside water | 74 |
| Figure 4-41 SEM images of the HV (high voltage) and LV (low voltage) cathode deposits of the test with an external electric field..... | 75 |
| Figure 4-42 SEM image of the cathode deposit of the copper cathode | 76 |
| Figure 4-43Cathode deposit of Flake test - image 1 | 77 |
| Figure 4-44Cathode deposit of Flake test - image 2 | 77 |
| Figure 5-1 Comparison of the standard Sigma CNT vs produced CNT | 78 |



LIST OF TABLES

| | |
|---|----|
| Table 2-1 Comparison of mechanical properties of CNT | 9 |
| Table 2-2 Top ten authors for CNT related publications (20) | 15 |
| Table 2-3 Top ten institute for CNT related publications (20) | 16 |
| Table 3-1 Specification of the commercial grade CNTs used for the analysis..... | 33 |
| Table 3-2 Description of the samples for different arcing time | 38 |
| Table 3-3 Sample description for the samples with different arcing currents | 39 |
| Table 3-4 Sample description for the samples with different arcing current by using forth arcing set up | 39 |
| Table 3-5 Sample description for the samples with different arcing environment pressure by using forth arc discharge set up..... | 40 |
| Table 3-6 : Sample description for the samples with different arcing environment.. | 41 |
| Table 4-1 Elemental analysis of vein graphite..... | 45 |
| Table 4-2 Elemental Analysis of Flake Graphite..... | 45 |
| Table 4-3 Temperatures at maximum decomposing rate of commercial MWCNT samples | 51 |
| Table 4-4 TGA results of the samples with different arcing time | 56 |
| Table 4-5 Results of the test with different arcing currents by using the second set up..... | 59 |
| Table 4-6 TGA results of the sample produced by varying the current (repeat) | 60 |
| Table 4-7 Temperature at the maximum decomposition rate and the CNT yield for the samples with different arcing environment pressure (taken from TGA results) | 65 |

LIST OF ABBREVIATIONS

| <u>Abbreviation</u> | <u>Description</u> |
|---------------------|---|
| Å | Angstrom |
| AFM | Atomic Force Microscope |
| Ar | Argon |
| CNT | Carbon nanotube |
| EDX | Energy Dispersive X-ray analysis |
| FTIR | Fourier Transform Infrared Spectroscopy |
| g | gram |
| kg | kilogram |
| kV | Kilo Volts |
| MWCNT | Multi wall carbon nanotube |
| SEM | Scanning Electron Microscope |
| SWCNT | Single wall carbon nanotube |
| TGA | Thermo Gravimetric Analysis |
| CVD | Chemical Vapor deposition |
| DC | Direct current |
| USA | United States of America |
| DWCNT | Double wall carbon nanotube |
| VPGCF | Vapor phase grown carbon fibers |



University of Sri Lanka
Electronic Theses & Dissertations
United States of America

Chapter 1 : INTRODUCTION

1.1 Background

Carbon nanotubes appear to have been discovered in the late 1970s by Morinobu Endo during his experiments to produce micron diameter carbon fibers. (1). During this time he published several TEM (Transmission Electron Microscope) images showing very small diameter carbon filaments, which he described as a tube formed by rolling up a plane of carbon atoms as found in graphite. Surprisingly, Endo's discovery passed unnoticed until 1991. In 1991 Iijima (2) demonstrated that CNTs could be produced in an arc discharge between carbon electrodes in He gas. Small quantities of CNTs then became available for study. Iijima and coworkers used this material and modern transmission electron microscope to provide evidence for the structure of CNTs that we know today. They found that the CNTs could be open-ended or closed with a hemi spherical cap reassembling half of a fullerene molecule. The work of Iijima and his coworkers resulted in a "feeding frenzy" by researches worldwide to learn how to produce CNTs in larger quantities and of better quality. The race was on to elucidate their properties and to develop new technology taking advantage of the unique properties of these atomic filaments. (3)

Endo, in his early review of "Vapor phase grown carbon fibers" (VPGCF), also reminds that he has observed a hollow tube linearly extended with parallel carbon layer phases near the fiber core. (1). This appears to be the observation of multi walled carbon nanotubes at the center of the fiber. This work by Endo also contains several relatively unknown and very early references to the growth of carbon whiskers by R J bacon and the earliest carbon fibers reported in 1890. The mass produced MWCNTs (Japan) today are strongly related to Vapor phase grown carbon fibers developed by Endo. In fact they called it the "Endo- Process", out of respect for his early work and patents. In fact these MWCNTs are really small diameter. Vapor phase grown carbon fibers subsequently subjected to a high temperature heat treatment (HTT) in an inert atmosphere. This high temperature heat treatment drives the structure into a more organized set of concentric tubes of carbon.

The covalent carbon-carbon bonds within a CNT are among the strongest known. In addition, CNTs are remarkably compliant, that is they are able to make sharp bends without fracture. It is therefore expected that CNTs could be incorporated in revolutionary light weight composites. To perfect these CNT composites, challenges exists in their dispersions into the host and also in developing strong covalent coupling of the CNT to the host medium. (4) Their large length (up to several microns) and small diameter (a few nanometers) result in a large aspect ratio. They can be seen as the nearly one-dimensional form of fullerenes. Therefore, these materials are expected to possess additional interesting electronic, mechanic and molecular properties. Especially in the beginning, all theoretical studies on carbon nanotubes focused on the influence of the nearly one-dimensional structure on molecular and electronic properties. (5)

1.1 Structure of CNT

Carbon nanotube has the similar atomic structure as graphene and graphite which consists three carbon atoms around each carbon atom. But in graphene and graphite atoms are bound with pure sp^2 bonds (Three σ bonds) whereas in carbon nanotubes the orbital structure of carbon is altered, because the bond length between carbon atoms decreases and the bond angle changes. σ - and π - orbitals are no longer perpendicular to each other. Overlap of the π -orbitals is introduced. As a consequence the parts of the π - orbitals inside and outside of a nanotube rearrange, in a way, that the outer contribution is much larger than the inner one .The curvature induces a mixed state of σ - and π -orbitals. The effect could also be explained by a mixture of sp^2 and sp^3 orbitals. (6) (Further details are described in the section **2.7 Introduction to graphite**). This mixing of the σ - and π -orbitals is varying with the nanotube type and the size. Because of this, the properties of the CNT are very different from that of graphene and graphite. Also due to the same reason there are differences between the nanotube types and the physical size of the nanotube. On the graphite, as seen on the Figure 1 site “A” is the part of an electron rich plane. Edge planes (site “C”) are highly reactive due to the partial saturation of valencies. Two different types of sites can be identified on the edge plane;

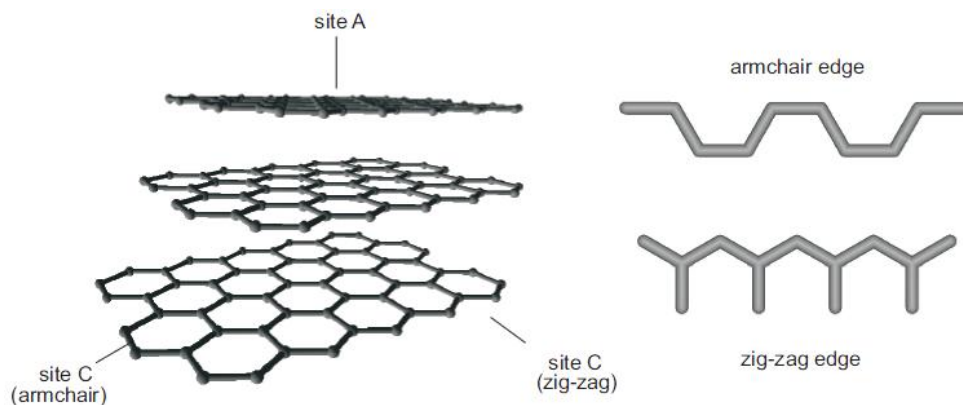


Figure 1-1 Schematic illustration of the basal and edge planes in graphite (7)

- An arm-chair site
- Zig-zag site.

These two sites display different reactivity with activated oxygen species, and results in different poly-functional organic surface groups. (7)

But there are no any raw edges on carbon nanotubes, as CNT has a tubular shape with two hemisphere caps on both sides. Due this unavailability of raw edges and the curvature structure, CNT exhibits different properties than graphite or graphene.



University of Moratuwa, Sri Lanka.
Electronic Theses & Dissertations
www.lib.mrt.ac.lk

1.2 Research objectives

1. Proof of concept after generation of carbon nanotubes.

To use arc discharge method by using Sri Lankan vein graphite to produce CNT and to carry out detailed study on Sri Lankan graphite, and to make a separate apparatus for the arcing.

2. Separation of carbon nanotubes and Characterization of carbon nanotubes.

To characterize produced CNT through SEM (Scanning Electron Microscope) and TGA (Thermo Gravimetric Analysis)

3. Optimizing of parameters to get good quality higher yield.

To study the quality of the produced CNT's through SEM and TGA to calculate the yield. Prepare several CNT samples in order to find out the behaviour of the arcing current, voltage, arcing time and the arcing environment.

Chapter 2 : LITERATURE STUDY

2.1 Different Structures of Carbon Nanotubes

2.1.1 Single Wall Carbon Nano Tubes (SWCNT)

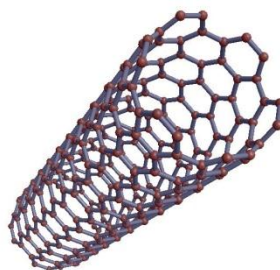


Figure 2-1 SWCNT (Original is in colour)

Single Walled Carbon Nanotubes (SWCNT) can be considered as long wrapped graphene sheets. Nanotubes generally have a length to diameter ratio of more than 1000 so they can be considered as nearly one-dimensional structures.

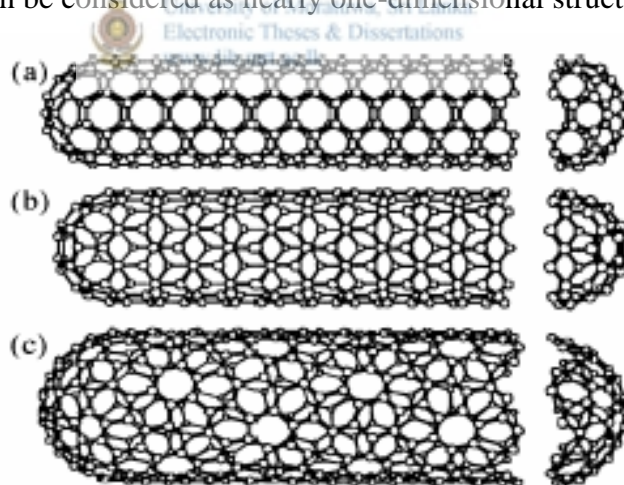


Figure 2-2 SWNTs with different chiralities.

The difference in structure is easily shown at the open end of the tubes. a) Armchair structure b) zigzag structure c) chiral structure

More detailed, a SWCNT consists of two separate regions with different physical and chemical properties. The first is the sidewall of the tube and the second is the end cap

of the tube. The end cap structure is similar to or derived from a smaller fullerene, such as C₆₀. (8)

C-atoms placed in hexagons and pentagons form the end cap structures. It can be easily derived from Euler's theorem that twelve pentagons are needed in order to obtain a closed cage structure which consists of only pentagons and hexagons. The combination of a pentagon and five surrounding hexagons results in the desired curvature of the surface to enclose a volume. A second rule is the isolated pentagon rule that states that the distance between pentagons on the fullerene shell is maximized in order to obtain a minimal local curvature and surface stress, resulting in a more stable structure. The smallest stable structure that can be made this way is C₆₀ the one just larger is C₇₀ and so on. (8)

SWCNT is generated when a graphene sheet of a certain size is wrapped in a certain direction. As the result is cylinder symmetric, we can only roll in a discrete set of directions in order to form a closed cylinder. **(Figure 2-3)** Two atoms in the graphene sheet are chosen, one of which serves the role as origin. The sheet is rolled until the two atoms coincide. The vector pointing from the first atom towards the other is called the chiral vector and its length is equal to the circumference of the nanotube. The direction of the nanotube axis is perpendicular to the chiral vector. (8)

SWNTs with different chiral vectors have dissimilar properties such as optical activity, mechanical strength and electrical conductivity. Depending on their chiral vector, carbon nanotubes with a small diameter are either semi-conducting or metallic. The differences in conducting properties are caused by the molecular structure that results in a different band structure and thus a different band gap. The differences in conductivity can easily be derived from the graphene sheet properties. It was shown that a (n,m) nanotube is metallic as accounts that: $n=m$ or $(n-m) = 3i$, where i is an integer and n and m are defining the nanotube. (9)

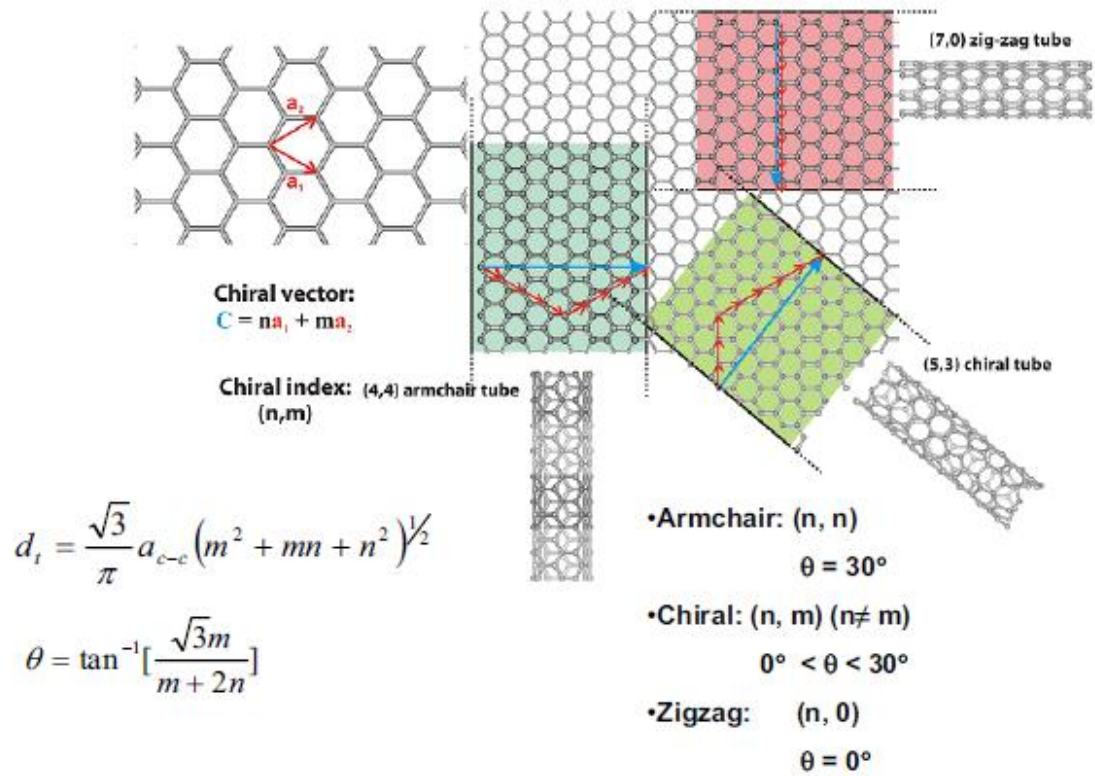


Figure 2-3 Chiral Vectors of SWCNT (10) original is in colour



University of Moratuwa, Sri Lanka.
 Electronic Theses & Dissertations
 www.lib.mrt.ac.lk

2.1.2 Multi Wall Carbon Nanotube (MWCNT)

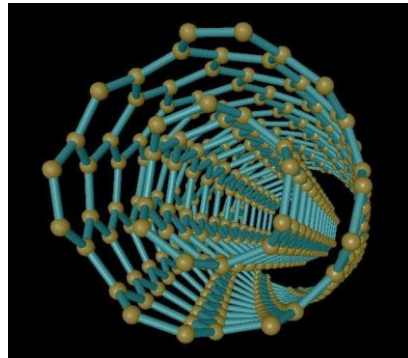


Figure 2-4: MWCNT(Original is in colour)- Generated from NINITHI software

Multi-walled nanotubes (MWNT) consist of multiple rolled layers (concentric tubes) of graphite. The interlayer distance in multi-walled nanotubes is close to the distance between graphene layers in graphite, approximately 3.4 Å. (11)

The length and diameter of these structures differ a lot from those of SWNTs and, of course, their properties are also very different. (Figure 2-5: Different structures of MWCNT)

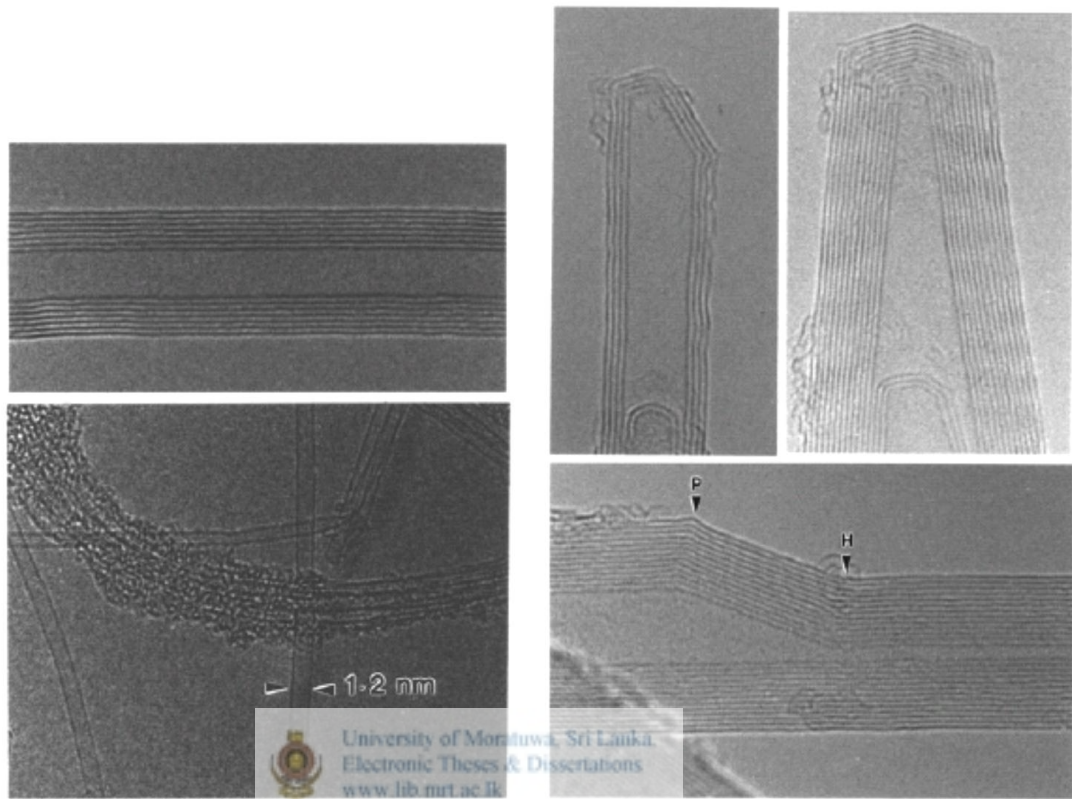


Figure 2-5: Different structures of MWCNT- TEM images

Top-left: cross-section of a MWNT the different walls are obvious, they are separated by 0.34nm. Rotation around the symmetry axis gives us the MWNT. Top-right: Symmetrical or non-symmetrical cone shaped end caps of MWNTs. Bottom-left: A SWNT with a diameter of 1,2 nm and a bundle of SWNTs covered with amorphous carbon. Bottom-right: A MWNT with defects. In point P a pentagon defect and in point H a heptagon defect. (9)

The special place of double-walled carbon nanotubes (DWNT) must be emphasized here because their morphology and properties are similar to SWNT but their resistance to chemicals is significantly improved. This is especially important when functionalization is required (this means grafting of chemical functions at the surface of the nanotubes) to add new properties to the CNT and thus modifying both

its mechanical and electrical properties. In the case of DWNT, only the outer wall is modified. (12)

2.2 Physical Properties of CNT

2.2.1 Strength

Carbon nanotubes are the strongest and the stiffest material yet discovered in terms of tensile strength and elastic modulus. This strength results from the covalent sp^2 bonds formed between the individual carbon atoms. In 2000, a multi-walled carbon nanotube was tested to have a tensile strength of 63 Giga- Pascal (GPa).. Since carbon nanotubes have a low density for a solid of 1.3 to $1.4 \text{ g}\cdot\text{cm}^{-3}$, its specific strength of up to $48,000 \text{ kN}\cdot\text{m}\cdot\text{kg}^{-1}$ is the best of known materials, compared to high-carbon steel's $154 \text{ kN}\cdot\text{m}\cdot\text{kg}^{-1}$. (11)

Under excessive tensile strain, the tubes will undergo plastic deformation, which means the deformation is permanent. This deformation begins at strains of approximately 5% and can increase the maximum strain when the tubes undergo fracture by releasing strain energy.

CNTs are not nearly as strong under compression. Because of their hollow structure and high aspect ratio, they tend to undergo buckling when placed under compressive, torsional or bending stress.

The Table 2-1 referred to axial properties of the nanotube, whereas simple geometrical considerations suggest that carbon nanotubes should be much softer in the radial direction than along the tube axis. (11)

Table 2-1 Comparison of mechanical properties of CNT

| Comparison of mechanical properties (11) | | | |
|--|--|--|---------------|
| Material | Young's | Tensile strength (GPa) | Elongation at |
| SWNT | ~1 (from 1 to 5) | 13–53 ^E | 16 |
| Armchair | 0.94 ^T | 126.2 ^T | 23.1 |
| Zigzag SWNT | 0.94 ^T | 94.5 ^T | 15.6–17.5 |
| Chiral SWNT | 0.92 | | |
| MWNT | 0.27 ^{E1} –0.8 ^{E-} | 11 ^E –63 ^E –150 ^E | |
| Stainless steel | 0.186 ^E –0.214 ^E | 0.38 ^E –1.55 ^E | 15–50 |
| Kevlar– | 0.06 ^E –0.18 ^E | 3.6 ^E –3.8 ^E | ~2 |

^E Experimental observation; ^T Theoretical prediction

2.2.2 Hardness



University of Moratuwa, Sri Lanka
Electronic Theses & Dissertations
www.lib.mrt.ac.lk

Diamond is considered to be the hardest material, and it is well known that graphite transforms into diamond under conditions of high temperature and high pressure. One study succeeded in the synthesis of a super-hard material by compressing SWNTs to above 24 GPa at room temperature. The hardness of this material was measured with a Nano indenter as 62–152 GPa. The hardness of reference diamond and boron nitride samples was 150 and 62 GPa, respectively. The bulk modulus of compressed SWNTs was 462–546 GPa, surpassing the value of 420 GPa for diamond. (13)

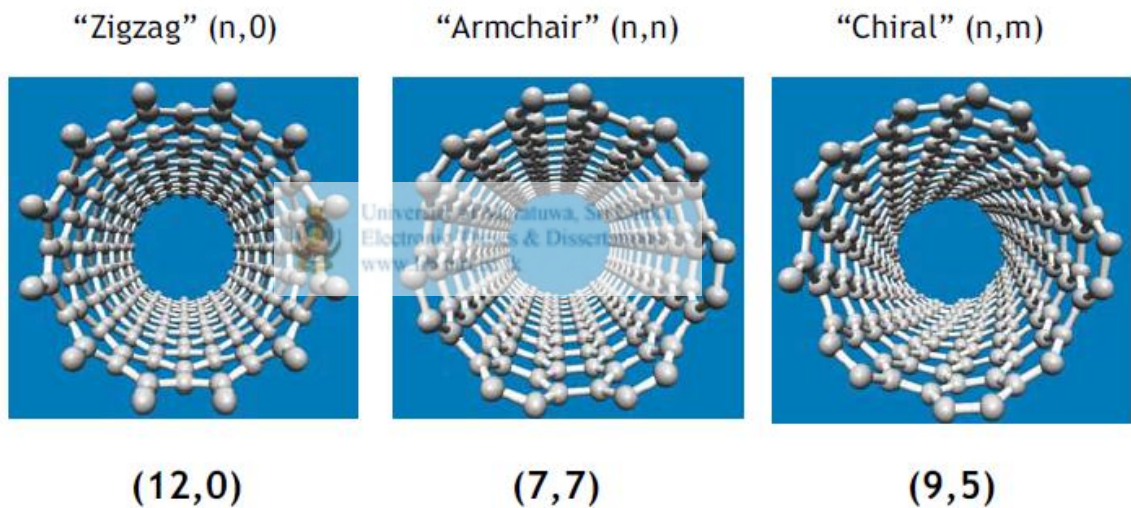
2.2.3 Kinetic

Multi-walled nanotubes, multiple concentric nanotubes precisely nested within one another, exhibit a striking telescoping property whereby an inner nanotube core may slide, almost without friction, within its outer nanotube shell thus creating an atomically perfect linear or rotational bearing. This is one of the first true examples

of molecular nanotechnology, the precise positioning of atoms to create useful machines. Already this property has been utilized to create the world's smallest rotational motor. Future applications such as a gigahertz mechanical oscillator are also envisaged. (14)

2.2.4 Electrical

The electronic structure of the CNT is also remarkable. The nature of the electrical conductivity along the tube axis was predicted theoretically to depend uniquely on the integers (n,m) described below. These predictions were soon confirmed by experiment. Energy band theory predicted that two thirds of all possible CNTs would be semiconducting with a gap $E_g \sim 0.6V/d$, where d is the diameter of the tube. The remaining one third of the all CNTs should be metallic due to band overlap. (3)



(n,n) : all metallic ; (n,m) : 2/3 semiconducting 1/3 metallic

Figure 2-6 Chiral notation of SWCNT (10)- original is in colour

Because of the symmetry and unique electronic structure of graphene, the structure of a nanotube strongly affects its electrical properties. For a given (n, m) nanotube, if $n = m$, or $n - m$ is a multiple of 3, the nanotube is metallic; otherwise the nanotube is a moderate semiconductor.

However, this rule has exceptions, because curvature effects in small diameter carbon nanotubes can influence its electrical properties. Thus, (5,0) SWCNT that should be semiconducting is in fact metallic according to the calculations and *vice versa*, zigzag and chiral SWCNTs with small diameters that should be metallic have a finite gap (armchair nanotubes remain metallic) (15). In theory, metallic nanotubes can carry an electrical current density of $4 \times 10^9 \text{ A/cm}^2$ which is more than 1,000 times greater than metals such as copper_(16)

2.2.1 Thermal

All nanotubes are expected to be very good thermal conductors along the tube, exhibiting a property known as "ballistic conduction", but good insulators laterally to the tube axis. Measurements show that a SWNT has a room-temperature thermal conductivity along its axis of about $3500 \text{ W}\cdot\text{m}^{-1}\cdot\text{K}^{-1}$ (17). Compared to copper, a metal well-known for its good thermal conductivity, which transmits $385 \text{ W}\cdot\text{m}^{-1}\cdot\text{K}^{-1}$. A SWNT has a room-temperature thermal conductivity across its axis of about $1.52 \text{ W}\cdot\text{m}^{-1}\cdot\text{K}^{-1}$, which is about as thermally conductive as soil. The temperature stability of carbon nanotubes is estimated to be up to $2800 \text{ }^\circ\text{C}$ in vacuum and about $750 \text{ }^\circ\text{C}$ in air. (18)

2.3 Applications of carbon nanotubes

There are numerous applications of CNT but only the application of MWCNT is mentioned below since the study is focused on MWCNT manufacturing. Three properties of MWCNTs are specifically interesting for the industry: The electrical conductivity (as conductive as copper), their mechanical strength (up to 15 to 20 times stronger than steel and 5 times lighter) and their thermal conductivity (same as that of diamond and more than five times that of copper). A combination of these impressive properties enables a whole new variety of useful and beneficial applications. (19)

Although there are numerous applications of CNTs, only limited applications are commercially used. Most of the applications related to electronics are still in research level and will be used in the near future. Reason for that is mostly due to the

difficulty in handling a single nanotube on the Si chips. Also controlled deposition of CNT on Si is also a challenge for the scientists.

Application of MWCNT is illustrated in Figure 2-7. Most of the present commercial applications which are in commercial scale production are based on mechanical strength of the MWCNT. Also light weight property is used in aircraft industry to fabricate light weight high strength aircraft parts.

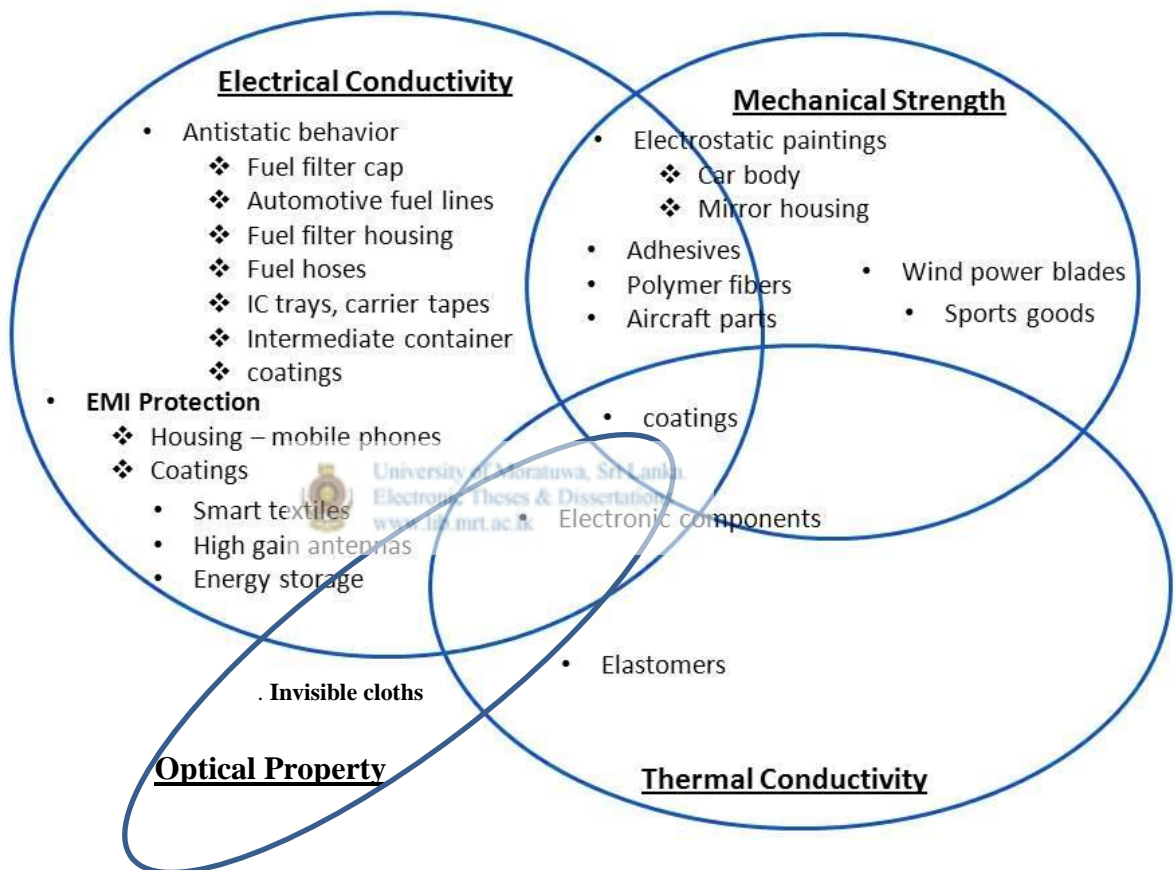


Figure 2-7 Application of MWCNT

2.3 Manufacturing of carbon nanotubes

Carbon nanotubes are generally produced by three main techniques.

1. Arc discharge
2. Laser ablation
3. Chemical vapor deposition.

Scientists are researching more economic ways to produce these structures. In arc discharge, a carbon vapor is created by an arc discharge between two carbon electrodes (mainly graphite) with or without catalyst. When arcing the electrons are coming out from the cathode and collide on the anode. This collision generates heat and due to this heat the carbon atoms on the anode evaporated and form carbon plasma at the temperature of around 4000K. The produced carbon plasma is quenched on the cathode and forms carbon nanotube.

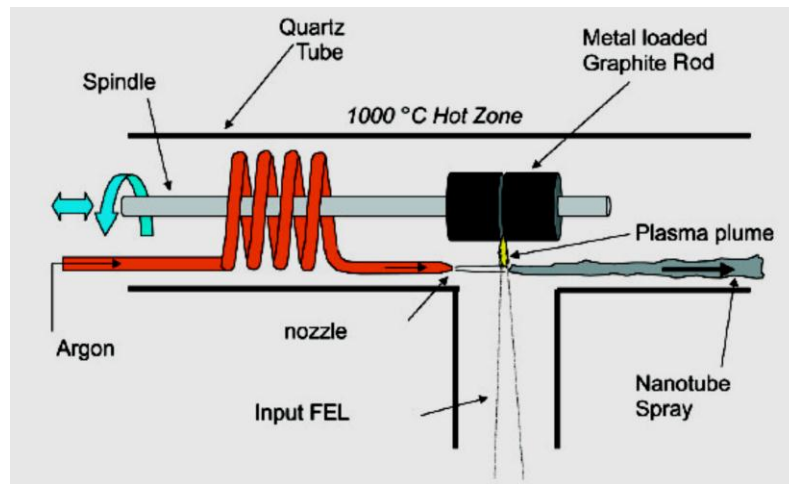


Figure 2-8 Schematic drawings of the laser ablation apparatus (8)

As shown on in Figure 2-8 in laser ablation technique, a high-power laser beam impinges on a volume of carbon containing feedstock gas (methane or carbon monoxide). At the moment, laser ablation produces a small amount of clean nanotubes, whereas CVD method generally produces large quantities of CNT.

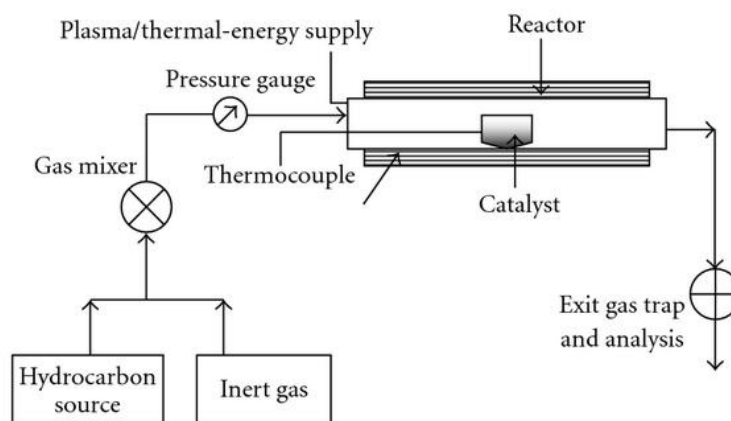


Figure 2-9 Schematic diagram of synthesis of CNT by CVD technique

As seen in the Figure 2-9, chemical vapor deposition (CVD) synthesis is achieved by putting a carbon source in the gas phase and using an energy source, such as plasma or a resistively heated coil, to transfer energy to a gaseous carbon molecule. Commonly used gaseous carbon sources include methane, carbon monoxide and acetylene. The energy source is used to “crack” the molecule into reactive atomic carbon. Then, the carbon diffuses towards the substrate, which is heated and coated with a catalyst (usually a first row transition metal such as Ni, Fe or Co) where it will bind. Carbon nanotubes will be formed if the proper parameters are maintained. Excellent alignment, as well as positional control on nanometer scale, can be achieved by using CVD. Control over the diameter, as well as the growth rate of the nanotubes can also be maintained. This method is very easy to scale up. Typical yields for CVD are approximately 30%. In general, chemical vapor deposition (CVD) results in MWNTs or poor quality SWNTs. The SWNTs produced with CVD have a large diameter range. (8)

2.4 Global trend for carbon nanotube

During past two decades CNT has been a popular name among the science community and the following table describes the trend towards publication in CNT related materials.

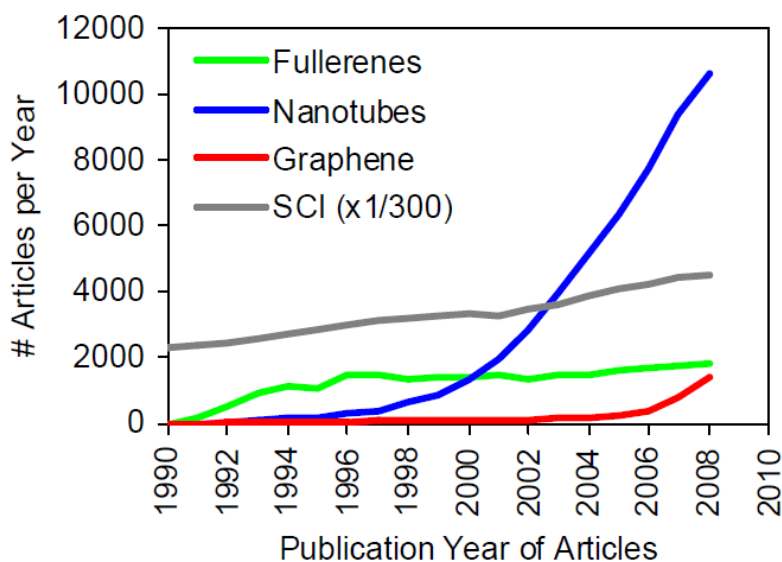


Figure 2-10 Comparison of CNT, Graphene and Fullerene (Original is in colour) publication [20]

According to Figure 2-10, the productivity (total number of articles per year) of the research activities dealing with nanotubes steadily increased, reaching about 11000 papers published in the year 2008 (compared to “only” 2000 fullerene papers published in the same year).

Google has become powerful search engine for web resources. Results for the word “Nanotube” on Google are given below.

- Jan 2011 : 17.7 Mn pages
- Mar 2012 : 92.4 Mn pages

There is a drastic increase of the results and it implies that the CNT is becoming popular worldwide day by day.

The following table shows the top ten authors for CNT related publications in terms of the number of publications.

Table 2-2 Top ten authors for CNT related publications (20)

|  Rank | Author | Country | # Articles |
|--|-----------------|-------------|------------|
| 1 | Iijima, S | Japan | 333 |
| 2 | Bando, Y | Japan | 307 |
| 3 | Ajayan, PM | USA | 294 |
| 4 | Dresselhaus, MS | USA | 291 |
| 5 | Chen, Y | PR China | 288 |
| 6 | Roth, S | Germany | 269 |
| 7 | Lee, YH | South Korea | 262 |
| 8 | Chen, J | PR China | 259 |
| 9 | Wang, J | USA | 258 |
| 10 | Wang, Y | PR China | 258 |

Most of the CNT related researches are carried out in top ranked universities and the Table 2-2 shows the top ten research centers with highest number of cnt related publications.

Table 2-3 Top ten institute for CNT related publications (20)

| Rank | Research Organization | # Articles | % Articles |
|------|--|------------|------------|
| 1 | Chinese Academy of Science | 2840 | 5.0 |
| 2 | Tsing Hua University | 903 | 1.6 |
| 3 | Russian Academy of Science | 881 | 1.5 |
| 4 | Peking University | 684 | 1.2 |
| 5 | Tohoku University | 630 | 1.1 |
| 6 | Rice University | 628 | 1.1 |
| 7 | University of Science and Technology china | 616 | 1.1 |
| 8 | University of Cambridge | 609 | 1.1 |

As seen in the table 2-3, most of the publications are from the Asian research organizations and there are few publications from USA. Also as seen on the Figure 2-11 around 50% of the total nanotube production is from Asian countries. China is the leading country in terms of both CNT related publications and also the CNT production.

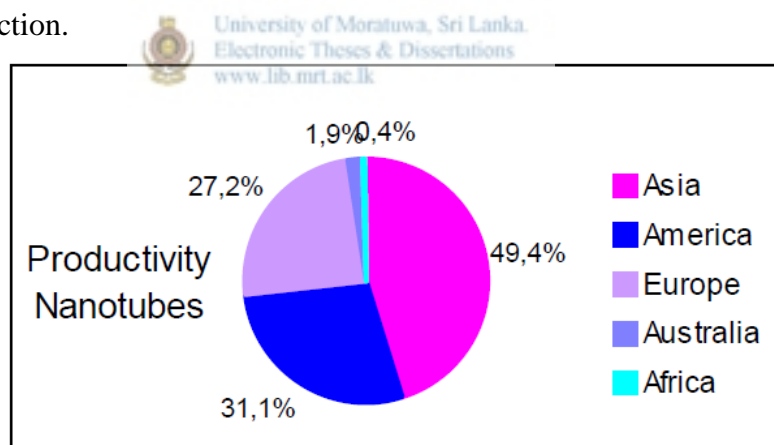


Figure 2-11 Productivity of Nanotubes

As seen on the Figure 2-12 most of the commercial scale manufactures use CVD technique for their CNT manufacturing. Only NRC CNRC in Canada produces CNT with Laser ablation method and there are two institutes namely carbolex in USA and Iljin Nanotec in Korea who use arc discharge method for their CNT manufacturing. As at today highest manufacturing is based on CVD and Cnano in china has the highest production capability of 500tons per year. (4).

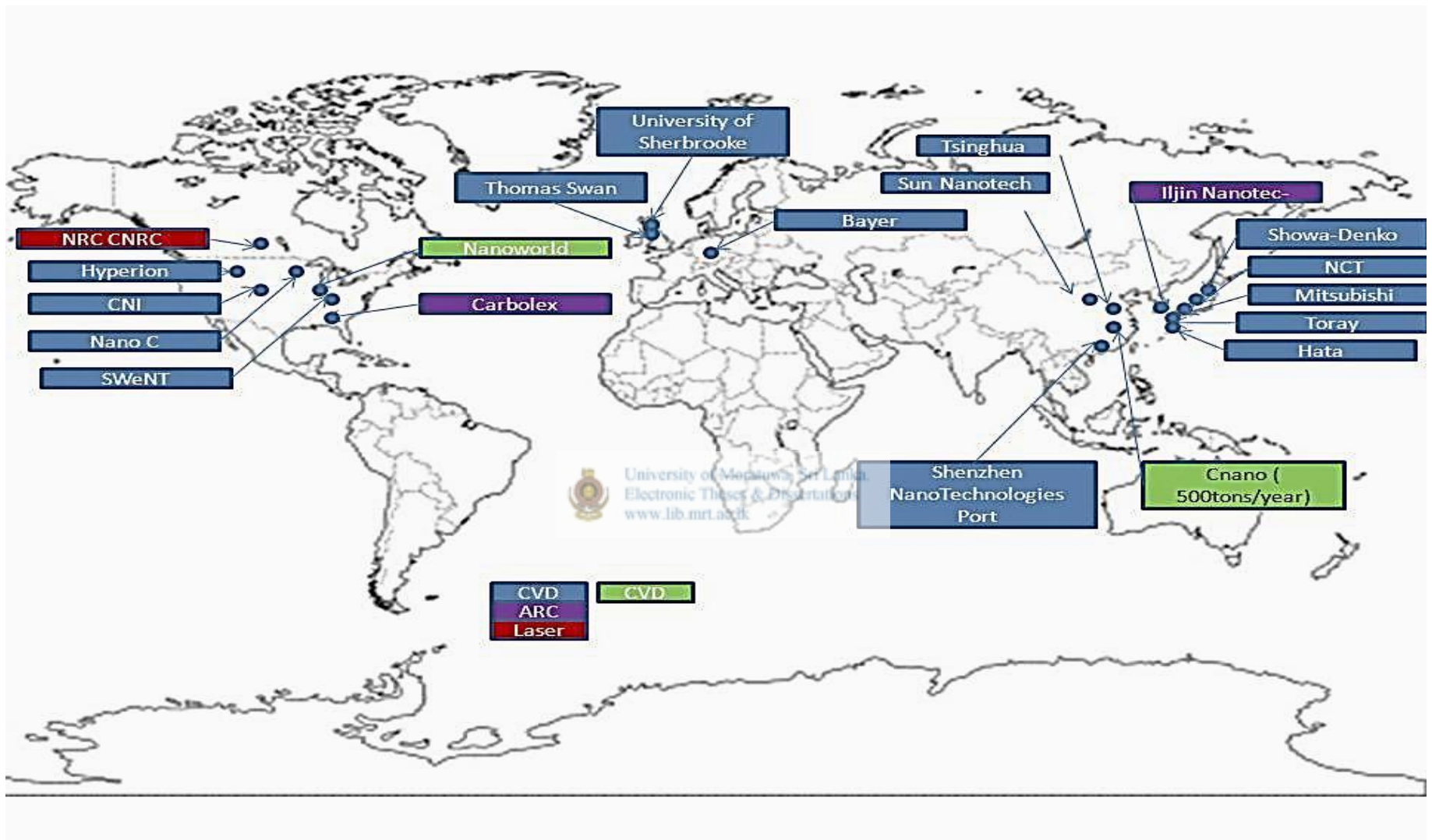


Figure 2-12 commercial scale CNT manufactures (Original is in colour)

2.7 Introduction to graphite

Long time after the era of the Celts, who already had used graphite in the production of ceramics, English shepherds in the year 1565 found a glossy anthracite-coloured mineral that was excellently suited for drawing and writing, and they gave it the name "plumbago". It was only in 1779 that a Swedish chemist discovered that this material was a type of carbon and not of lead. The name commonly used today is derived from the Greek word for to write: Graphein. (21)

Large quantities of carbon can be found in the sun and in the atmosphere of most planets. Although on the earth the content of carbon is less than 0.1 percent, it still is the basis of organic chemistry and of life itself. This is because of graphite's property to form composites with itself and with other elements such as oxygen, hydrogen, or nitrogen. Crystalline carbon is only known in four allotropic forms: (21)

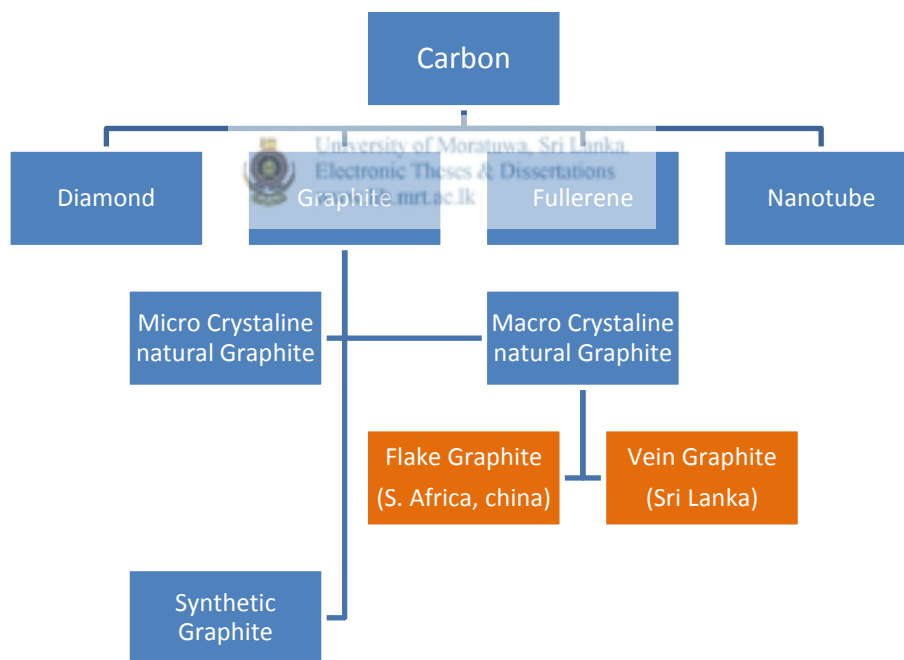


Figure-2-13 Different form so Carbon (Original is in colour)

Graphite and diamond are both made from carbon, which has 4 electrons in outer shell which occupy the electron configuration of $(1s)^2(2s)^2(2p)^2$. In the ground state there are two unpaired electrons in the outer shell. In diamond assembling many

different sp^3 - hybridized carbon atoms to one crystal, it achieves the typical diamond structure (Figure 2-14).

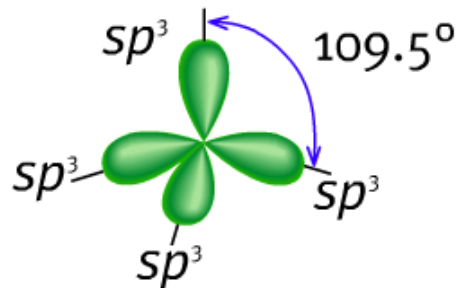


Figure 2-14 sp^3 -hybrid orbital

Due to the three dimensional sp^3 -structure the binding strength between neighboring carbon atoms is equal for each atom and very strong. Therefore, diamond is one of the hardest materials known; it is used as a cutting tool. The corresponding band structure reveals a large band gap due to unavailability of free electrons, which corresponds to an insulator. The electrical conductivity is very low. Furthermore, the transparent appearance of diamond corresponds to the fact that electrons cannot be excited out of the valence band into the conduction band with a wavelength in the optical range. In graphite the sp^2 hybridization is there. As seen in Figure 2-15 the sp^2 -hybridization is the combination of one s-orbitals with only two p-2 orbitals, namely p_x and p_y .

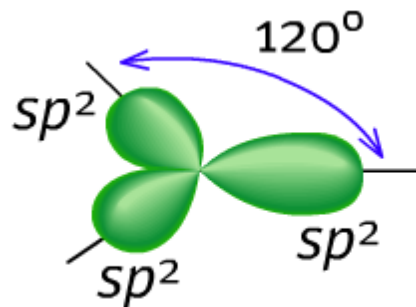
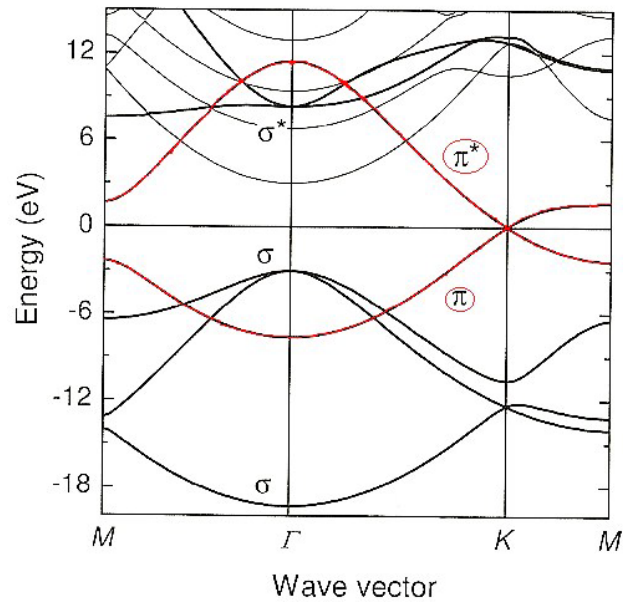


Figure 2-15 sp^2 Hybridization

Graphite has planar assembly with a characteristic angle of 120 degree between hybrid orbitals forming a σ -bond. The additional p_z -orbital is perpendicular to the sp^2 -hybrid orbitals and forms a free electron cloud. It consists of parallel carbon

layers. Within a layer the planar sp^2 -hybrid orbitals align themselves to a structure with strong binding. Between the layers the π -orbitals give rise to weak Van-der-Waals-forces. As a result graphite is one of the softest materials known and is used in pencils.



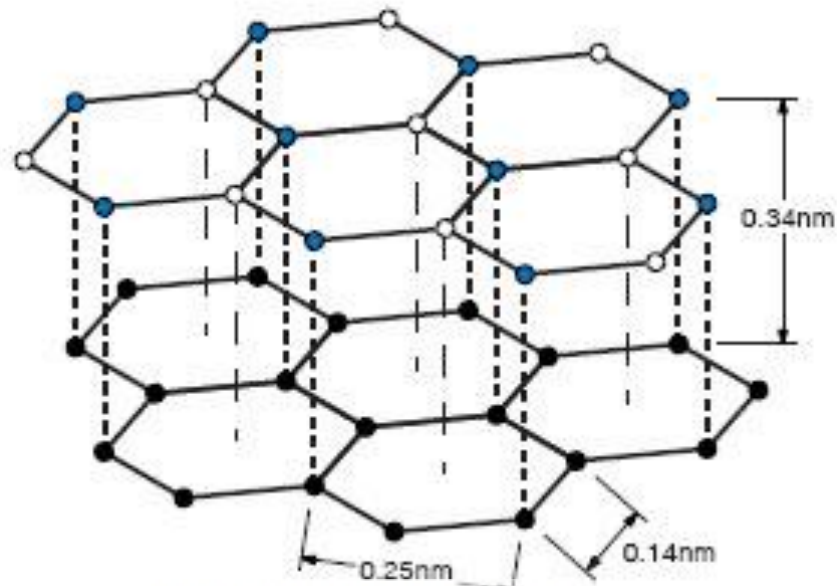
University of Moratuwa, Sri Lanka
 Figure 2-16 Band structure of graphite
www.lib.mrt.ac.lk

The band structure of graphite (Figure 2-16) reveals valence and conduction band, consisting of the bonding and anti-bonding π - and π^* - orbitals, which touch at the K-point. Due to this fact graphite can be described as a semimetal. The connections of the two bands influence the possibility to easily excite electrons out of the valence into the conduction band, independent of the wavelength, so that graphite is a very good electrical conductor and opaque. (6)

Graphite is chemically inert, eco-friendly, and absolutely safe. It is classified as micro-crystalline and macro-crystalline natural graphite and synthetic graphite. Six hexagonally arranged carbon atoms form the basic unit of the graphite crystal. The two-dimensional lattices are highly stable within themselves, but they can be easily shifted against each other. (21)

As seen on the Figure 2-12 commercial quantities of Vein graphite can only be found in Sri Lanka. Therefore it is known as Ceylon graphite. As the name describes, the

vein graphite is formed inside rocks as veins of our body. The diameter ranges from 4 inches to several feet. But flake graphite is found within prevalently rocks and cannot be found in large lumps. Therefore as-mined vein graphite is more pure than flake graphite. Further details are described in section 3.3.1 Characterization of raw materials.



University of Moratuwa, Sri Lanka
Electronic Theses & Dissertations
www.theses.lanka.ac.lk
Figure 2-17 Lattice Structure of Graphite

As seen on the *Figure 2-17* distance between the two adjacent carbon atoms in graphite is 0.14 nm and distance between the layers is 0.34 nm.

2.7.1 Application of natural graphite

- Carbon brushes (electrical conductivity and low friction and self-lubrication).
- Refractories (thermal resistance, thermal conductivity and low wettability by liquid metals).
- Electrodes for electric arc furnaces (thermal resistance and electric conductivity).
- Molds for continuous casting from isostatically pressed graphite (thermal conductivity, thermal resistance, low friction and self-lubrication, low wettability).
- Lubricants (low friction and self-lubrication).

- Graphite powder as a solid lubricant.
- Graphite powder added to oils and greases.
- Polymer coatings containing graphite powder.
- Bronze-graphite composites for sliding bearings.
- Friction materials (low friction, self-lubrication, thermal conductivity, and thermal resistance) contain up to 15% graphite powder for controlling coefficient of friction and dissipation of friction energy.
- Clutches.
- Brake drums and pads.
- Graphite foil (thermal resistance, chemical resistance) is made of a graphite powder treated by sulfuric acid and rolled to a required thickness. Graphite foil is used for manufacturing high temperature gaskets and packages.
- Cathodic material in zinc-carbon and lithium-ion batteries (electrical conductivity and chemical resistance) contains fine high purity graphite powder.
- Moderators in nuclear reactors (resistance to neutron radiation, thermal resistance).
- Carbon fibers for Carbon Fiber Reinforced Polymer Composites (high strength, low density). Automotive, marine and aerospace parts, sport goods (golf clubs, skis, tennis racquets, fishing rods), bicycle frames are made of Carbon Fiber Reinforced Polymer Composites.
- Carbon-Carbon Composites (low CTE, high Modulus of Elasticity and strength, low density). High performance braking systems, refractory components, hot-pressed dies, heating elements, turbojet engine components.
- Pencils (low friction) consist of a mixture of microcrystalline graphite and clay. (22)



Chapter 3 : MATERIALS AND METHODS

All vein graphite used in this study were taken from the Bogala graphite mine, Sri Lanka and were of as-mined highest grade (99.9%) was used without further purification. All gasses were purchased from Industrial Gasses Pvt Ltd, Sri Lanka and were of high purity grade. Reference analytical grade carbon nanotube samples were purchased from Sigma Aldrich, Germany and used without further purification. Further, the commercial grade carbon nanotube samples with five different diameters were purchased from Chengdu Organic Chemicals Pvt Ltd, Chinese Academy of Science, China. (www.timesnano.com)

The characterization techniques, equipment and the methodologies used in this study are described below.

3.1 Characterization techniques

3.1.1 Thermo gravimetric analysis (TGA)

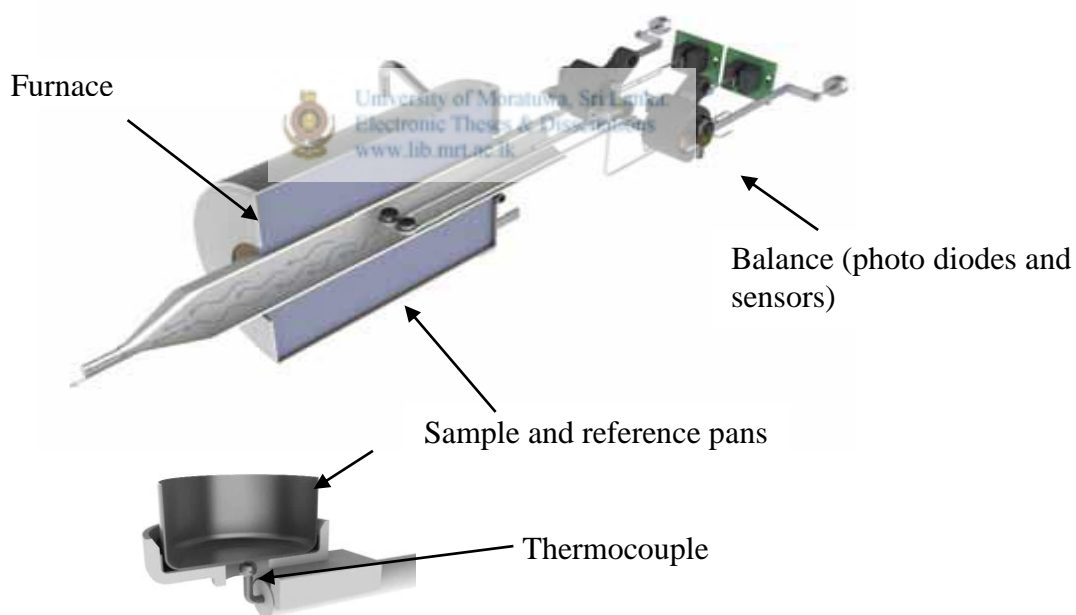


Figure 3-1 Schematic diagram of TGA (Original is in colour) (www.tainstruments.com)

In TGA, the sample is heated in a controlled environment and the weight of the sample is accurately measured as a function of the temperature. When the sample is heated in a controlled environment the weight losses occur due to decomposition

of the internal compounds in the sample at different temperature levels. The composition of the sample can be calculated as a percentage of the weight and since the initial weight is known the final weight composition can be calculated. The heat flow to the sample over the heating period can also be measured from the same equipment.

In the field of carbon nanotube, TGA is a powerful technique to quantify the amount of CNT and the amount of impurities. (23) (24) (25) Also a separate technique to compare the diameters of multi wall carbon nanotubes was developed using TGA in this study.

The thermal behavior of produced CNT samples was examined using Thermo Gravimetric Analysis (TGA), TA Instruments SDTQ600, at the Sri Lanka Institute of Nanotechnology, Sri Lanka. The samples (10-15 mg) were heated from ambient temperature to 1000 °C (ramp 10 °C/min) in air (100 l/min flow rate) environment using an alumina sample holder. Quantitative analysis (Yield) of the CNTs was done using the TGA.

Specifications of SDTQ600: (Source: SDTQ600 Manual)

System Design Horizontal Balance and Furnace

Balance Design Dual Beam (growth compensated)

Sample Capacity 200 mg (350 mg including sample holder)

Balance Sensitivity 0.1 µg

Furnace Type Bifilar Wound

Temperature Range Ambient to 1500 °C

Heating Rate – Ambient to 1000 °C 0.1 to 100 °C/min

Heating Rate – Ambient to 1500 °C 0.1 to 25 °C/min

Furnace Cooling Forced Air (1500 to 50 °C in < 30 min,

1000 °C in 50 °C in < 20 min)

Thermocouples Platinum/Platinum-Rhodium (Type R)

Temperature Calibration Curie point or Metal Standards (1 to 5 Points)

DTA Sensitivity 0.001 °C

Calorimetric Accuracy/Precision ± 2% (based on metal standards)

Mass Flow Controller with Automatic Gas Switching Included

Vacuum to 7 Pa (0.05 torr)

Reactive Gas Capability Included – separate gas tube

Dual Sample TGA Included

Auto-Stepwise TGA Included

Sample Pans Platinum: 40 μ L, 110 μ L

Alumina: 40 μ L, 90 μ L

(www.tainstruments.com)

3.1.2 Scanning electron microscopy (SEM)

SEM is an instrument which is capable of imaging in the range which cannot be seen by optical microscope. (Resolution below 2 μ m). Due to this reason SEM is one of the most routinely used imaging technique to study the morphological properties of nano-materials.

Here an electron beam is used to construct the morphological image of the sample. The electron beam is generated via a heated tungsten filament and it is extracted with about 1 to 5 kV high voltages. The extracted electron beam is then accelerated with a help of an external high voltage (around 1~30 kV) which is commonly known as the acceleration voltage. The accelerated electron beam is focused with an electromagnetic lens to get a higher concentrated energy on to the sample. When the sample is hit with this high energy electron beam, the atoms in the sample emit secondary electrons and these electrons are captured by the detector. The captured current signal is then amplified and converted in to an image.

In the SEM, the sample is kept in a vacuum and the sample needs to be conductive to avoid charging by the electrons. Since the CNT samples were not 100% conductive a tiny layer of gold was sputtered on to each sample before testing in this study.

Scanning electron microscope (SEM) is used to study the quality of the CNT in this study. When the CNTs are straight and clean the quality of the CNT is good and also CNT should be free of impurities such as graphitic particles and fullerenes. These properties of CNTs can be seen by using the SEM.

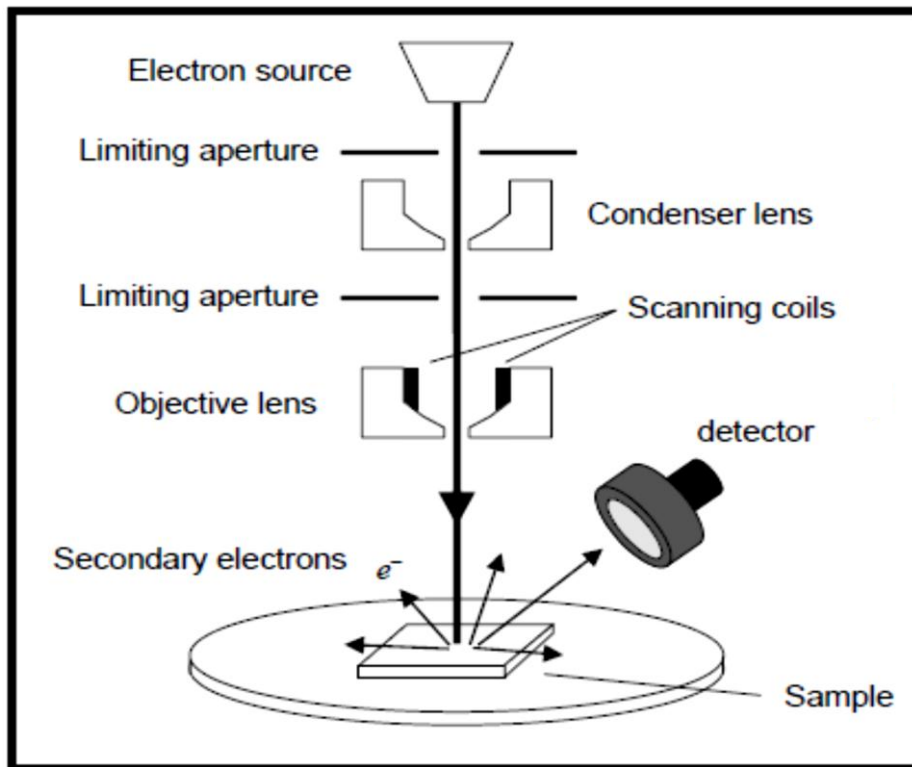


Figure 3-2 Typical Schematic diagram of a SEM set-up



University of Moratuwa, Sri Lanka.
Electronic T1 (Zadeh, 2008) ons
www.lib.mrt.ac.lk

HITACHI SU6600 Scanning Electron Microscope at the Sri Lanka Institute of Nanotechnology with the following specifications was used to characterize the produced CNTs. Hitachi SU6600 SEM was equipped with an iron sputtering unit Hitachi E1010. This was used to coat the samples with tiny layer of gold.

Specifications:

- Type : FESEM (Field emission SEM)
- Resolution : 1.2 nm for standard gold sample
- Maximum acceleration : 30KV
- Maximum extraction voltage : 5KV
- Detectors attached : Secondary electron detector
- : Back scatter electron detector
- : Transmission electron detector
- : EDX detector

3.1.3. Atomic force microscopy (AFM)

AFM is one mode of the scanning probe microscopy technique which consists of a cantilever with a sharp tip (probe) at its end that is used to scan the specimen surface. Other modes are MFM (Magnetic Force Microscopy), EFM (Electrostatic Force Microscopy) and STM (Scanning Tunneling Microscopy). The cantilever is typically silicon or silicon nitride with a tip radius of curvature on the order of nano meters. When the tip is brought into proximity of a sample surface, forces between the tip and the sample lead to a deflection of the cantilever.

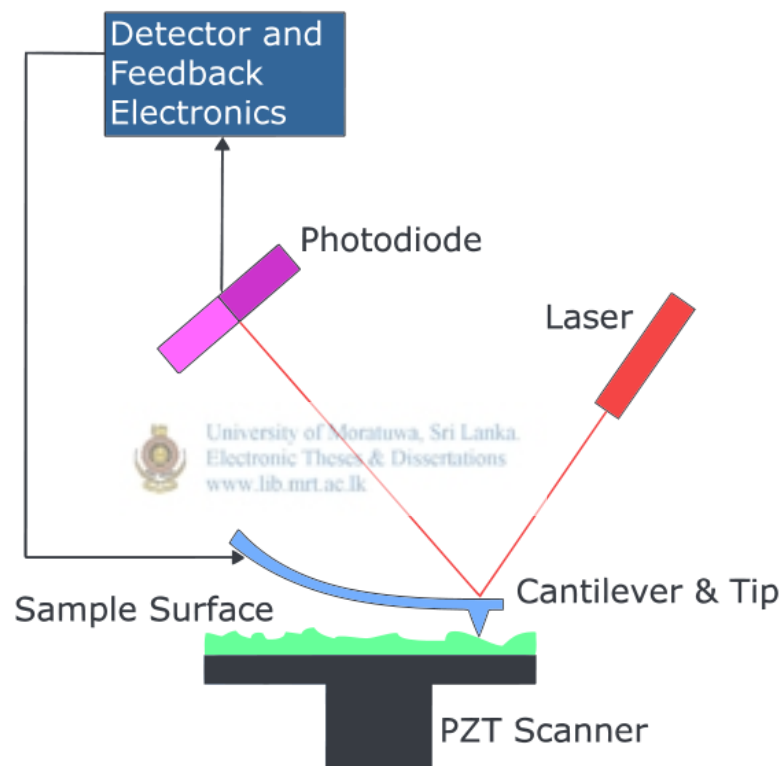


Figure 3-3 An AFM probe scans over a sample surface (Original is in colour)

Laser is reflected from the back of the reflective AFM lever and onto a position sensitive photo detector. While scanning the sample the topology image is created. The contact mode where the tip scans the sample in close contact with the surface is the common mode used in AFM imaging. In non-contact mode, the tip hovers 50 - 150 Å above the sample surface.

Unlike the SEM, AFM can give atomic level 3D images but the process is not straight forward. Sample preparation and the time taken per sample in analysis are in days. Therefore only one CNT sample was tested with AFM in this study.

3.1.4 Elemental analysis

SU6600 SEM at SLINTEC PVT LTD, which was used in this study, was equipped with an Energy Dispersive X-ray analysis (EDX) system from Thermofisher Scientific GmbH, Germany. When the high energy electron beam hits the samples, the atoms closer to the sample surface energies and emits X-rays. The wave lengths of these x- rays are characteristic for the elements and by detecting the wave length of the emitted x-rays the element percentages within the sample can be identified. This EDX system along with the SU6600 SEM was used to measure the purity of the raw material used and also used to compare flake graphite and vein graphite.

3.2. Other equipment used

3.2.1 Vacuum pump

Vacuum pump with following specifications was used to evacuate the arc discharging set up before arcing.  Electronic Theses & Dissertations
arcimg.lib.mrt.ac.lk

Brand : Vaccubrand
Model : RZ 2.5
Max : 2.3~2.8 m³/h, 4x10⁻⁴ mbar
Input : 230 V, 50 Hz, 1.6 A

The arcing chamber was evacuated down to 75 Torr and filled with the relevant inert gas (N₂, Ar or He) up to 1300Torr. This procedure was repeated three times before fixing the relevant parameters. This is to ensure the inert atmosphere for arcing to take place.

3.2.2 High current DC power supply

Initially Miller Dimension 400 dc welding transformer was used as the DC power supply source. Later to get higher accurate results Matsusada RE series high current DC power supply with following specifications was used to generate the arc.

Input : 200 V, 3 phases, 50/60 Hz, Out Put : 115 A, 35 V

The output current of the instrument is controlled accurately nearest to 1 A. In this study, the constant current mode was selected and the current was varied from around 30A to 115A. Since the unit was operated at 110 V an extra three phase step down transformer was used at the input. (Locally fabricated 10 kVA transformer from Hemal Electricals, Kadawatha, Sri Lanka)

3.2.3 High voltage generator

Arc discharge CNT production was carried out under an external electric field by using a high voltage generator with the following specifications.

Brand : Matsusada

Model No : AU-60R1-L(220 V)

Input : 230 V, 50 Hz

Output : up to 30 kV with 0.1 kV resolutions. (Negative output is also possible by changing the negative output electronics)

3.2.4 Stop watch

Isolab brand laboratory grade analogue stop watch was used to measure the timing of the arcing.

3.2.5 Glove box



University of Moratuwa, Sri Lanka.
Electronic Theses & Dissertations
www.lib.mrt.ac.lk

Specifications of the glove box which was used to create the enclosed inert chamber are given below.

Brand : Iteco, Italy

Input : 230 V, 50 Hz

3.3 Methodologies

3.3.1 Characterization of raw materials

Since the study was focused on Sri Lankan vein graphite, comprehensive study was carried out on the vein graphite. As-mined vein graphite from Bogala Graphite lumps without further purifications and flake graphite from Asberry Carbon, USA were used. Powdered samples (50 mg) were prepared from both types and used for analysis.

3.3.1.1 Characterization on SEM (Imaging and elemental analysis)

15mm diameter sample holder was taken and cleaned with distilled water. Then a conductive double side carbon tape was pasted on the sample holder. A small amount of sample was sprinkled on to the tape with the help of a cotton bud. Sample was then put inside the gold sputtering unit, Hitachi E1010 and a tiny layer of gold was sputtered on to the sample. This gold layer is needed for the non-conductive samples to avoid the charging effect. For all the samples gold was sputtered for 15 seconds. During this time period around 2 nm thick layer of gold is formed on the sample.

Because of the conductive carbon tape and the gold layer the charging electrons on the sample are grounded and a clear image of the samples can be obtained. Finally the samples were fed in to the SEM and images were obtained from the secondary electron detector. Both elemental analysis report and the images were taken from the SEM examined.

3.3.1.2 Characterization on TGA

Each sample (10mg) was taken from both Bogala Graphite (known as Vein graphite) and flake graphite from Asberry carbon, USA. Alumina sample pan was used for the analysis and initially it was heated without the sample up to 1100⁰ C with a heating rate of 30⁰C per minute to oxidize all impurities in the sample holder. Once it was cooled to room temperature the balance was reset and removed from the instrument. The sample was loaded with the help of the spatula. Then all samples were run with a heating rate of 10⁰ C/min up to 1000⁰ C. Final results were analyzed through TA Universal Analysis 2000 software from TA instrument, USA.

The weight loss (Figure 3-4 – Y-1, Green curve), derivative weight loss (Figure 3-4- Y-3, Maroon curve) with respect to the temperature (since the heating rate is fixed, this axis is same as the time axis) and also the heat flow graph (Figure 3-4 – Y-2, Blue curve) were plotted against the temperature using the software. The peak on the derivative curve represents the maximum rate of weight loss or maximum rate of decomposition. As seen in the Figure 3-4, in most of the cases the heat flow curve also follows the derivative curve and also gives a peak at the same temperature referring to the maximum weight loss.

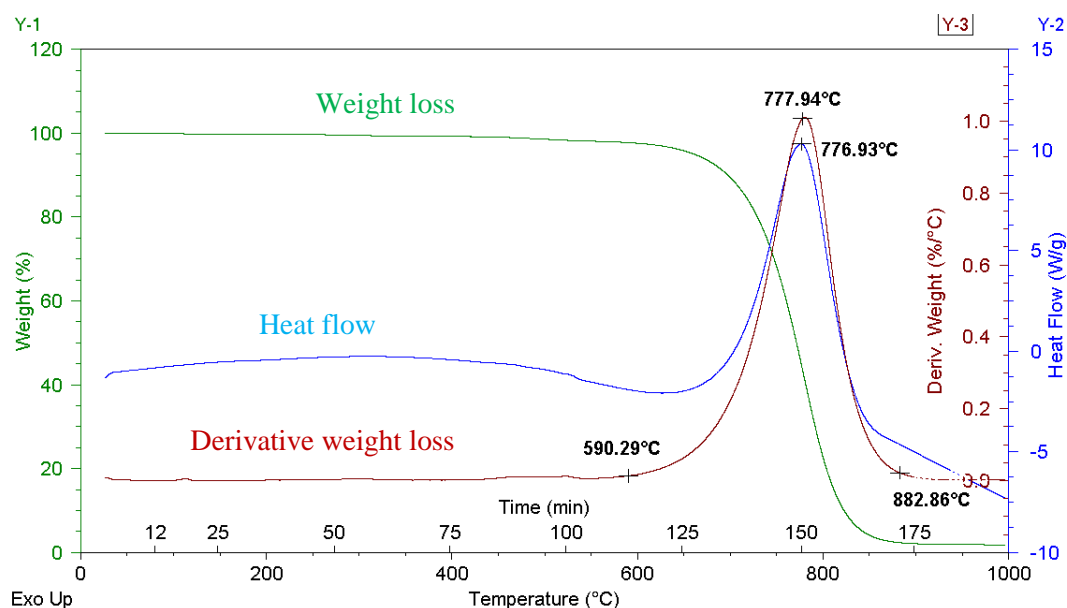


Figure 3-4 TGA Analysis example

According to the Figure 3-4 decomposition starts at 590⁰C and ends at 882⁰C. The maximum rate of weight loss is at 777.9⁰C and it is similar to temperature at maximum heat flow. This means that the decomposition rate is also at its maximum at this point because more heat is required for more decomposition of the sample.

As seen in Figure 3-5 on the DTG curve (Derivative Thermo Gravimetric curve), there are two peaks referring to sample A and sample B. Sample B is decomposed quickly and by selecting the appropriate decomposing range on the software we can calculate the weight percentage of the sample B (61.28%). Similarly weight percentage of the sample A also can be measured (38.6%). Balance could be some residue material which is not decomposing below 1000⁰C or some moisture content. This technique can be used to identify the composition of the unknown samples.

This method was used to calculate the CNT yield in this study and there were two distinguishing peaks for all the samples. One peak referred to the graphitic particles and the other to CNT. Normally the graphitic peak was observed at the temperatures around 820~850⁰C which did not change much from the sample to sample. This temperature range is slightly higher than what we observed for pure graphite (Figure 4-3). This is due to the thermal annealing due to the high temperature of around 4000K during the arc discharge. Due to this annealing effect

the pure graphite could turn in to different thermally treated graphitic particles which have higher thermal stability than raw graphite.

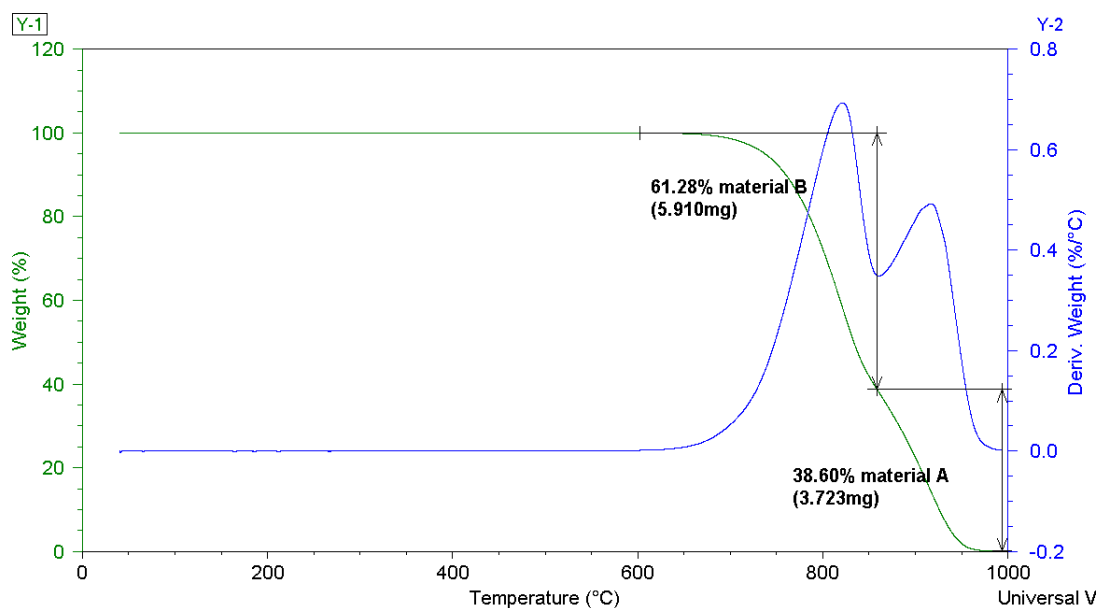


Figure 3-5 Weight % calculation from DTG curve (Sample: CNT produced with arc discharge)

3.3.2 Characterization of standard CNT samples

Standard analytical grade CNT samples (MWCNT, DWCNT, and SWCNT) purchased from Sigma Aldrich, Germany were characterized. As described in the section **Characterization techniques** all samples were characterized using SEM and TGA. Final results were analyzed through TA Instruments Universal Analysis 2000 software from TA instrument, USA.

3.2.3 Experiments with commercial grade CNT

Five commercial grade CNT samples were purchased from Chengdu Organic Chemicals Pvt Ltd, Chines Academy of Science, China (www.timesnano.com) with following specifications.

Table 3-1 Specification of the commercial grade CNTs used for the analysis

| Product code | Specification |
|--------------|---|
| TNM1 | MWCNTs, OD:<8nm, Purity:>95% Length:10-30um, |
| TNM3 | MWCNTs, OD:10-20nm, Purity:>95%, Length:10-30um, |
| TNM5 | MWCNTs, OD:20-30nm, Purity:>95%, Length:10-30um, |
| TNM7 | MWCNTs, OD:30-50nm, Purity:>95%, Length:10-20um, |
| TNM8 | MWCNTs, OD:>50nm, Purity:>95%, Length:10-20um, |

As described in the section **Characterization techniques** all five samples were characterized using SEM and TGA. Final results were analyzed through TA Instruments Universal Analysis 2000 software from TA instrument, USA. Same tests were repeated for first two samples for checking the repeatability.

3.2.4 Setting up of the arc discharge apparatus

Initially two carbon rods from a battery were used to generate the arc in normal atmosphere. The carbon rods were cleaned by removing the chemical on the outer surface by wiping with a paper towel with distilled water. Then the rods were connected to the linear motion system and connected to a 12V, 75Ah car battery. The electrodes were moved slowly manually until they came in to contact with each other. Then gap between the electrodes was increased to generate the arc.

Initial set up

Power connection from the battery
Carbon Electrodes

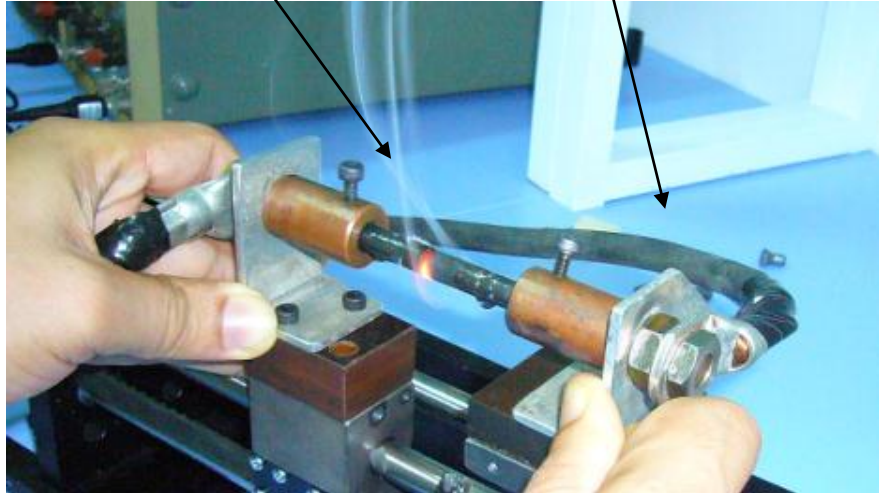


Figure 3-6 First generation arcing setup in open air(Original is in colour)

Following to the initial trial the set up was changed as follows to get the inert atmosphere and continuous DC supply.

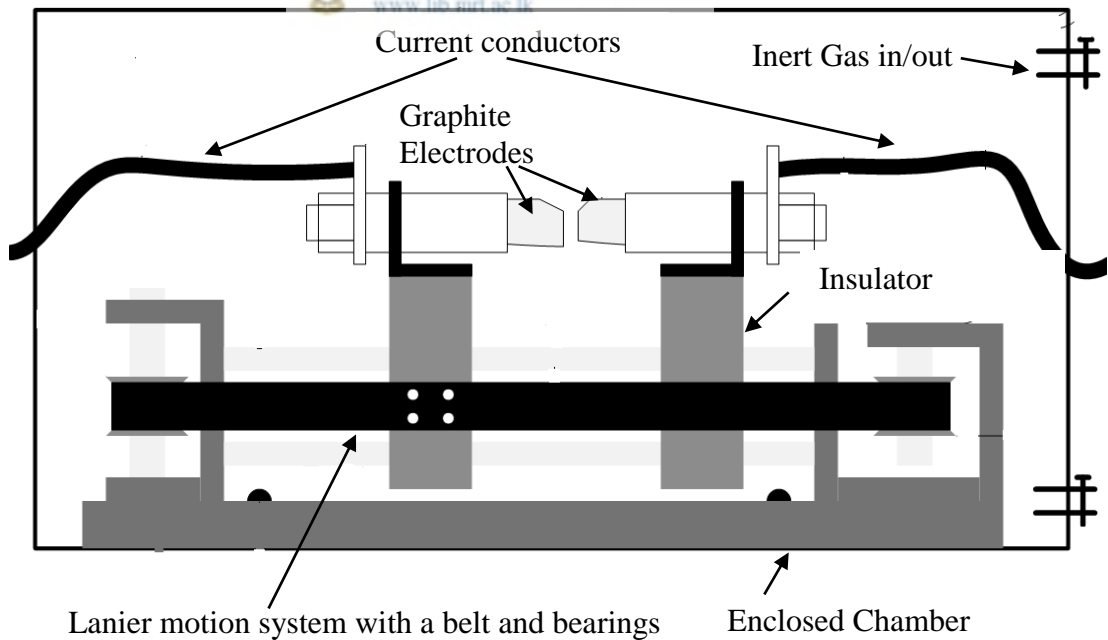


Figure 3-7 schematic view of the arc-discharge apparatus (26)

Second generation arc discharge set up



 University of Moratuwa, Sri Lanka
Electronic Theses & Dissertations
Figure 3-8 Second generation arc discharge set up (Original is in colour)

In the second setup, two pure vein graphite electrodes were connected to a linear motion system inside a glove box. The glove box was used to create a closed inert atmosphere and it was fitted with Argon (Ar). The system was evacuated with a vacuum pump (Described in section 2.2).The minimum tolerable pressure limit for the glove box was $-150\text{mmH}_2\text{O}$ (750Torr). A rented direct current welding transformer (Brand Miller, Model: dimension 400) was used to generate the arc. The output of the transformer was directly connected to the graphite anode and the cathode by using 20mm^2 shielded flexible copper conductors.

As described in section **3.2.1 Vacuum pump**, the glove box was evacuated and purged with Ar. This was repeated three times to get a proper inert atmosphere. The transformer setting was set for constant current mode with 50A, 20V as described by Samaranyake L. (26). Potentiometer meter used to change the current had half turn for its full scale and it was difficult to set for exact 50A.

The electrodes were moved slowly manually until they came in to contact with each other. Then gap between the electrodes was increased to generate the arc. Separate clip-on meter was used to measure the current since the dc transformer was not incorporated with an accurate current display. Arcing time was captured using the stop watch.

Note: for safety reasons welding goggles were used.

Third generation arc discharge setup

To rectify the issue of not getting constant current with the welding transformer that was replaced with a new digital high current DC power supply as described in section 3.2.2 *High current DC power supply*. The current setting was digitally controlled on this instrument. All the experiments thereafter were carried out using this Matsusada RE-115 high current DC power supply.

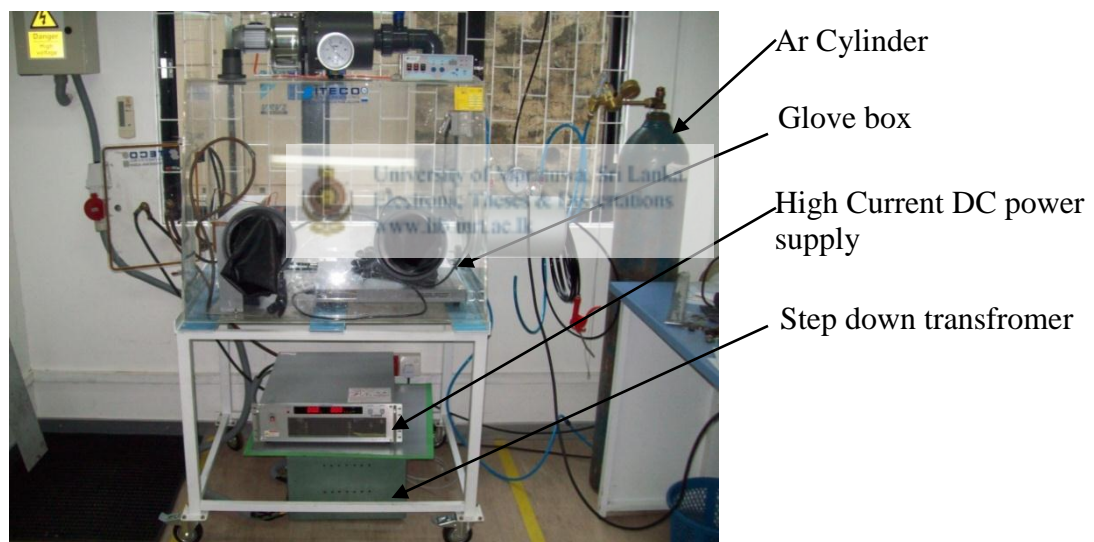


Figure 3-9 Third generation arc discharge setup(Original is in colour)

Fourth generation arc discharge setup

In the third arc discharge setup the minimum tolerable pressure of the glove box was around 745Torr. (Only 150 mmH₂O less than the atmospheric pressure).The fourth arc discharge set up was developed as below (Figure 3-10) by replacing the glove box with a mild steel (W-350mm*H400mm*L750mm) enclosure. Thickness of the metal enclosure was 8mm. Vacuum gauge used was capable to measure from 0

Torr to 1520 Torr. (Figure 3-10 –A) A 10mm thick glass window was fixed to the side of the chamber to see the arc. Figure 3-10-D. One side of the chamber was manufactured using an ebonite (12mm) sheet to get the insulation for the supply wires. Through the same wall the linear motion system was extended by using a stainless steel shaft (10mm) and two lip type oil seals were used as the air insulator at the wall as shown in Figure 3-10-C. The chamber was fitted with two air lines for evacuation and filling of the gas. The system was connected to the same Matsusada high current DC power supply.

A pressure relief valve was incorporated to the chamber with a set point of 5 bars as a safety precaution.



Figure 3-10 Final Arc discharge set up(Original is in colour)

(A: overall setup, B: vacuum gauge, C: power connection and fixing of the linear motion system. D: view through the glass window)

3.2.5 Cross section analysis of the arc soot

As described in section 3.2.1 *Vacuum pump* the glove box was evacuated and purged with Ar. This was repeated three times to get a proper inert atmosphere. Current was set for 50A and the glove box pressure was set to 1 atm. The electrodes were moved manually until they came in to contact with each other. Then gap between the electrodes was increased to generate the arc. The arc was maintained manually by moving the electrodes slowly for 1 minute. The system was kept for cooling for 30 minutes and the arc soot was scraped out from the cathode by using a paper knife. The soot was cut in to two and as described in the section 3.3.1.1 *Characterization on SEM (Imaging and elemental analysis)*, the sample was prepared for SEM analysis by keeping the cutting edge of the sample soot facing up. Sample was coated with gold as described in the previous section and the sample was analyzed through the SEM.

3.2.6 Testing with different arcing times

By using the second arc discharge set up 10 CNT samples were prepared with different arcing time as shown on the below table. All other conditions were kept constant as much as possible. Other conditions:

1. Arc Current : Around 100 A
2. Arc Voltage : 12 ~ 24 V
3. Arcing pressure : 1 atm

Table 3-2 Description of the samples for different arcing time

| Sample | Time (s) | Sample | Time (s) |
|----------|------------|-----------|------------|
| sample 1 | 10 | sample 7 | 45 |
| sample 2 | 15 | sample 8 | 50 |
| sample 3 | 20 | sample 9 | 55 |
| sample 4 | 25 | sample 10 | 60 |
| sample 5 | 30 | Sample 11 | 90 |
| sample 6 | 40 | Sample 12 | 120 |

Each sample was grounded by using a motor and pastel. All the samples were characterized SEM and TGA as described in section *Characterization techniques*

3.2.7 Testing with different arcing current

By using the second arc discharge set up 05 CNT samples were prepared with different arcing current as shown on the below table. All other conditions were kept constant as much as possible.

Other conditions:

1. Inert Gas : Ar
2. Arc time : 60 s
3. Arc Voltage : 12~24 V
4. Arcing pressure : 450 Torr

Table 3-3 Sample description for the samples with different arcing currents

| Sample | Current(A) | Sample | Current(A) |
|--------|------------|--------|------------|
| A1 | 60 | A4 | 100 |
| A2 | 70 | A5 | 115 |
| A3 | 90 | | |

Each sample was grounded by using a motor and pastel. All the samples were characterized SEM and TGA as described in section *Characterization techniques*

This experiment was repeated by using the fourth arc discharge set up with the following parameters.

1. Inert Gas : He
2. Arc Time : 60 s
3. Arcing pressure : 1 atm

Table 3-4 Sample description for the samples with different arcing current by using forth arcing set up

| Sample | Current (A) | Sample | Current (A) | Sample | Current (A) |
|--------|-------------|--------|-------------|--------|-------------|
| A2.1 | 65 | A2.4 | 85 | A2.7 | 100 |
| A2.2 | 75 | A2.5 | 90 | A2.8 | 110 |
| A2.3 | 80 | A2.6 | 95 | A2.9 | 118 |

The weight of each sample soot was measured by using the analytical balance. Each sample was grounded by using a motor and pastel. All the samples were characterized using the SEM and TGA as described in section *Characterization techniques*.

3.2.8 Testing with different arcing environment pressure

By using the fourth arc discharge set up 12 CNT samples were prepared with different arcing environment pressure as shown on the below table. All other conditions were kept constant as much as possible.

1. Inert Gas : Ar
2. Arc time : 60 s
3. Arc Voltage : 12 ~ 24 V
4. Arcing Current : 100 A

Table 3-5 Sample description for the samples with different arcing environment pressure by using forth arc discharge set up.

| Sample | Pressure (Torr) | Sample | Pressure (Torr) | Sample | Pressure (Torr) | Sample | Pressure (Torr) |
|--------|-----------------|--------|-----------------|--------|-----------------|--------|-----------------|
| P1 | 75 | P4 | 300 | P7 | 600 | P10 | 1050 |
| P2 | 150 | P5 | 375 | P8 | 750 | P11 | 1200 |
| P3 | 225 | P6 | 450 | P9 | 900 | P12 | 1560 |

The weight of each sample soot was measured by using the analytical balance. Each sample was grounded by using a motor and pastel. All the samples were characterized with SEM and TGA as described in section *Characterization techniques*

3.2.9 Testing with different arcing environment

By using the final arc discharge set up 13 CNT samples were prepared with different arcing environment as shown on the below table. All other conditions were kept constant as much as possible.

Other conditions:

1. Arc time : 60 s
2. Arcing Current : 100 A

Table 3-6 : Sample description for the samples with different arcing environment

| Sample | Pressure (Torr) | Environment | Sample | Pressure (Torr) | Environment |
|-------------------|-----------------|-------------|-------------------|-----------------|---|
| Ar-1 | 760 | Argon | N ₂ -1 | 950 | Nitrogen |
| Ar-2 | 950 | Argon | N ₂ -1 | 1350 | Nitrogen |
| Ar-3 | 1350 | Argon | W-1 | 760 | DI- water. (Top surface, middle ,bottom samples and cathode surface) |
| He-1 | 760 | Helium | W-2 | 760 | |
| He-2 | 950 | Helium | W-3 | 760 | |
| He -3 | 1350 | Helium | W-4 | 760 | |
| N ₂ -1 | 760 | Nitrogen | | | |

First nine samples were taken by using the forth arc discharge set up and the weight of each sample soot was measured by using analytical balance. Each sample was grounded by using a motor and pastel. All the samples were characterized using SEM as described in section *Characterization techniques* .Last sample was taken inside the deionized water, as seen on the Figure 3-11 the linear motion system was submerged in de ionized water with the graphite electrodes and the electrodes were moved slowly by hand until they came in to contact with each other. Then gap between the electrodes was increased to generate the arc. Arcing time was captured using the stop watch. After 60 seconds four samples were taken as per the above table.

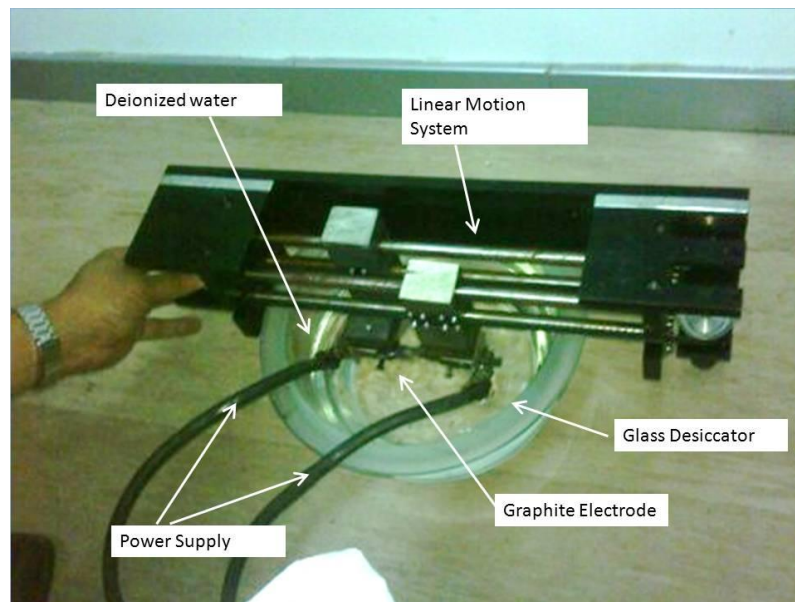


Figure 3-11 Arcing inside de ionized water. (Original is in colour)

3.2.10 Testing with an external electrical field

As seen on the Figure 3-12, an external electrical field was introduced to the arcing set up on the same direction as the dc power source by using a high voltage generator which is described in section 3.2.3 *High voltage generator*.

Several arc experiments were done bay varying the external electrical field from 1kV to 13kV with following parameters.

1. Inert Gas : Ar
2. Arc time : 60 s
3. Arc Voltage : 12 ~ 24V (Constant current)
4. Arcing Current : 100A

All the samples were characterized using SEM and TGA as described in section *Characterization techniques*.

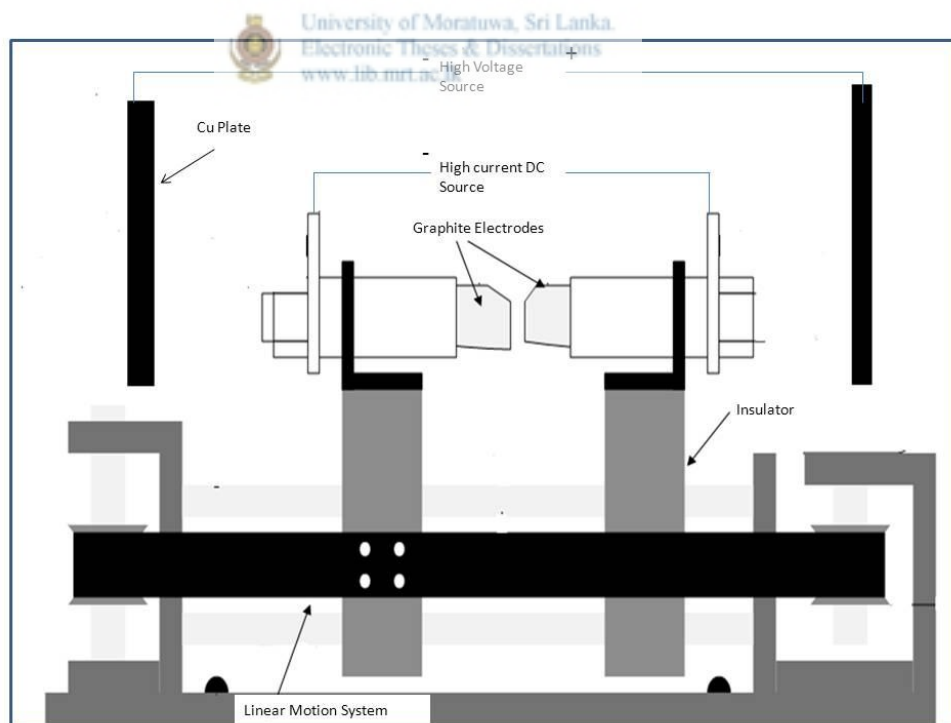


Figure 3-12 Schematic diagram of set up with external electric field

3.2.11 Testing with different shapes and materials of anode/cathode

Testing was carried out using the fourth arc discharge set up with the following anode cathode combinations.

- Graphite flat surface anode (10 mm diameter) with flat graphite surface cathode (25 mm diameter)
- Graphite pointed anode with graphite flat surface cathode (25 mm diameter)
- Graphite pointed anode with copper flat surface cathode (25 mm diameter)

3.2.12 Testing with Flake graphite anode and cathode

Flake graphite powders purchased from Asberry carbon were compressed with a hydraulic press (50 ton pressure) by using a 10mm and 25mm dies and the graphite anode and the cathode were made by using the fourth arc discharge set up with the following parameters.

1. Inert Gas : Ar
2. Arc time : 60 s
3. Arc Voltage : 12~24V (Constant current)
4. Arcing Current : 100A

Chapter 4 : RESULTS AND DISCUSSIONS

4.1 Characterization of raw materials

SEM images of the vein graphite and that of the flake graphite is given below.

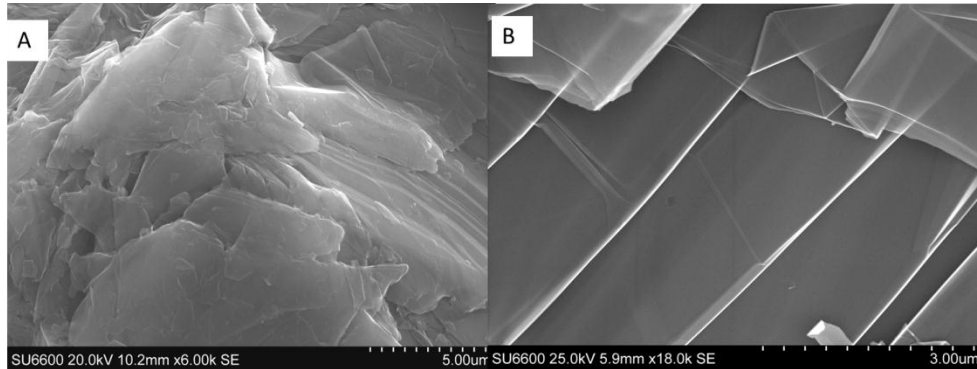


Figure 4-1 - SEM images of (A) Flake graphite, (B) Vein Graphite

As seen in **Figure 4-1** flake graphite has more disordered planes whereas the vein graphite shows well defined clear graphite planes and this is in line with the data published by Asbury Carbon Inc. (27). This is confirmed by the following XRD pattern of the vein and flake graphite.

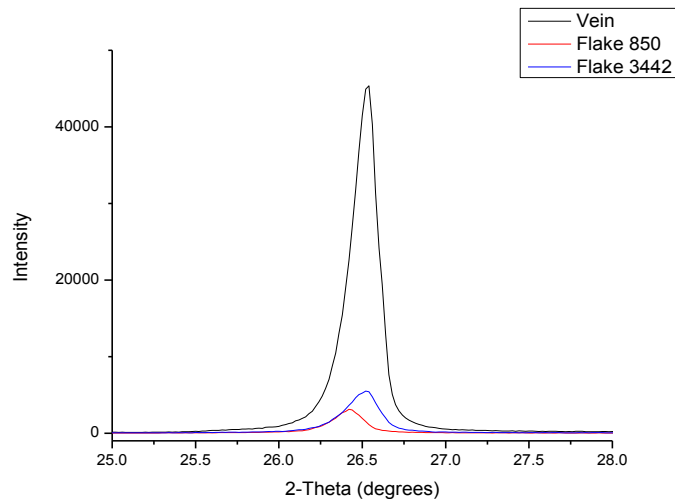


Figure 4-2 XRD Analysis of Vein and Flake graphite

As seen in the Figure 4-2, the peak around 2-Theta = 26.5⁰ degrees represents the graphite peak and the intensity is higher in vein than flake. That means vein graphite is more crystalline than flake graphite.

As described in section 2.1.4 the elemental analysis results of vein and flake graphite are given in Table 4-1 Elemental analysis of vein graphite and Table 4-2 Elemental Analysis of Flake Graphite respectively.

Table 4-1 Elemental analysis of vein graphite

| Element Line | Weight % | Atom % |
|---------------------|-----------------|---------------|
| C K | 99.82 | 99.95 |
| Si K | 0.07 | 0.03 |
| Fe K | 0.11 | 0.02 |
| Total | 100 | 100 |

Table 4-2 Elemental Analysis of Flake Graphite

| Element Line | Weight % | Atom % |
|---------------------|-----------------|---------------|
| C K | 93.79 | 96.48 |
| O K | 2.88 | 2.22 |
| Al K | 0.09 | 0.04 |
| Si K | 1.83 | 0.8 |
| S K | 0.86 | 0.33 |
| Ca K | 0.12 | 0.04 |
| Zn K | 0.42 | 0.08 |
| Total | 100 | 100 |

As seen in Table 4-1 and Table 4-2, the carbon percentage of vein graphite is 99.82% and that of flake graphite is 93.79%. Based on these results it can be concluded that the Sri Lankan Vein graphite is much more pure than flake graphite.

As described in section 2.3.1 the thermal behavior of flake and the vein graphite was examined on the TGA. Using the “Universal Analysis 2000” software the weight loss, derivative weight loss and the heat flow was plotted against temperature.

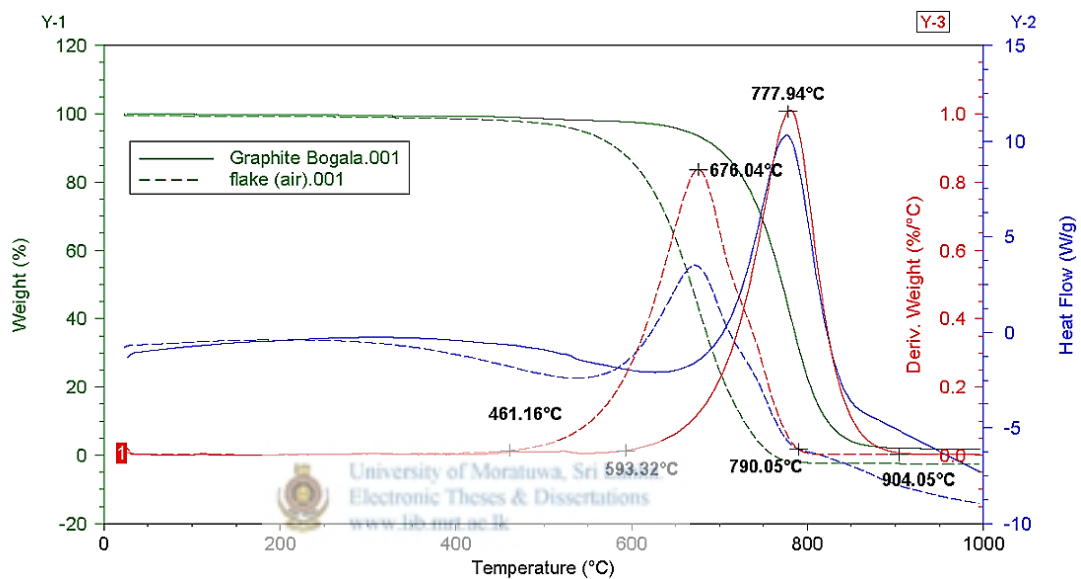


Figure 4-3 TGA results of Vein graphite (solid line) and Flake graphite (Dotted line) (Original is in colour)

The weight percentage is on axis Y1 (Green) and the heat flow is on axis Y-2 (Blue), derivative weight percentage is on axis Y3 (Red). From the derivative weight graph the temperature refers to the maximum rate of weight loss (or temperature refers to the maximum rate of decomposing) can be taken. The heat flow is also following the derivative graph and it also has the maximum heat flow at the same temperature. This means most of the sample is decomposed at the temperatures around this temperature at which the maximum weight loss is occurred.

As seen in the Figure 4-3, the temperatures refer to the maximum rate of weight loss of flake graphite is around 675°C and that of vein graphite is 778 °C. Also the decomposing is started at 461 °C for the flake graphite and that of vein graphite is

593°C. At around 790°C all the flake graphite has decomposed but up to that point only 40% of the vein graphite is decomposed and it goes up to 904°C for the complete decomposition.

As seen in the Figure 4-1, flake graphite has more disordered graphite layers than vein graphite which leads to more raw edges. When the raw edges are increased it can be easily attacked by oxygen and hence it is decomposed before vein graphite. This implies that vein graphite is more thermally stable than flake graphite. Due to this special feature of vein graphite it is used for high temperature applications. (27)

4.2 Characterization of standard CNT samples

Two samples of standard SWCNT and MWCNT from Sigma Aldrich GmbH were analyzed.

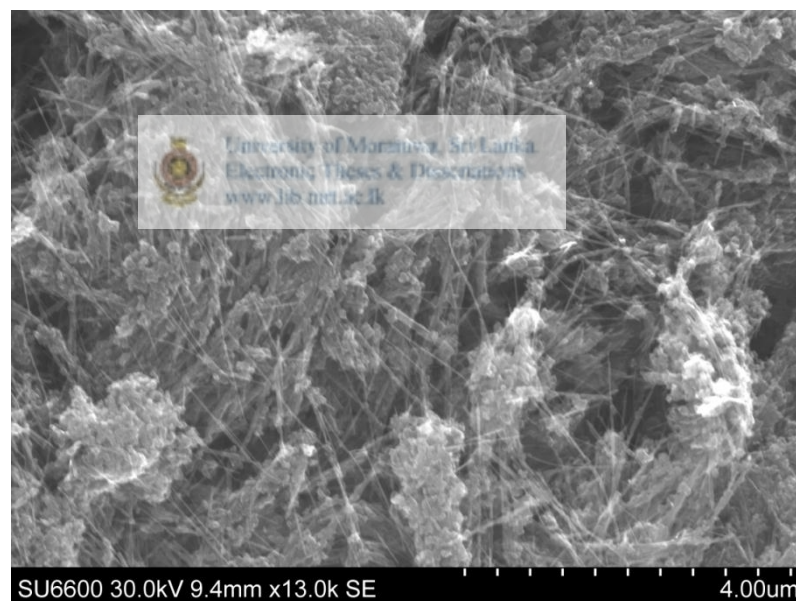


Figure 4-4 SEM image of Standard MWCNT from Sigma with 13000 magnification

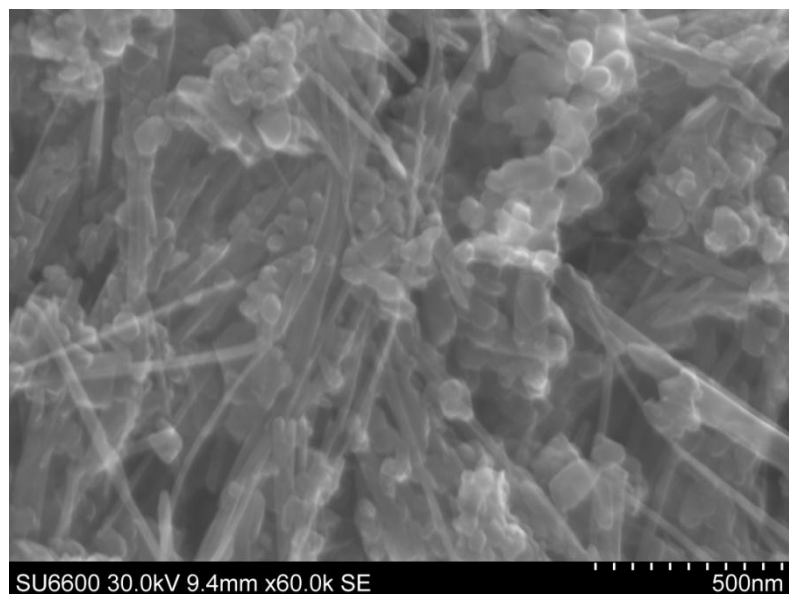


Figure 4-5 SEM image of Standard MWCNT from Sigma with 60000 magnification

Figure 4-4 is with a magnification of 16,000 and the other Figure 4-5 is with a magnification of 60,000. It is clear that the CNT sample is not pure and there are impurities. Small ball like of particle are fullerene and the other disordered particles are small graphitic particles (8).



University of Moratuwa, Sri Lanka
Electronic Theses & Dissertations
www.lib.mrt.ac.lk

Thermal analysis results are given in Figure 4-6 for the standard SWCNT and MWCNT. As seen in the TGA results, Figure 4-6 (dotted line), SWCNT decomposes around 300~450⁰C and MWCNT (solid line) around 650~875⁰C. These results are in line with the data published by Caoimhe de Frein (24). In the SWCNT sample, only 63.75% of SWCNT is available. Even at the 1000⁰C around 36% of the sample is available without decomposing and this is due to the catalyst used for the SWCNT production.

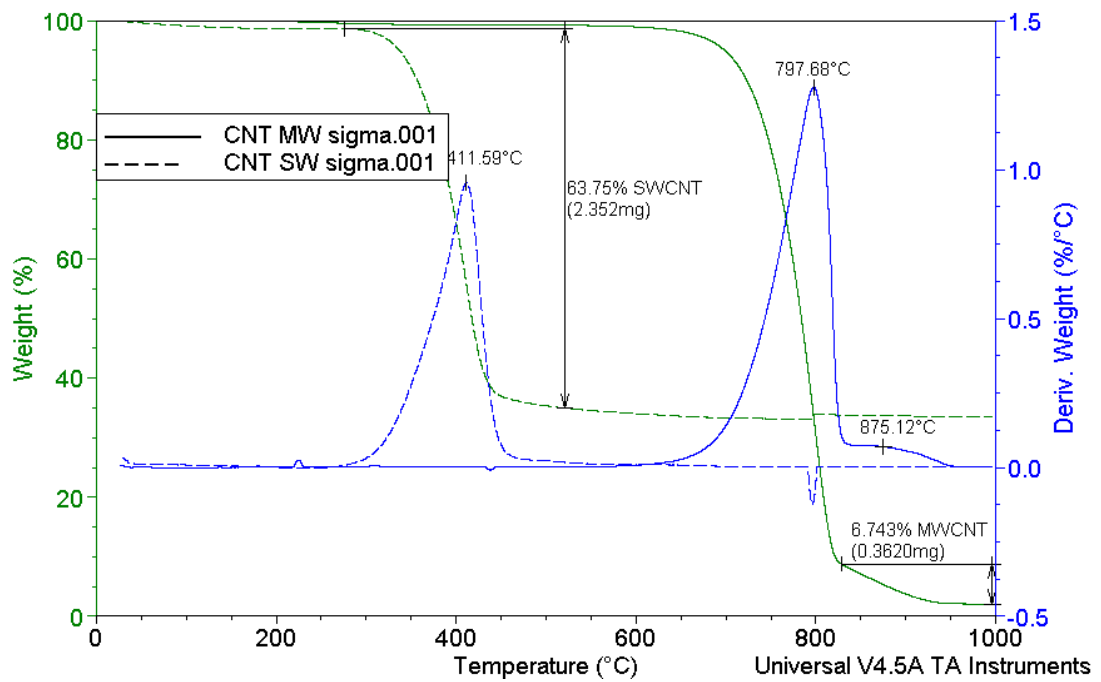


Figure 4-6 TGA Analysis of Sigma MWCNT (solid line) and Sigma SWCNT (dash line)
(Original is in colour)

On the MWCNT graph there are two distinguishable peaks at 797.88⁰C and 875⁰C. Comparing the TGA results of MWCNT in figure 4-6 with the graphite results in Figure 4-3, it can be concluded that the peak at 797.88⁰C is due to the graphitic particles. In conclusion the sample of MWCNT contains only 6.743% of MWCNT. Also 2% of the sample remained after 1000⁰C because of the metallic impurities.

Only MWCNT sample was analyzed by AFM. One MWCNT was found on the scan area of 800nm*800nm. The diameter of the MWCNT can be taken from Figure 4-7 as 32.8 nm. It is very difficult to find an individual CNT with AFM and also it is not straight forward imaging like in the SEM.

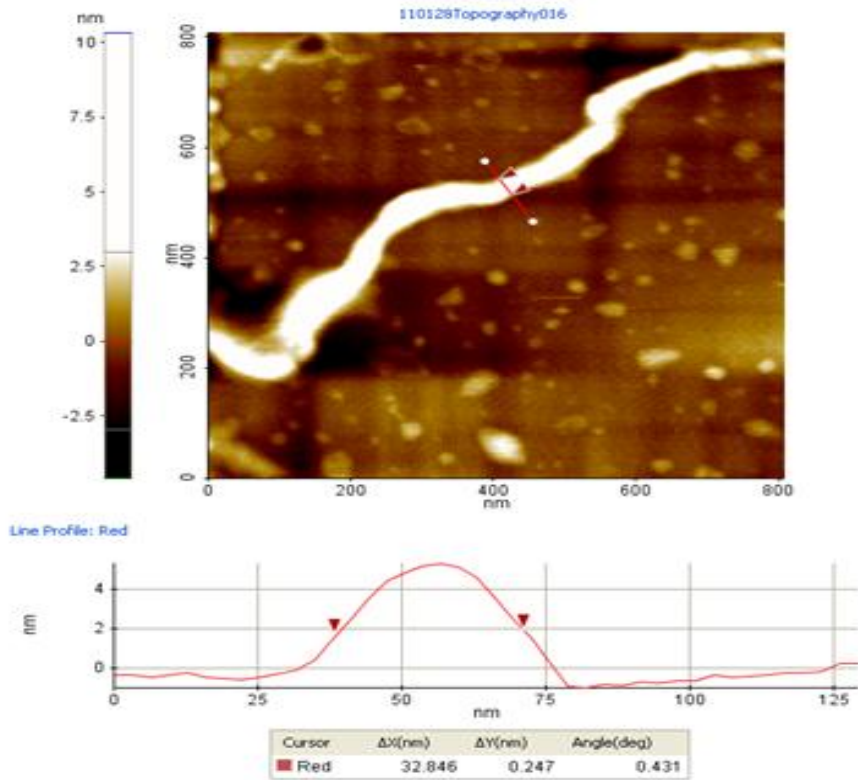


Figure 4-7 AFM analysis of MWCNT(Original is in colour).

4.3 Experiments with commercial grade CNT

All five samples were analyzed with TGA with a heating rate of 5⁰C/ Min.

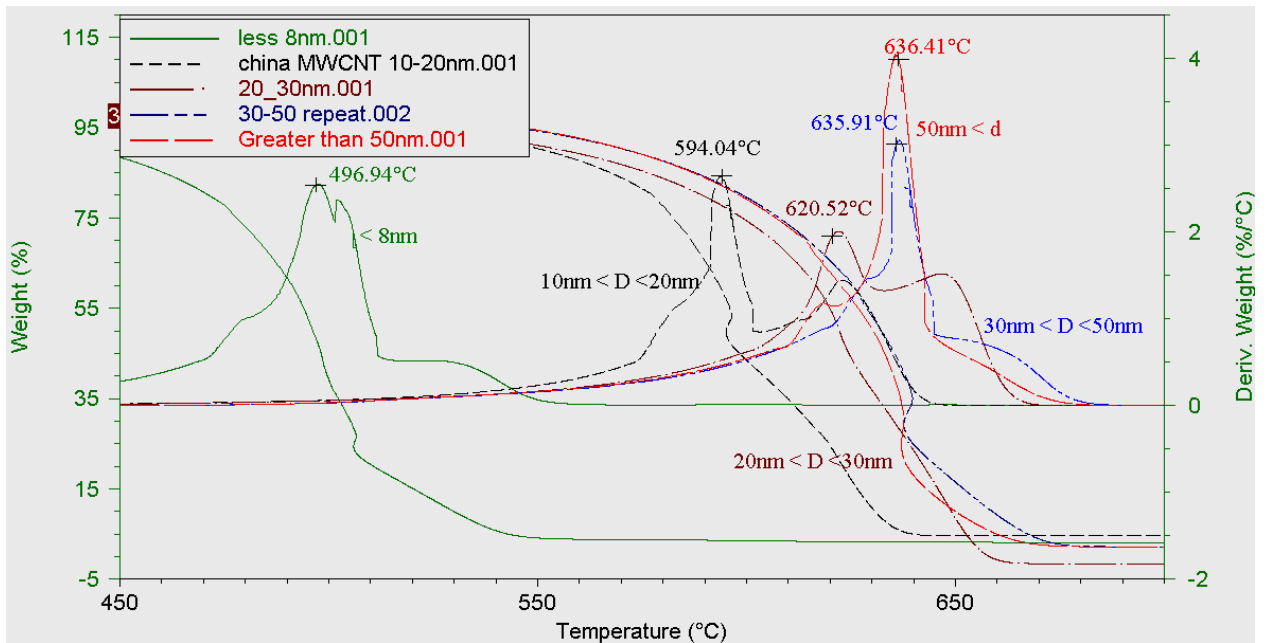


Figure 4-8 TGA analysis of commercial MWCNT samples (Original is in colour)

As seen on the TGA graph, the sample with diameters less than 8 nm has the maximum decomposing rate at 497⁰C (as described in section 3.1.1 Thermo gravimetric analysis (TGA)). Similarly all other samples have the maximum decomposing rate at 594⁰C, 620⁰C, 635⁰C and 636⁰C, respectively. The analysis was done using TA universal V4 software and the summary of the results are tabulated below.

Table 4-3 Temperatures at maximum decomposing rate of commercial MWCNT samples

| Product code | Specification | Temperature at Maximum Decomposing rate |
|--------------|---|---|
| TNM1 | MWCNTs, OD:<8nm, Purity:>95% Length:10-30um, | 497 ⁰ C |
| TNM3 | MWCNTs, OD:10-20nm, Purity:>95%, Length:10-30um, | 594 ⁰ C |
| TNM5 | MWCNTs, OD:20-30nm, Purity:>95%, Length:10-30um, | 620 ⁰ C |
| TNM7 | MWCNTs, OD:30-50nm, Purity:>95%, Length:10-20um, | 635 ⁰ C |
| TNM8 | MWCNTs, OD:>50nm, Purity:>95%, Length:10-20um, | 636 ⁰ C |

The above experiment was repeated for two samples with a heating rate of 10⁰C/min. The result of the repeat experiment of the commercial samples is given below.

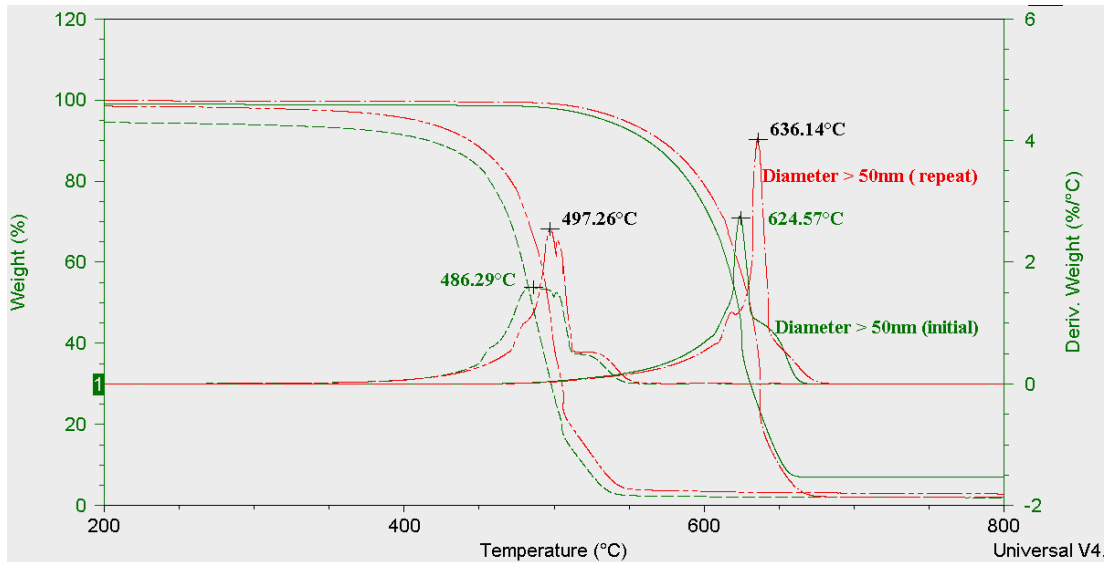


Figure 4-9 Repeat TGA analysis of commercial grade MWCNT samples (Original is in colour)

As seen from the graph, there is a shift of both the curves by around 10°C . This is due to the heating rate difference of 5°C but the results remain as before. When the heating rate is increased, the temperature at maximum decomposing rate increases slightly. Because when the heating rate is low the sample is exposed more to a particular temperature and therefore decomposition becomes easier. Considering all the results, following graph can be drawn.

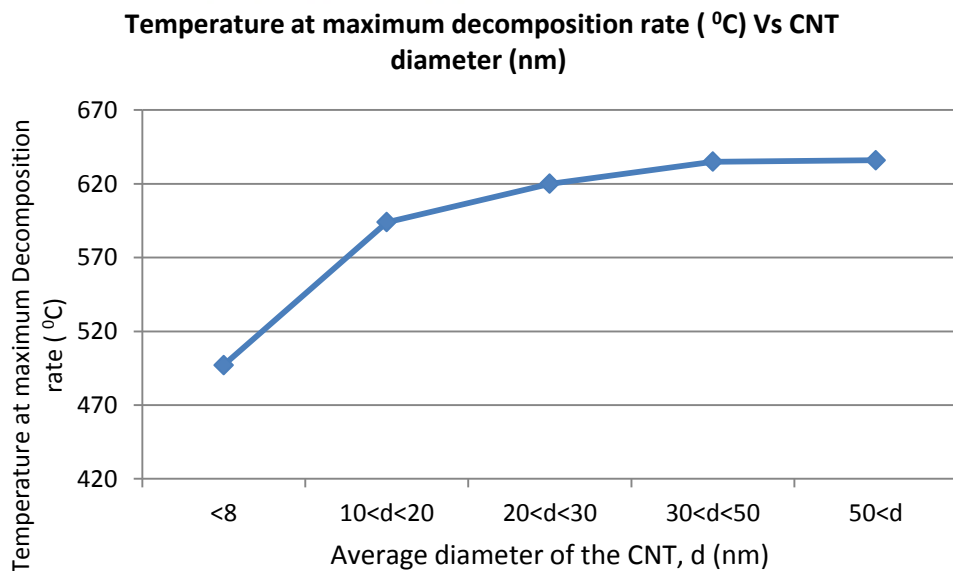


Figure 4-10 Temperature at maximum decomposition rate or the maximum heat flow while decomposing of the CNT Vs CNT Diameter for commercial samples (Original is in colour)

Based on the above results, it can be concluded that the temperature at the maximum decomposition rate increases with the increase of the diameter. These results can be used as an analytical technique to compare diameters of two samples made by same manufacturing technique and it was used in this study to compare the diameters of produced CNTs.

4.4 Setting up the arc discharge apparatus

In the initial set up carbon rods were burnt in open air due to presence of oxygen. As such there was no CNT formation. On the second set up, there was room for formation of CNT but the evacuation was not good enough to remove all the oxygen inside. The minimum tolerable pressure was 740Torr whereas the fourth set up gave 75Torr as the minimum pressure. Also the repeatability was not good due to varying current with the analog winding transformer. But with the MatsusadaTM high current power supply along with the small metal chamber, both problems were solved. It can be concluded that a good evacuation system and a constant current set up are needed for CNT manufacturing.

4.5 Cross section analysis of the arc soot

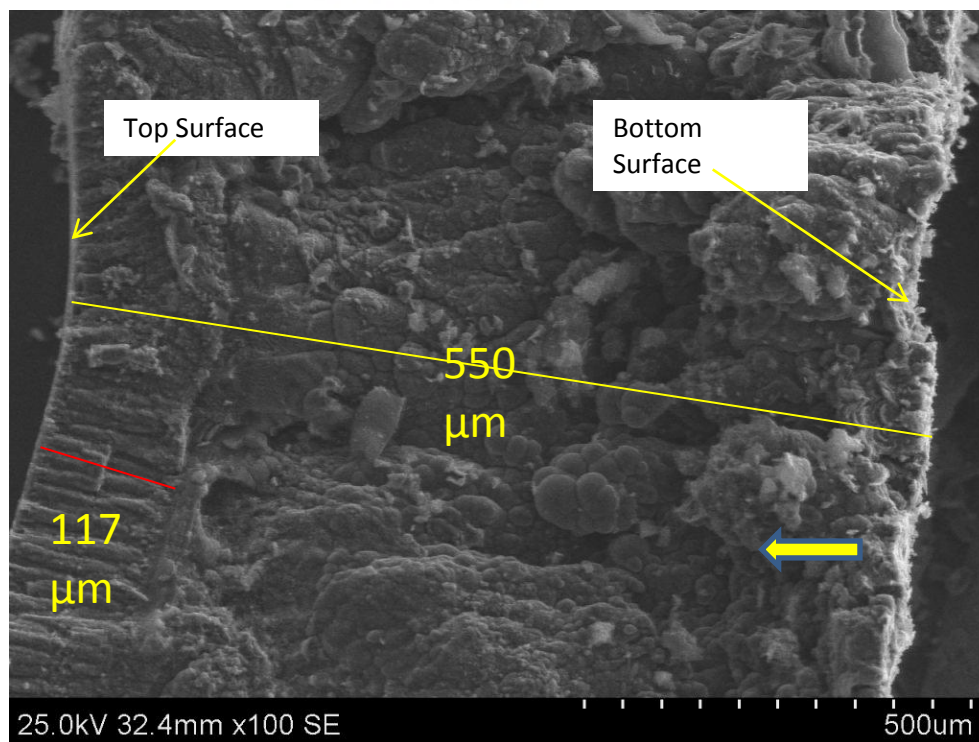


Figure 4-11 SEM image of Cross section of the Arc soot (Original is in colour)

As seen in the Figure 4-11, the thickness of the arc soot is around 550 μm for an arcing time of 60s with a constant current of 50A. On the top surface, CNT is formed up to 117 μm . This is around 21.27%. The experiment was done by using the second arc discharge set up where the current value was not fixed and also the evacuation was not good. This value for the yield would have increased up to around 30% if the fourth set up which is described in section 2.2.4 was used.

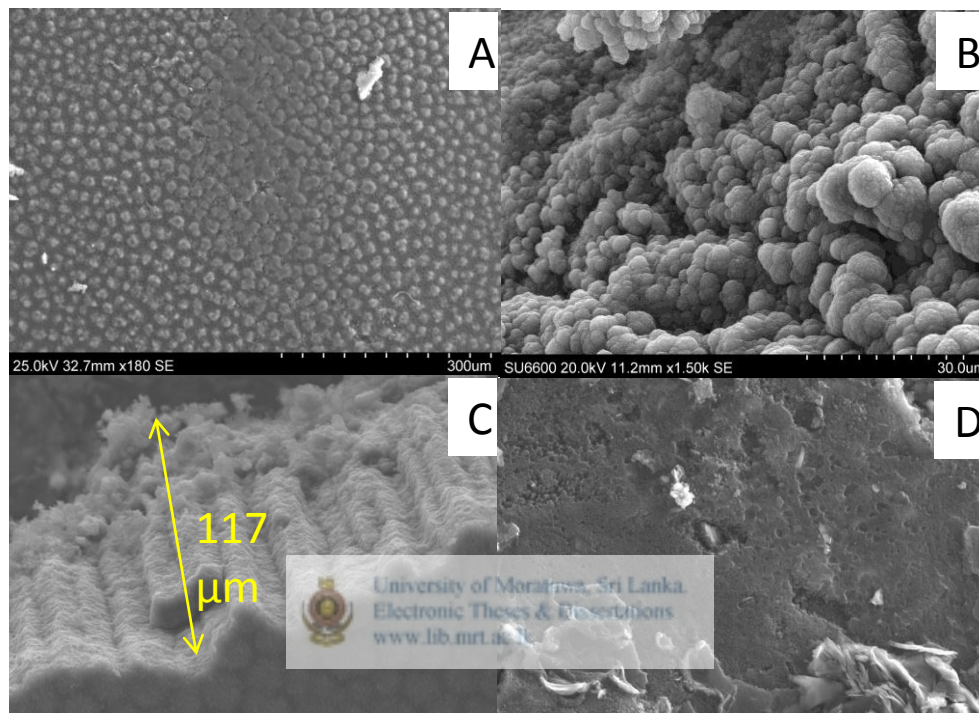


Figure 4-12 SEM image of the arc soot A) view from the top B) image of the middle structure c) image of the formed CNT layer D) view of the bottom surface

Figure 4-12-A and C shows that the top surface of the arc soot and is rich with CNT. The thickness of the CNT layer is around 117 μm . As seen in the Figure 4-12-B, the middle layer consists of ball shape graphitic particles. There are no CNTs in this area. Also as seen in the Figure 4-12-D, the bottom surface consists of raw graphite particles and some form of disordered graphitic particles. There is no CNT formation in this area too. One of the reasons for this might be the higher temperature inside the arc soot & due to that the formed CNT is damaged & formed new graphitic particles.

In summary, it can be concluded that the CNT is formed only on the top most layer around 100~120 μm .

4.6 Testing with different arcing time

SEM analysis of the samples with different arcing time is given below.

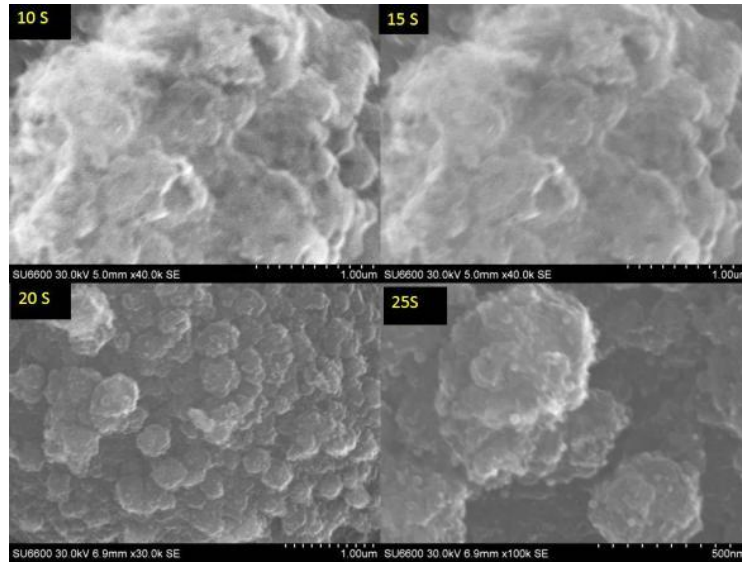


Figure 4-13 SEM images of the cathode deposit for arc time of 10s, 15s, 20s and 25s

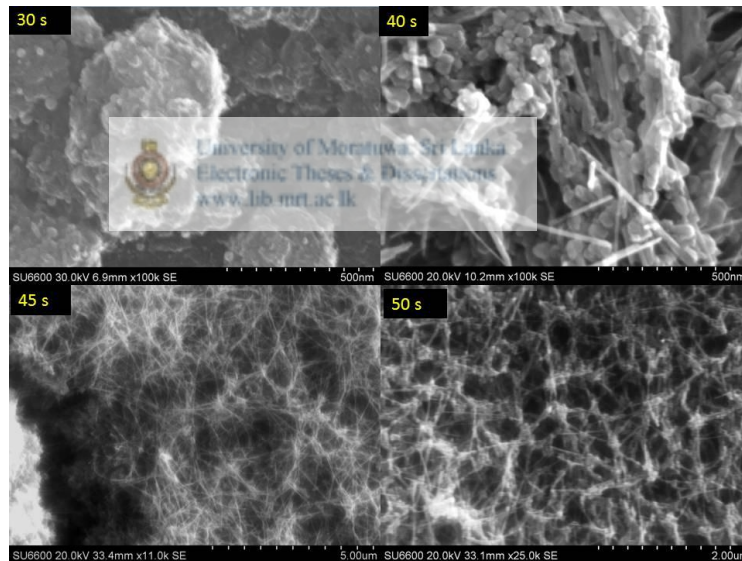


Figure 4-14 SEM images of the cathode deposit for arc time of 30s, 40s, 45s and 50s

As seen in the Figure 4-13 and Figure 4-14 there is no CNT formation up to 30s. At around 40s CNT formation starts with spherical particles like fullerene. Figure 4-15 clearly shows good quality CNTs without many defects after 55s. Based on the quality, it can be concluded that above 55s of arcing time is suitable for the arc discharge CNT production using the Sri Lankan vein graphite together with the other suitable physical conditions.

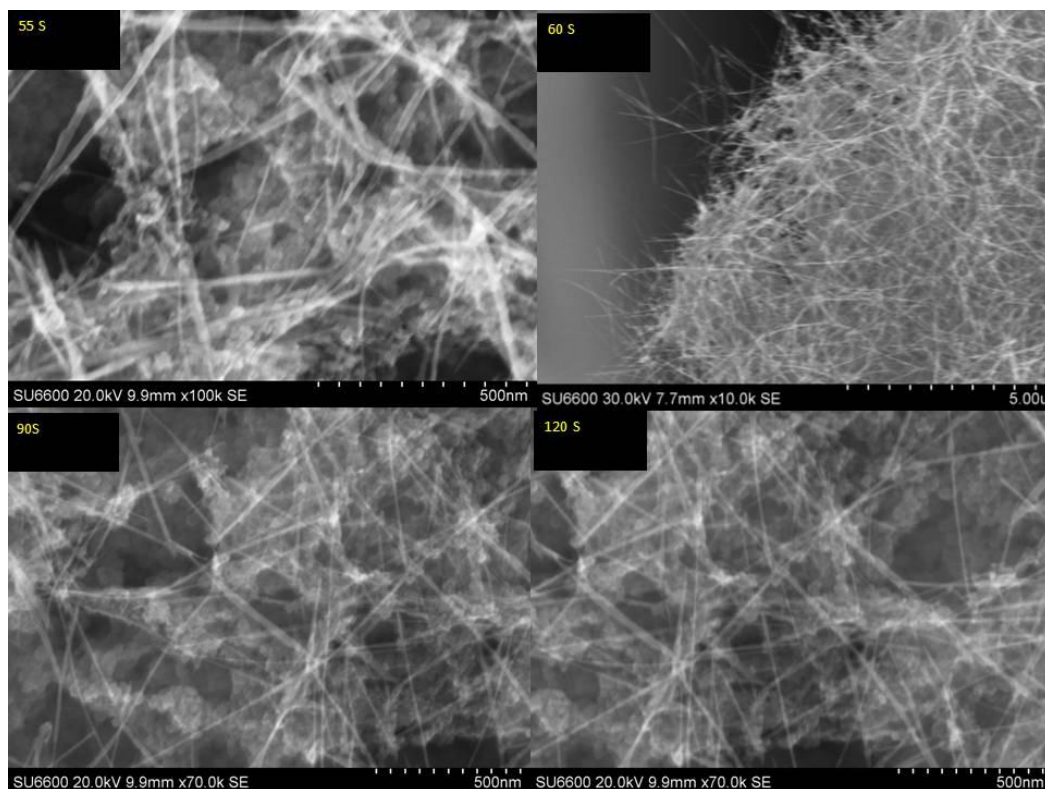


Figure 4-15 SEM images of the cathode deposit for arc time of 55 s, 60s, 90s and 120 s

TGA results of the sample with different arcing time are as follow.

Table 4-4 TGA results of the samples with different arcing time

| Sample | Time (s) | Temperature at the highest decomposition rate (°C) | CNT Yield % |
|-----------|------------|---|-------------|
| sample 1 | 10 | - | - |
| sample 2 | 15 | - | - |
| sample 3 | 20 | - | - |
| sample 4 | 25 | - | - |
| sample 5 | 30 | - | - |
| sample 6 | 40 | 841 | 15% |
| sample 7 | 45 | 853 | 23% |
| sample 8 | 50 | 844 | 17% |
| sample 9 | 60 | 930 | 32% |
| Sample 10 | 90 | 940 | 23% |
| Sample 11 | 120 | 942 | 21% |

The above results can be plotted as follow.

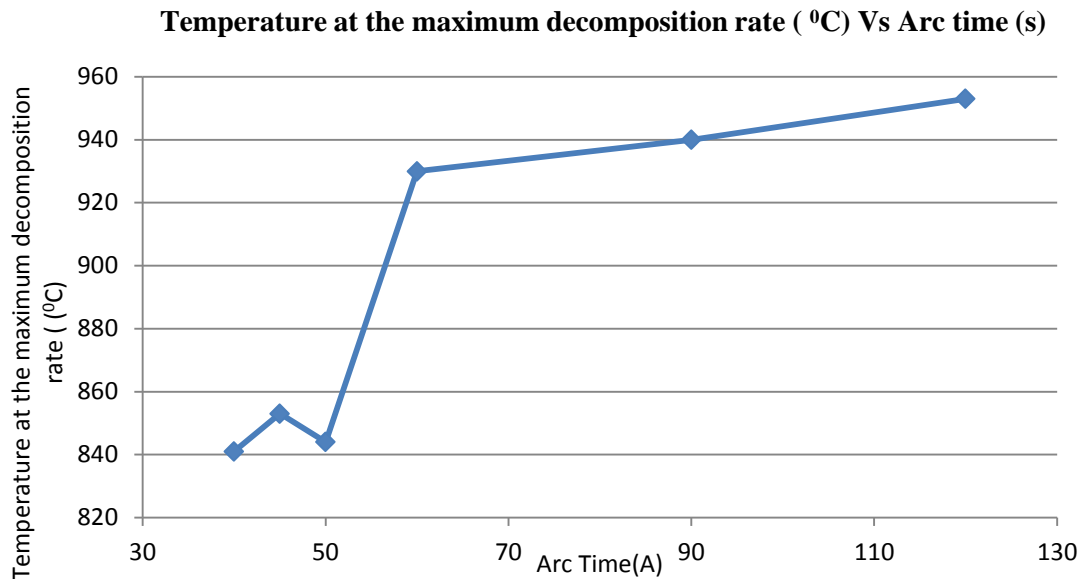


Figure 4-16 Temperature at the maximum decomposition of the samples with different arcing time (Original is in colour)

As seen in the Figure 4-16 the temperature at the maximum decomposition rate of the CNT increases with increase of arcing time. Based on the analytical technique developed in section **4.3 Experiments with commercial grade CNT**, it can be concluded that the diameter of the produced CNT is increasing with increase of the arcing time.

Figure 4-17 shows the CNT yield variation with arcing time. Based on the graph, it can be concluded that the CNT yield is increasing up to around 60s & slightly decreasing with increase of arcing time. As described in **4.5 Cross section analysis of the arc soot**, the CNT is formed only on the top most layer of the arc soot. When time increases top layer of CNT remains & the other graphitic particles are increasing. Because of that the percentage of yield decreases slightly after 60s.

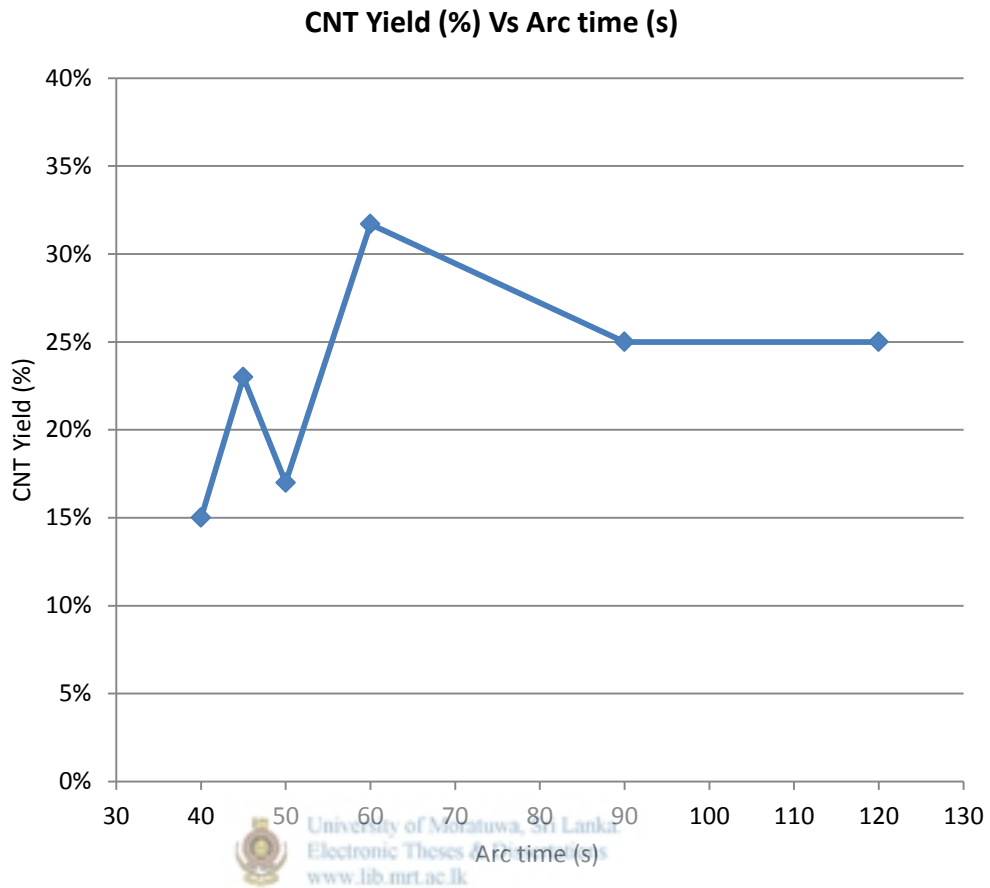


Figure 4-17 CNT yield of the samples with different arcing times (Original is in colour)

Based on the TGA and SEM results, it can be concluded that the best possible arcing time for the arc discharge CNT production using Sri Lankan vein graphite is around 60s.

4.7 Testing with different arcing currents

TGA results of the test done by using the second arc discharge set up are given in Table 4-5. For each sample a separate thermogram was drawn on TA universal software and the temperature at the maximum decomposition rate and the CNT percentage were calculated and tabulated. Based on those data two graphs were drawn.

Table 4-5 Results of the test with different arcing currents by using the second set up

| Current (A) | Temperature at the maximum decomposition rate for CNT (°C) | Graphitic Particles % | CNT % | Total arc soot weight (mg) | Yield (mg) |
|-------------|--|-----------------------|-------|----------------------------|------------|
| 60 | 863 | 66.34 | 33.18 | 0.105 | 34.84 |
| 70 | 867 | 58.00 | 42.00 | 0.21 | 88.20 |
| 90 | 914 | 58.00 | 42.00 | 0.04 | 16.80 |
| 100 | 916 | 56.00 | 44.00 | 0.03 | 13.20 |
| 115 | 925 | 58.00 | 39.00 | 0.04 | 15.60 |

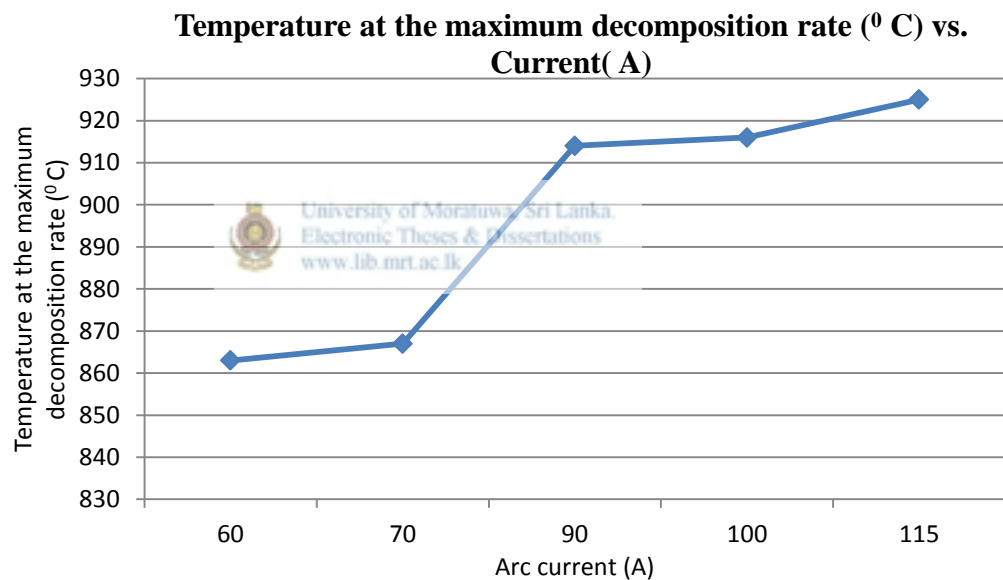


Figure 4-18 Temperature at the maximum decomposition rate vs arcing time

As seen in the Figure 4-18 and Figure 4-19, there is a clear trend that the CNT yield is increasing with increase of the current. Also since the decomposition temperature increased with the increase of the current, it can be concluded that the diameter increase with increase of the arcing current. This is in line with the data published by M. Cadeka (28).

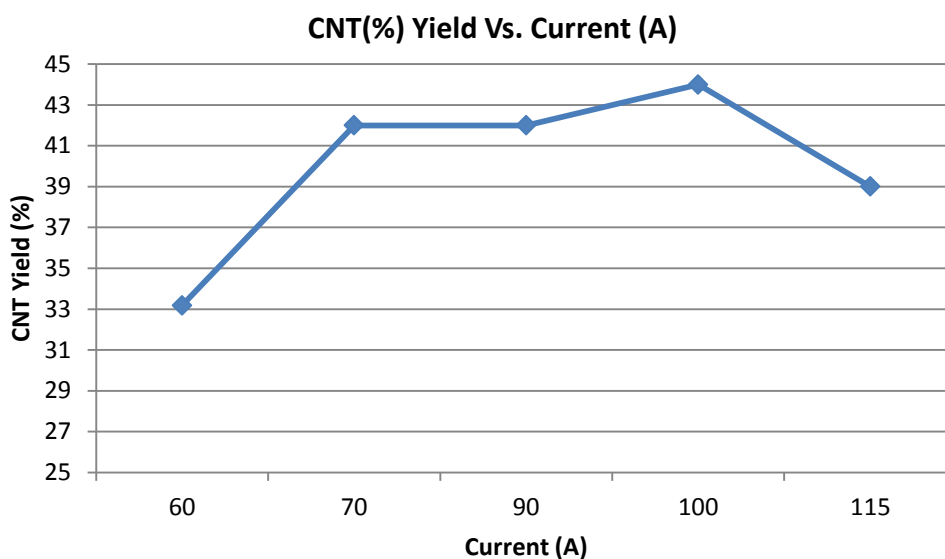


Figure 4-19 CNT yield vs. arcing current (Original is in colour)

According to Figure 4-19, the yield decreases after 100A and this phenomenon is further discussed below with the test done on the final arc discharge setup. A set of 12 samples were analyzed with arcing media of helium. The results were analyzed through TA universal software and tabulated below.

Table 4-6 TGA results of the sample produced by varying the current (repeat)

| Current (A) | Temperature at maximum decomposition rate (°C) | Total CNT % | Total soot weight | Yield (Mg) |
|--------------|---|-------------|-------------------|-------------|
| 55 | 900.00 | 27% | 5 | 1.34 |
| 65 | 928.50 | 12% | 8 | 0.99 |
| 75 | 910.00 | 29% | 11 | 3.16 |
| 85 | 955.00 | 32% | 12 | 3.84 |
| 90 | 938.00 | 43% | 20 | 8.56 |
| 95 | 948.00 | 36% | 23 | 8.21 |
| 100 | 951.00 | 40% | 27 | 10.67 |
| 110 | 919.80 | 40% | 47 | 18.93 |
| 118 | 950.00 | 63% | 60 | 37.64 |

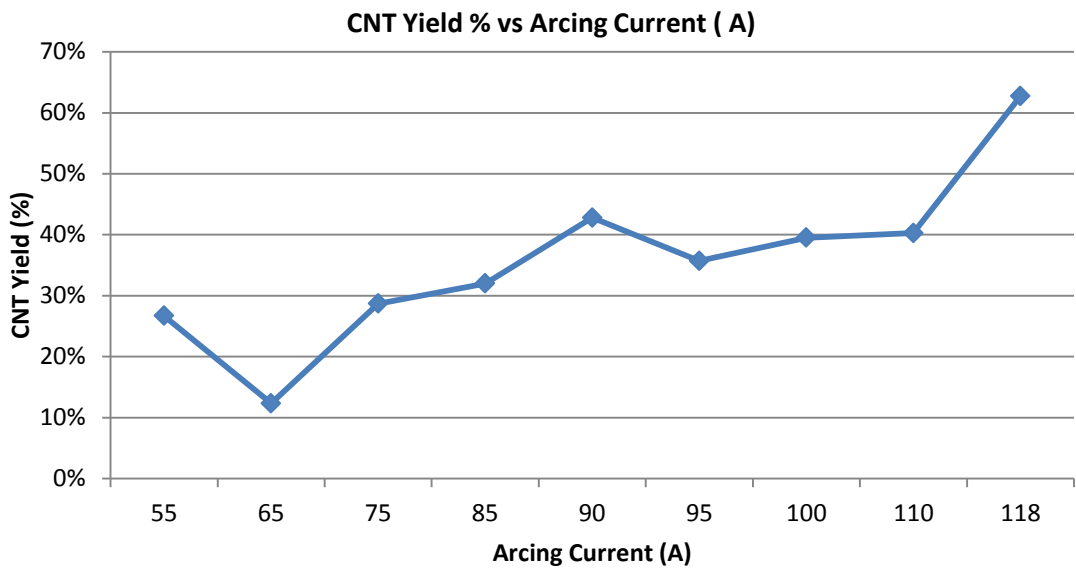


Figure 4-20 CNT yield % vs. arcing current (Repeat experiment) (Original is in colour)

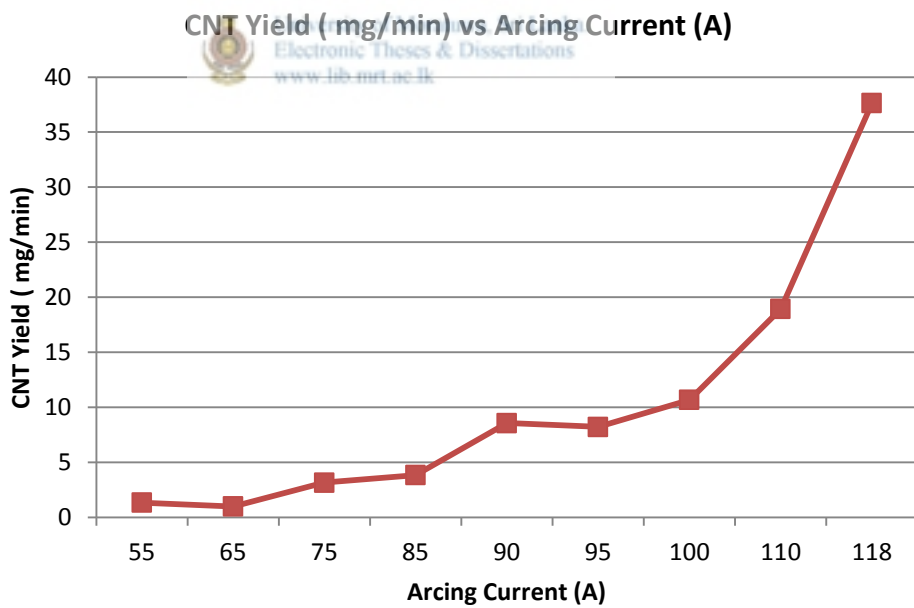
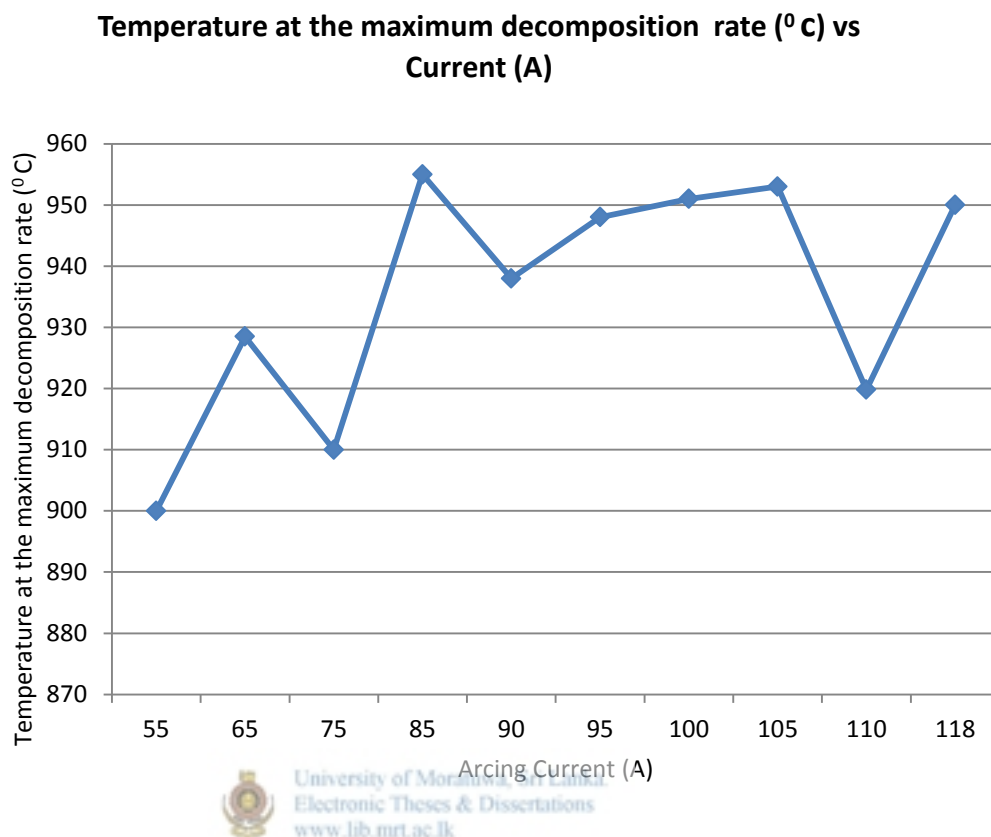


Figure 4-21 CNT yield vs. arcing current (Repeat test) (Original is in colour)

As seen in Figure 4-20 and Figure 4-21, it can be concluded that the CNT yield increases with the increase of the arcing current. The reason for this

phenomenon is that the generation of the carbon plasma is more with the higher current due to more heat generation.



*Figure 4-22 Temperature at the maximum decomposition rate vs .arcing current (Repeat experiment)
(Original is in colour)*

Figure 4-22 confirms the earlier results that the temperature at the maximum decomposition rate is increasing with increase of the arcing current.

In summary (based on the TGA results) it can be concluded that;

1. CNT yield is increasing with increase of the arc current
2. CNT diameter is increasing with increase of the arc current

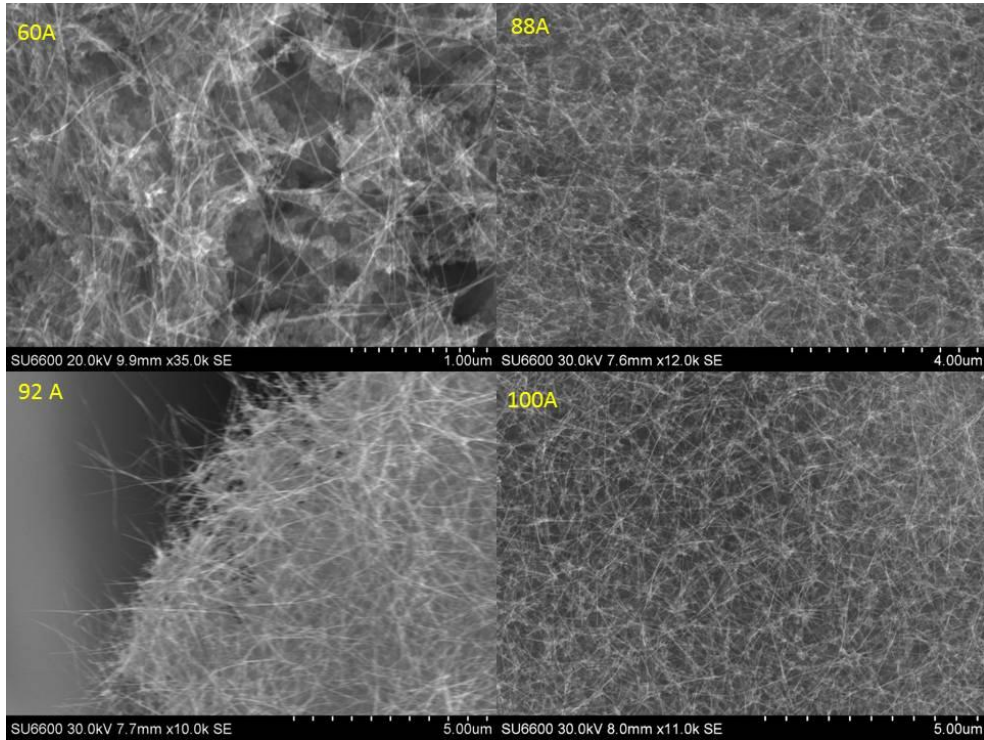


Figure 4-23 SEM images of CNTs produced with different arcing current (60A, 88 A, 92 A, 100A)

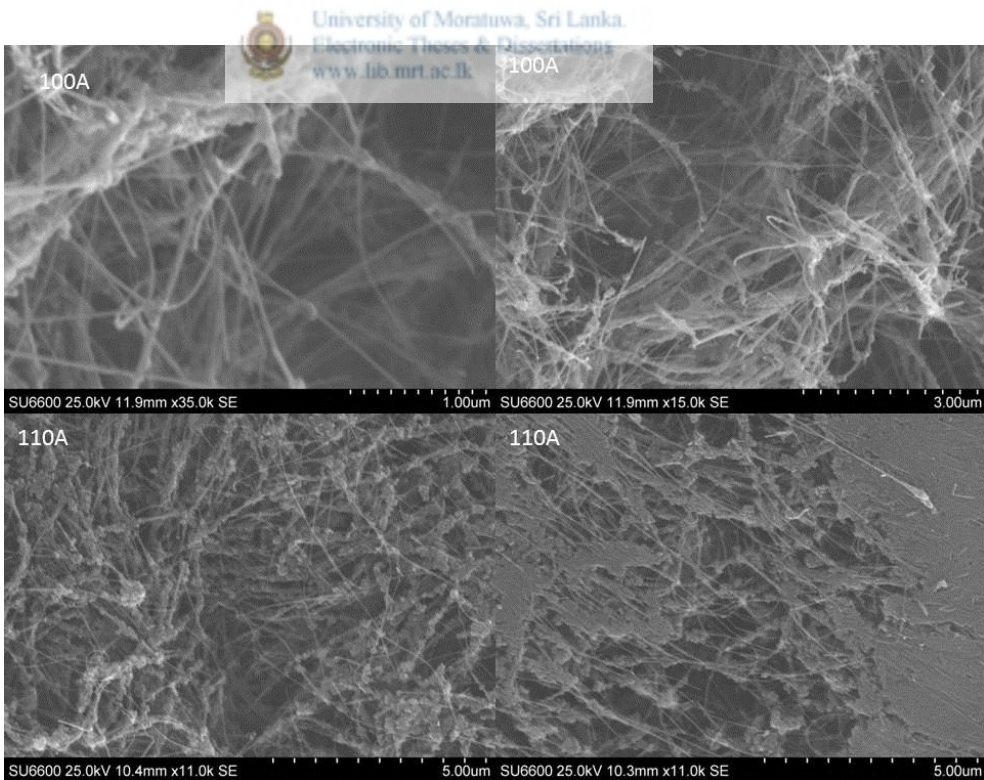


Figure 4-24 SEM images of CNTs produced with different arcing current (100A and 110A)

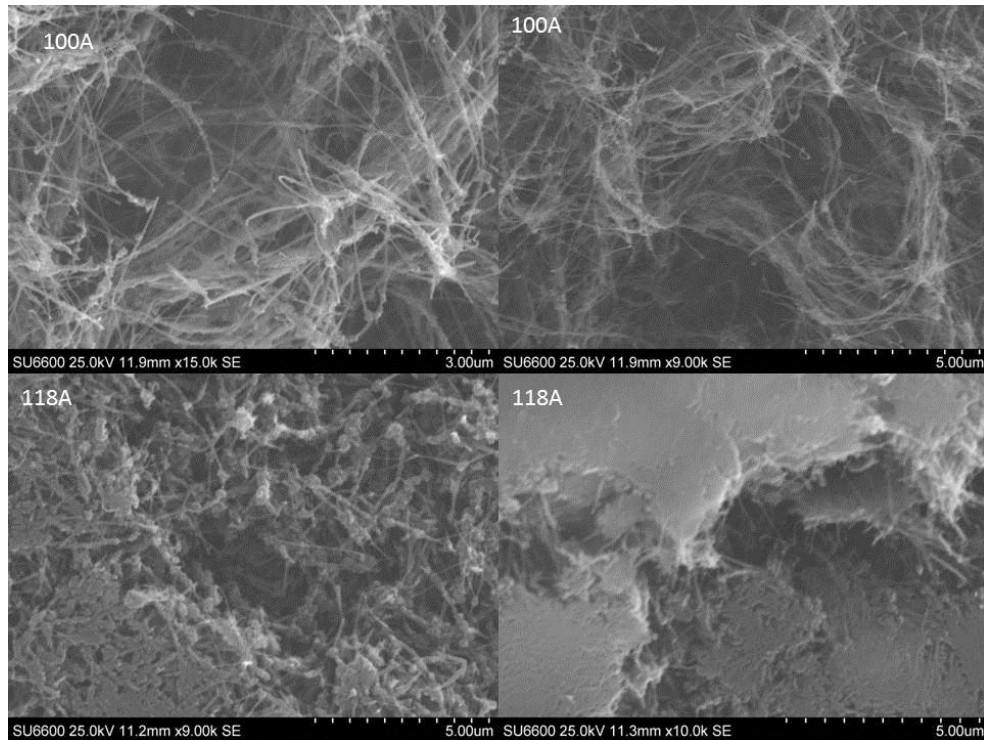


Figure 4-25 SEM images of CNTs produced with different arcing current (100A and 118A)

As seen in Figure 4-24, Figure 4-23 and Figure 4-25, at higher currents the CNTs are buried in the carbonized particles. This result is similar to that obtained with low pressure arcing. But around 90~100 A, CNTs are formed freely. There are lots of defects on the CNTs which are produced with currents less than 80 A.

Considering all the above facts (both yield and the quality) it can be concluded that the best arcing current for CNT production with Sri Lankan vein graphite is around 90~100A.

4.8 Testing with different arcing environment pressures

The initial weight of the arc soot of all 12 samples with different arcing pressure was measured using an analytical balance after the cathode was cooled down to room temperature

As described in the section 3.1.1 Thermo gravimetric analysis (TGA), the temperature at the maximum decomposition rate and the CNT yields were calculated for all other samples and tabulated in Table 4-7.

Table 4-7 Temperature at the maximum decomposition rate and the CNT yield for the samples with different arcing environment pressure (taken from TGA results)

| Pressure (Torr) | Graphitic peak (°C) | CNT Peak (°C) | CNT % | Total weight (mg) | Yield (Mg) |
|------------------|----------------------|----------------|-------|--------------------|-------------|
| 75 | 853.00 | 877 | 26.09 | 44 | 11.48 |
| 150 | 839.31 | 867.06 | 29.49 | 85 | 25.07 |
| 225 | 838.96 | 887.66 | 33.04 | 48 | 15.86 |
| 300 | 826.35 | 870.14 | 21.00 | 55 | 11.55 |
| 375 | 855.9 | 920.97 | 41.46 | 122 | 50.58 |
| 450 | 848.64 | 872.35 | 37.44 | 32 | 11.98 |
| 600 | 823.00 | 877.15 | 20.67 | 186 | 38.45 |
| 750 | 840.00 | 858.72 | 34.51 | 10.7 | 3.69 |
| 900 | 825.98 | 910 | 43.26 | 40 | 17.30 |
| 1050 | 821.31 | 916.74 | 38.20 | 72 | 27.50 |
| 1200 | 838.57 | 880.19 | 39.49 | 39 | 15.40 |
| 1520 | 856.00 | 905 | 53.00 | 40 | 21.20 |

As seen in the Table 4-7, there is no specific relationship between the weight of the arc soot (Anode ablation rate) and the arcing pressure. The weight varies from 10mg to 180 mg. This result is different from the data published by Erik Waldorff (29). In his experiment, the anode ablation rate which is proportional to the arc soot weight was increased with the increase of pressure. This may be due to the catalyst and the impure graphite raw materials that they have used in their experiment. The above details are plotted below.

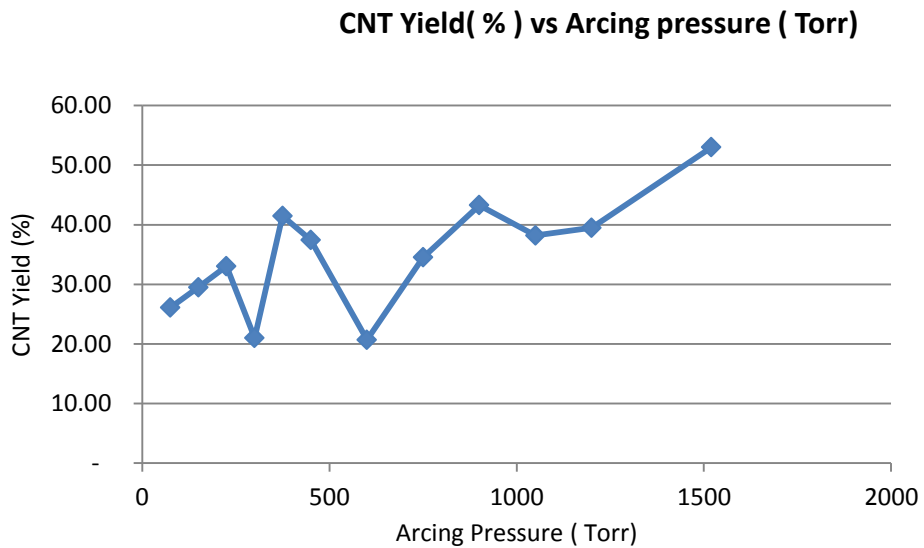


Figure 4-26 CNT yield Vs. Arcing pressure (Original is in colour)

As seen on the Figure 4-26, CNT yield is slightly increasing with arcing environment pressure. In most of the cases, the CNT yield was in the range of 10~40 mg/min.

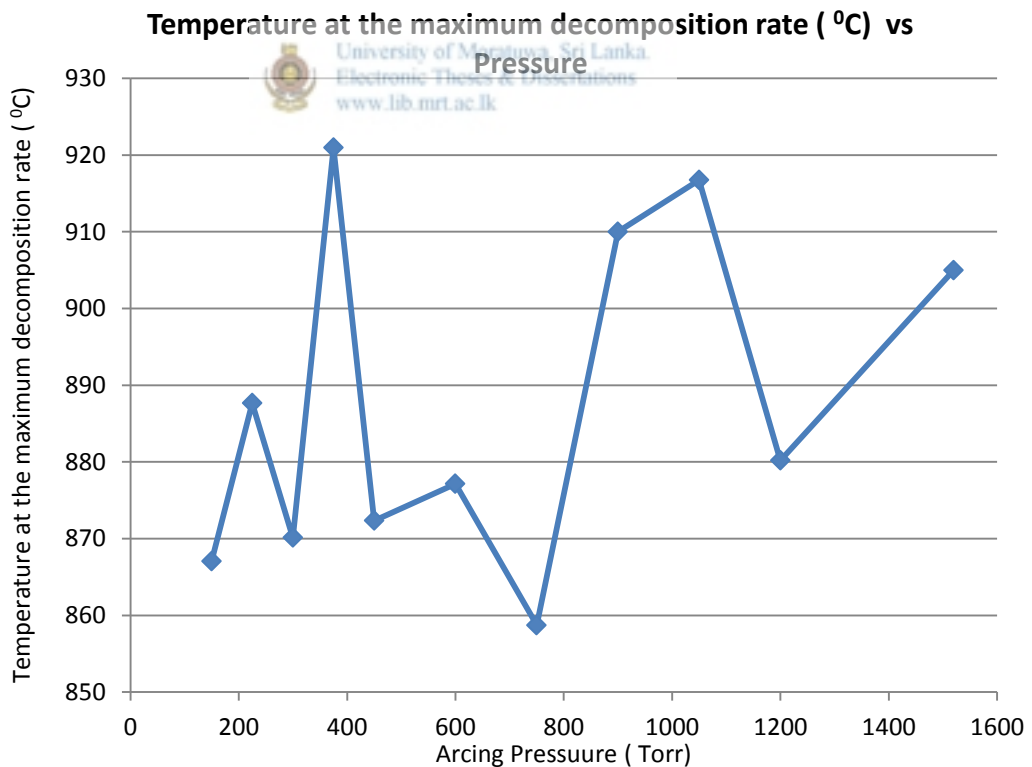


Figure 4-27 temperature at the maximum decomposition rate vs. arcing environment pressure (Original is in colour)

Figure 4-27 shows the temperature at the maximum decomposition rate of the CNT vs. arcing environment pressure. There is no significant relationship between the temperature at the maximum decomposition rate of the CNT and the pressure. Based on the analytical technique developed in section 4.3 *Experiments with commercial grade CNT*, it can be concluded that there is no significant relationship between the diameter of the CNT and the production environment pressure.

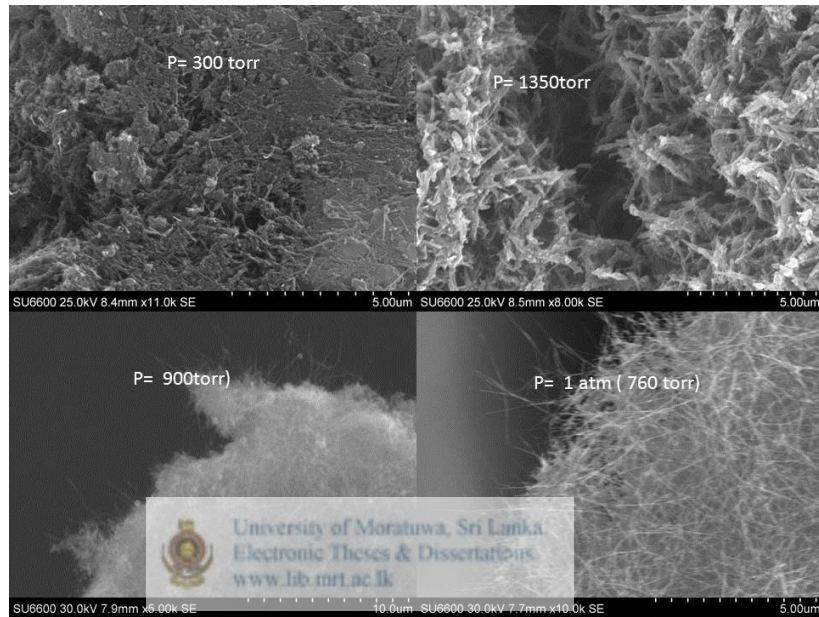


Figure 4-28 SEM images of produced CNT for different arcing pressure

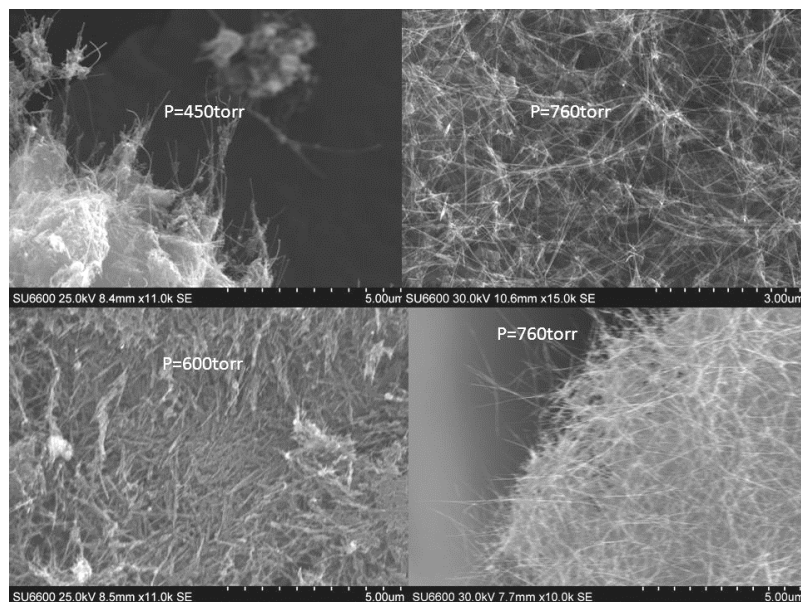


Figure 4-29 SEM images of produced CNT for different arcing pressure

As shown on the Figure 4-29, at the pressure of 300 Torr, the CNTs are not clear in the images. But as per the TGA results on Figure 4-26, 21% of the sample is CNT. This means that the CNTs are formed and burried in the graphitic particles. When the pressure is increased upto around 700~900 Torr, CNTs are formed freely. However, when the pressure reaches to around 1350Torr, the quality of the CNT gets poor. CNT walls are not straight and also all the CNT walls are full of defects when the quality is poor.

Based on all the above results, it can be concluded that the optimum pressure for the arc discharge cnt production using Sri Lankan vein graphite is around 700~900Torr.

4.9 Testing under different arcing environments

As seen in the Figure 4-30 and Figure 4-31, CNT yield can be calculated as 49.73% and 51.6 %. But on previous trials, average results were around 30% and it can be concluded that the yield can be increased by changing the inert media to N₂. At the same time, quality of the CNT also needs to be looked at as described in the next section.

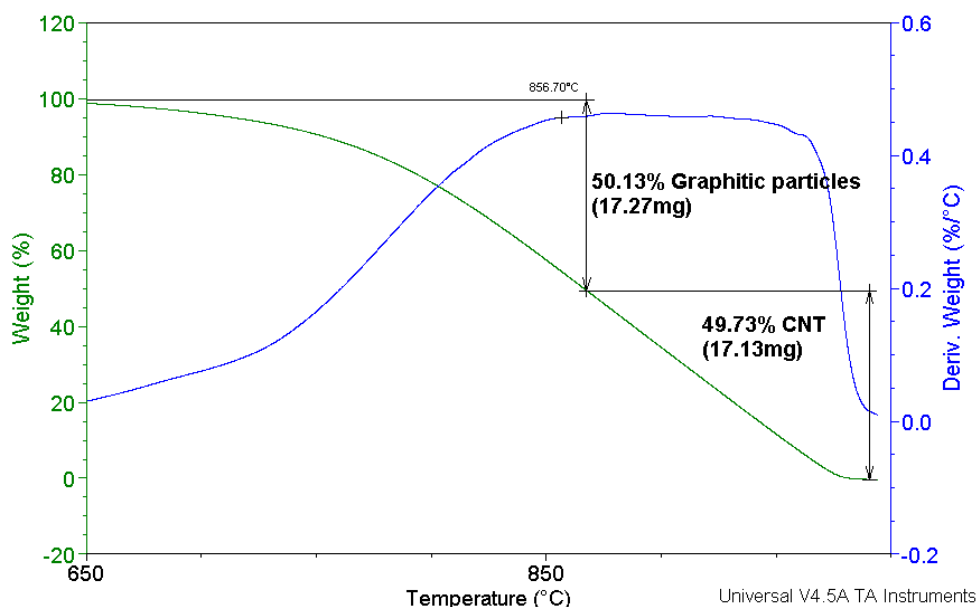


Figure 4-30 TGA analysis of the sample with N₂ at 1 atm, 100 A (Original is in colour)

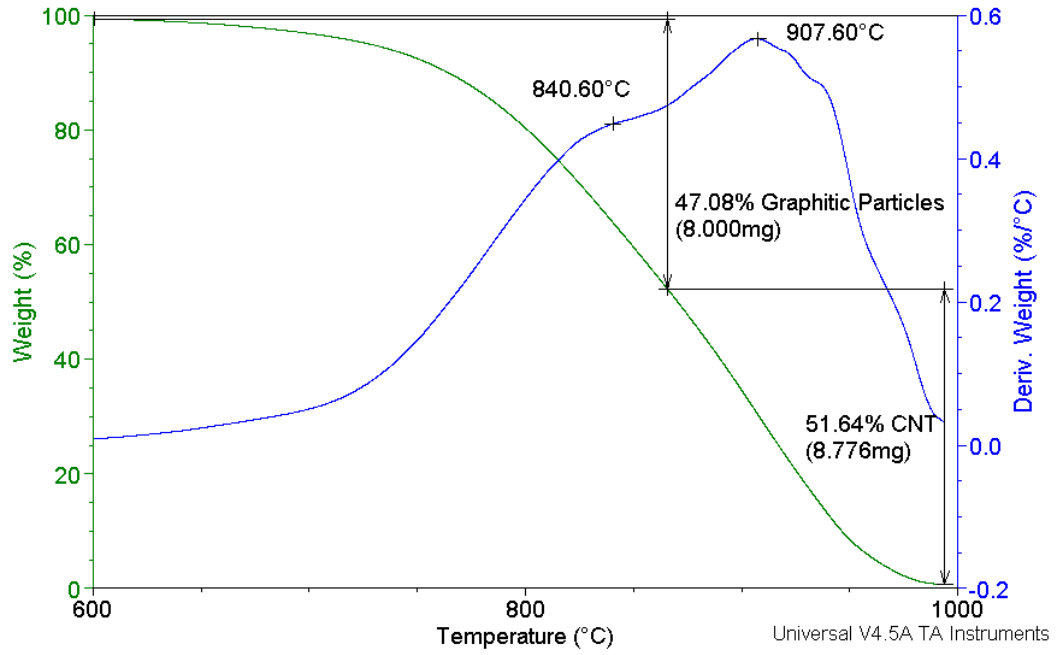


Figure 4-31 TGA analysis of the sample with N₂ at 900Torr, 100 A

Results of the test carried out using He as inert gas are given below.

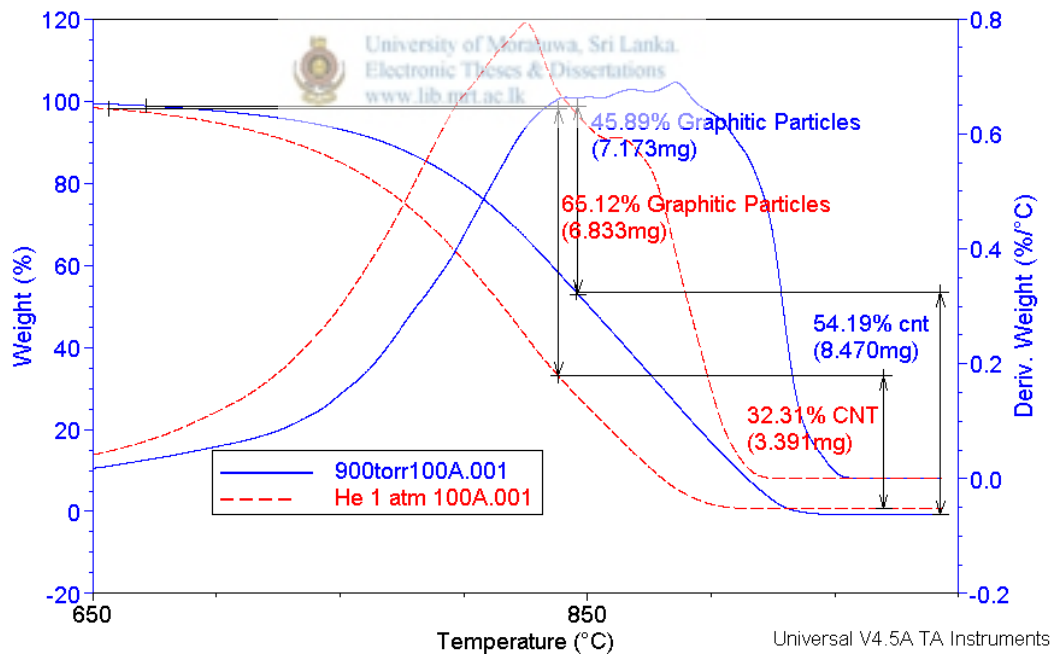


Figure 4-32 TGA results of the test with He gas (Solid line: 900Torr, 100A, 60s Dash line : 1 atm, 100A, 60s) (Original is in colour)

CNT Yield with different inert gases

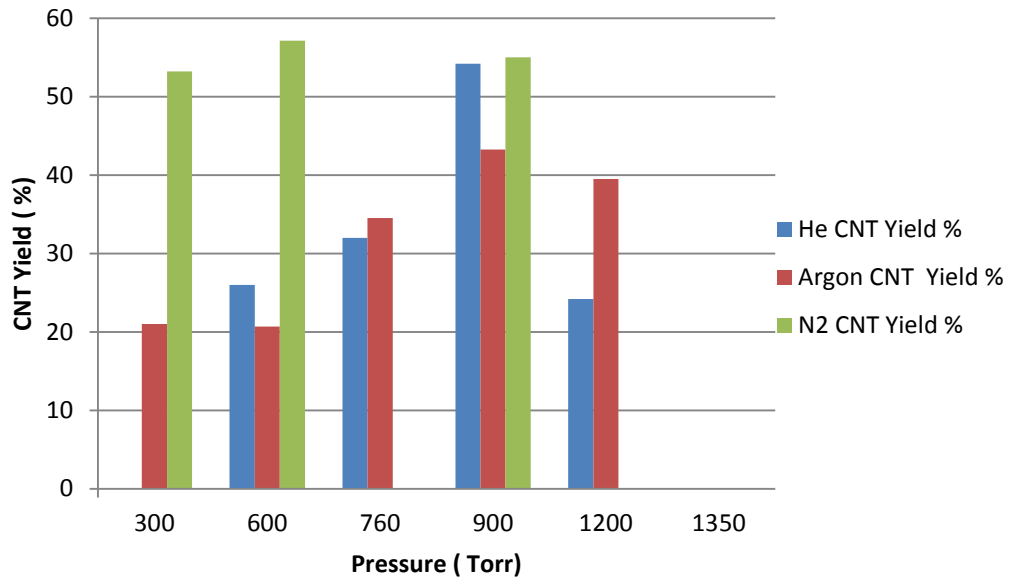


Figure 4-33 CNT Yield with different gases

As shown on the Figure 4-32 and Figure 4-33, the average CNT yield for He gas is around 40%. This is higher than that of Ar but less than that of nitrogen.

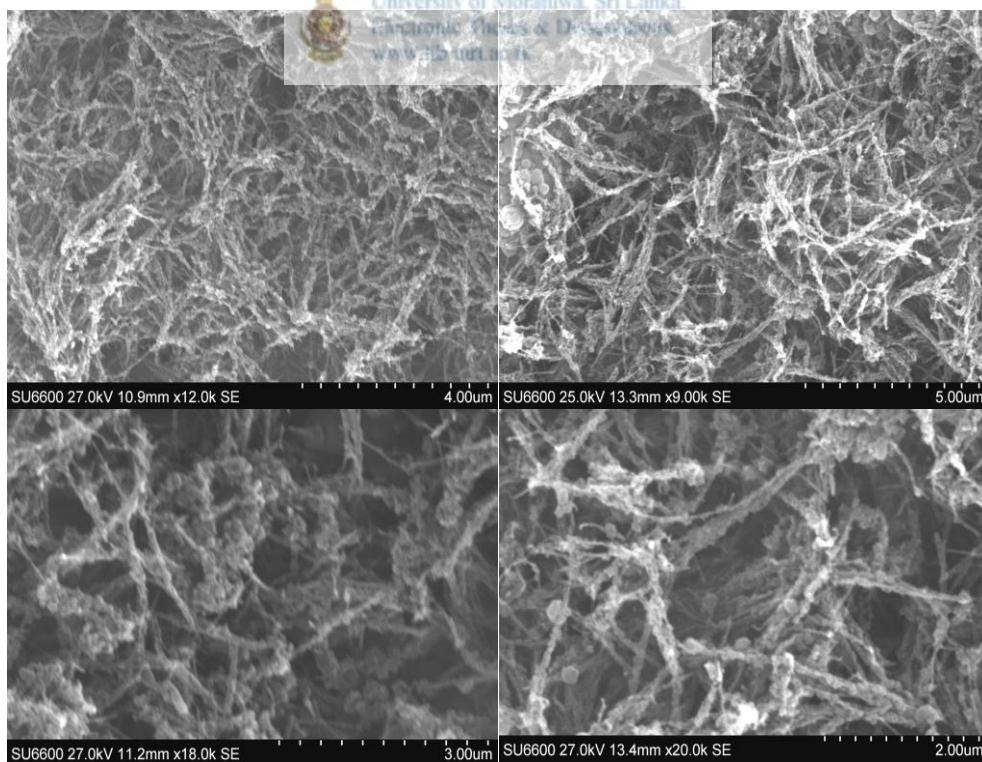


Figure 4-34 SEM images of the CNT produced with Nitrogen as the inert gas

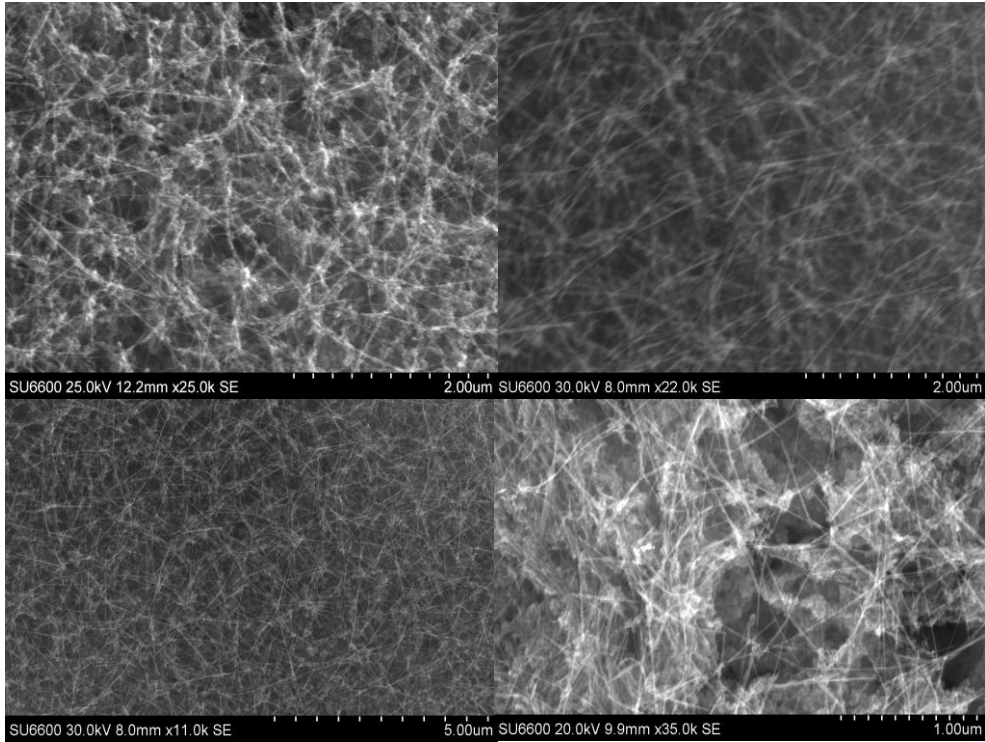


Figure 4-35 SEM images of the CNT produced with Argon as the inert gas

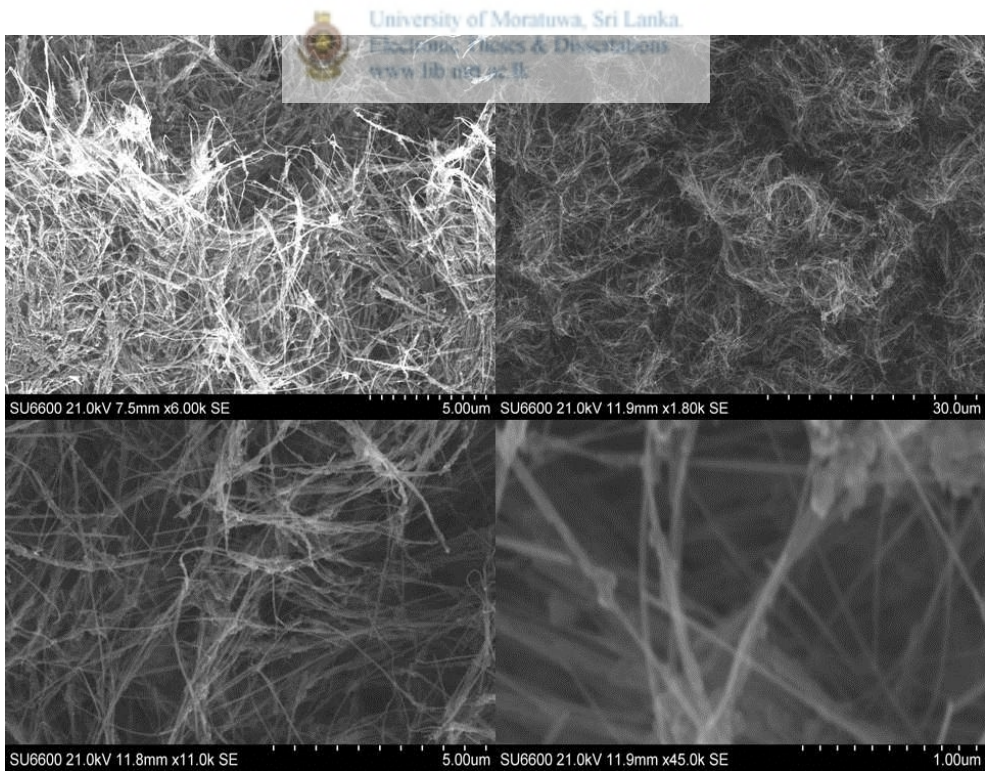


Figure 4-36 SEM images of the CNT produced with Helium as the inert gas

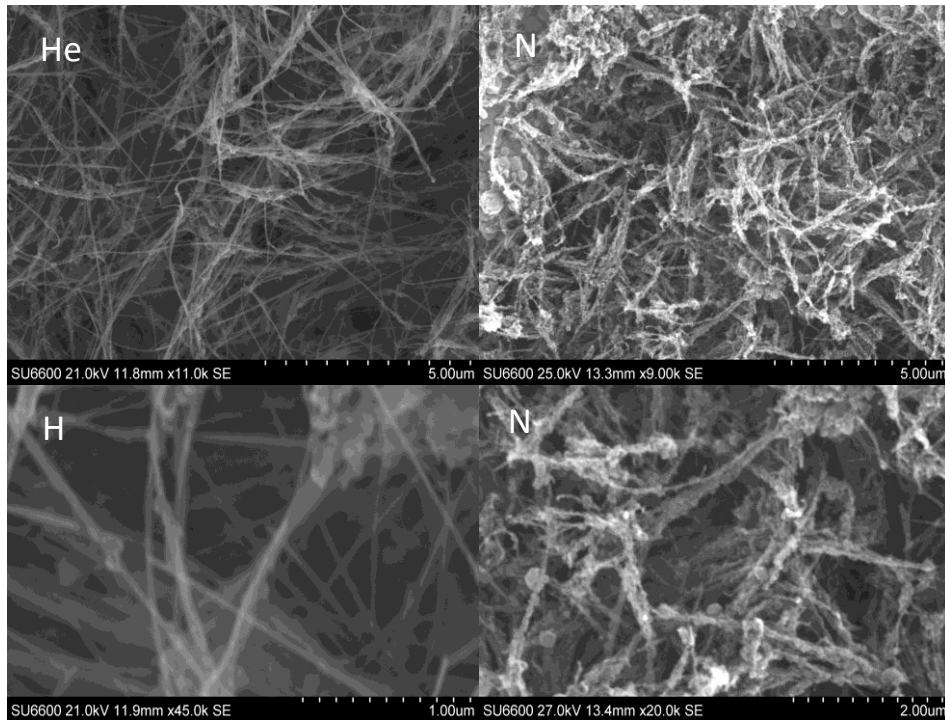


Figure 4-37 Comparison of SEM images of arc with He (left) and N2 (Right)

According to Figure 4-34 and Figure 4-37 it is clear that the CNT produced with nitrogen has lot of defects. All the CNT walls are bound with graphitic particles. These particles are known as the carbon onions.

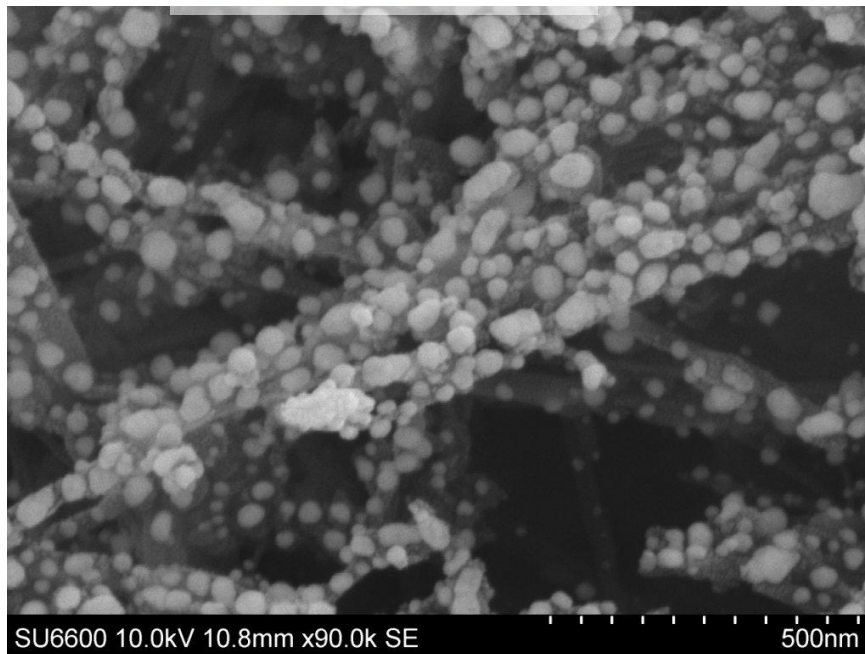


Figure 4-38 Carbon onion formation on the CNT produced with nitrogen gas as the inert media

Figure 4-38 clearly shows the formation of carbon onions on the CNT. Also the CNTs are not straight. But as shown in Figure 4-35, CNT produced with Ar is slightly better than that with N₂. But as seen on the Figure 4-39, the CNT produced with He has the best quality among all. These CNTs are straight, less defects and formed freely.



Figure 4-39 Clean CNT formation with He

One reason for this is due to the higher thermal conductivity of the Helium compared with other gases. When arcing, due to the thermal energy produced by collision of the electrons on to the anode, the anode erodes and carbon plasma is produced. Some of this carbon plasma is then cooled and deposited on the cathode. If the environmental thermal conductivity is higher it is easier to generate the plasma and also it supports for the quenching process.

This process is happening at the temperatures around 4000K & thermal conductivities of He, N₂ & Ar at 4000K are given below. (30), (31)

- He: 1020 mW/mK
- N₂ : 168 mW/mK
- Ar : 110 mW/mK

SEM images of the samples which were taken inside water arcing are given below.

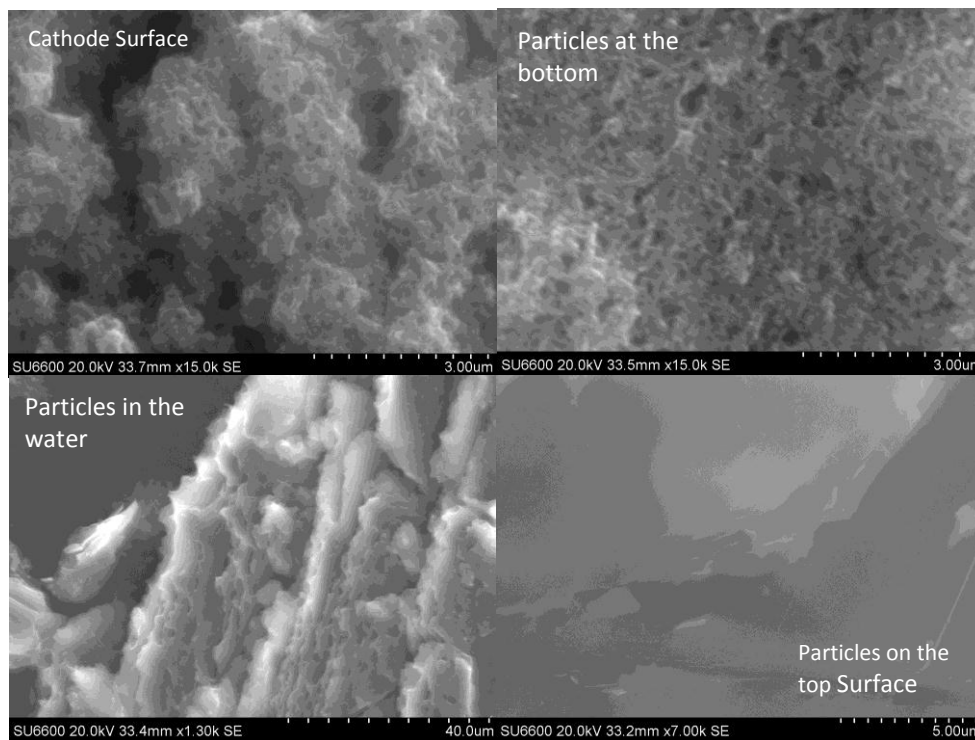



Figure 4-40 SEM images of the samples from arcing inside water

As shown on the  Figure 4-40, none of the samples consists with CNT and it can be concluded that the deionized water cannot be used as the media for CNT production using Sri Lankan vein graphite.

Considering both the quality and the yield, it can be concluded that the best candidate for the inert gas for arc discharge CNT production using Sri Lankan vein graphite is He.

4.10 Testing with an external electric field

Tests were carried out with external high voltage on the same direction as the low voltage supply. This setup produced two carbonized particles on,

1. Deposit on high voltage Copper (Cu) cathode
2. Normal low voltage DC graphite cathode

With the external high voltage it was very easy to maintain the electric arc. This means that the electric field between the graphite electrodes matters for the arc.

i.e higher the electric field easier to maintain the arc. The SEM analysis of the high voltage cathode deposit and the low voltage cathode deposits are given below.

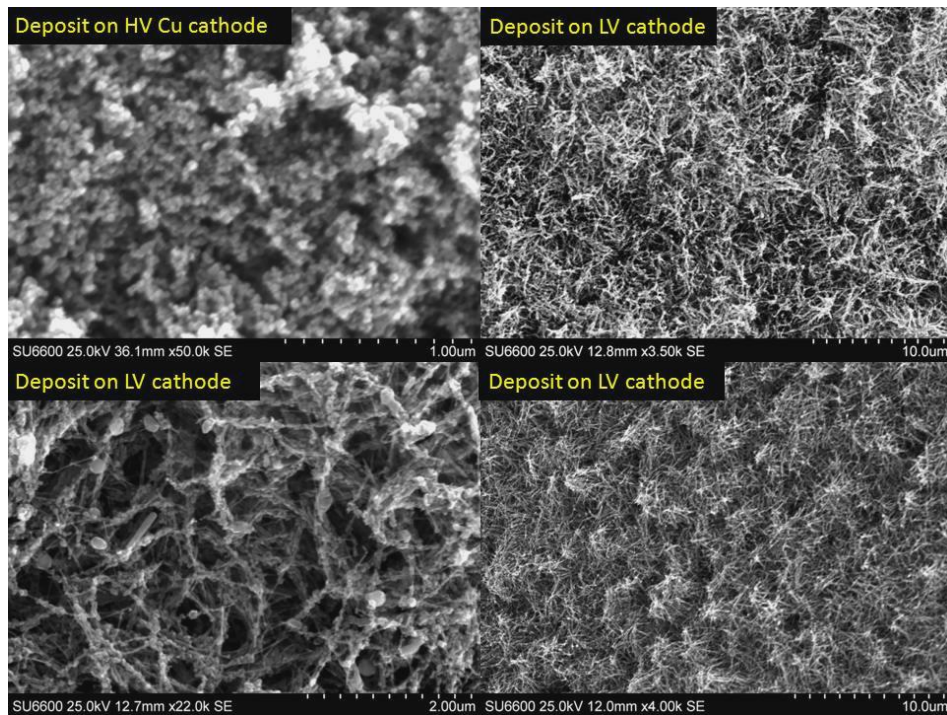


Figure 4-41 SEM images of the HV (high voltage) and LV (low voltage) cathode deposits of the test with an external electric field

As seen on the Figure 4-41 high voltage cathode deposit consists of small round shape fullerene shape of particles. There was no CNT formation on the high voltage Cu cathode. But as usual on the graphite cathode CNT was formed. As seen on the right side images, the CNT yield was high but according to the lower left image the produced CNTs are full of defects. The walls are not clear and are bound with carbonized particles.

In conclusion, there is no need of introducing an external electric field for CNT production which costs an extra amount.

4.11 Testing with different shapes and materials of anode/cathode

When the anode surface is flat it was difficult to maintain the continuous arc. Because the arc initiates through the least resistant path and when the anode is eroded, the selected least resistant path may no longer be valid. At this point, the point of arcing is moved to a different point to find a new least resistant path. Due to this, the formation of the CNT has to start again which takes another minimum of

40s. By using the pointed anode these issues can be resolved. Also a flat cathode is needed to support the above phenomena.

SEM analysis of the cathode soot of the test conducted with copper cathode with vein graphite anode is given below.

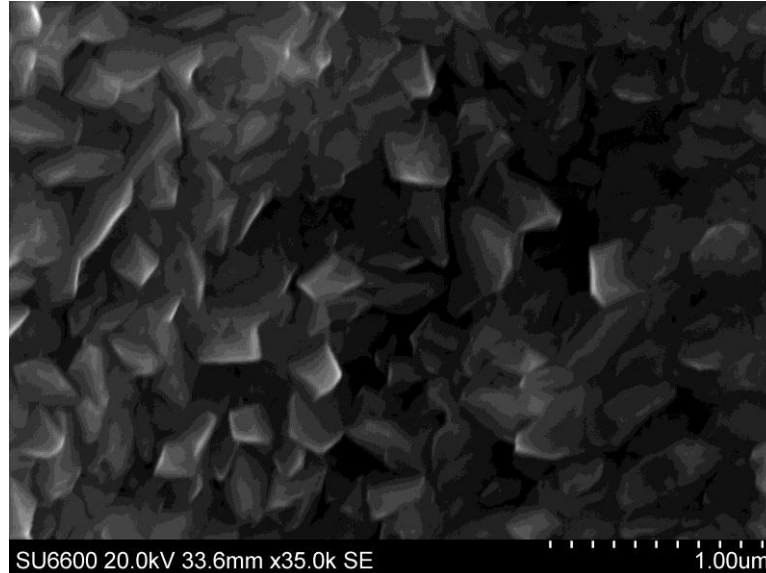


Figure 4-42 SEM image of the cathode deposit of the copper cathode

As seen on the Figure 4-42, there is no CNT formation when the cathode was changed to copper. In conclusion, it is mandatory to use graphite for both the electrodes.

4.12 Testing with flake graphite

There was no good arc with flake graphite. At around 40s of arcing time the anode was broken due to the internal arcing inside anode since it was made by compressing the powdered flake graphite which was compressed with a hydraulic press under a 50T load. The compressed pressure of 50 T might not be sufficient to prepare the anode.

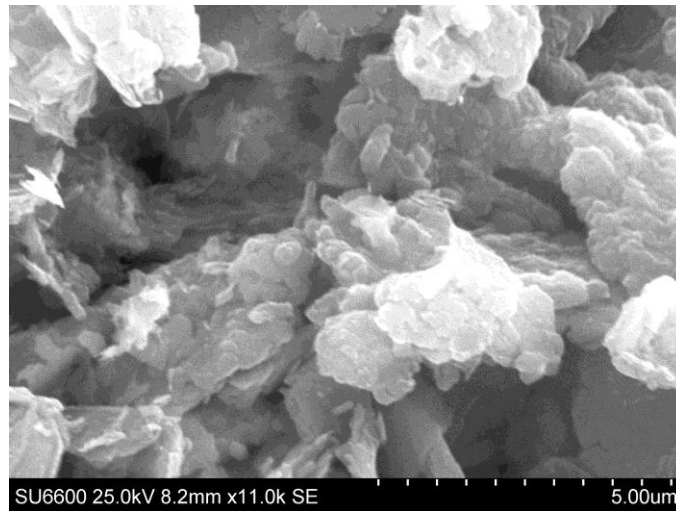


Figure 4-43 Cathode deposit of Flake test - image 1

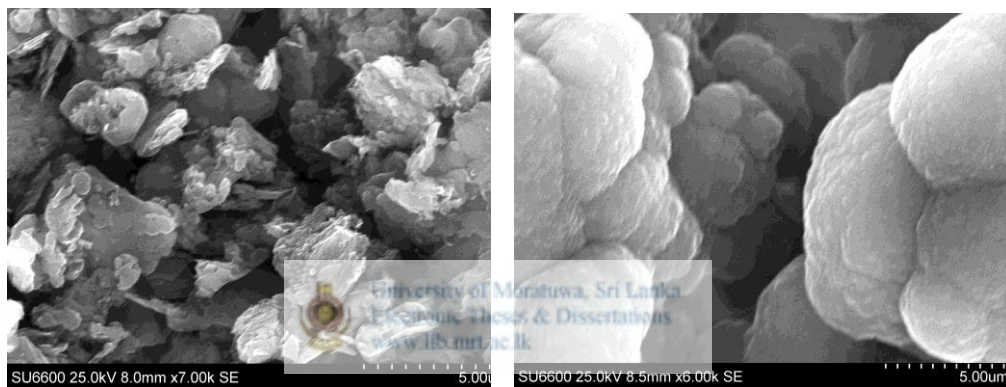


Figure 4-44 Cathode deposit of Flake test - image 2

As seen on the above images no CNT is formed with flake graphite and it can be concluded that the vein graphite is the form of graphite that we should use to produce arc discharge CNT using the method described in this study.

Chapter 5 : CONCLUSIONS

Following main objectives were covered in this study.

1. Producing of CNT

Four different arc discharge setups were developed to produce CNT and with the final arc discharge setup (fourth set up) good quality CNTs could be produced. This is due to the good vacuum system where, the system was evacuated down to less than 75Torr before filling the inert gas. Also the system should be capable to withstand the pressure of 1500Torr when the inert gas was filled for purging. Further development is needed to incorporate automation system to collect the final arc soot and also to automate the linear moving system.

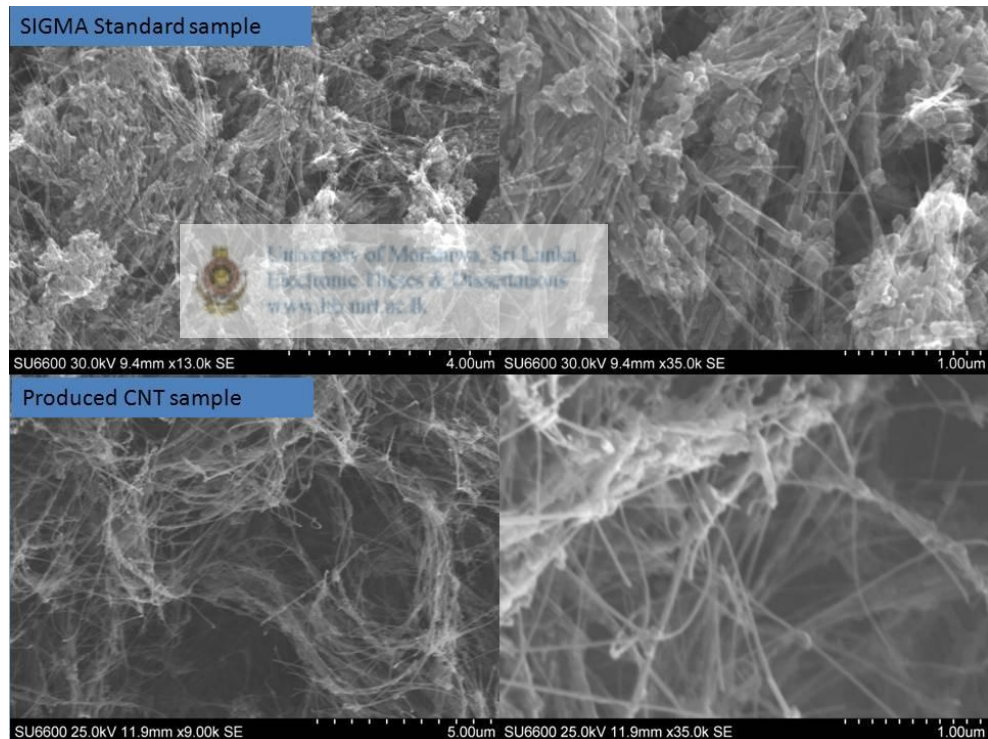


Figure 5-1 Comparison of the standard Sigma CNT vs produced CNT

As seen on the image Figure 5-1, the produced CNT in this study is much more pure than the standard MWCNT sample purchased from Sigma Aldrich, Germany. The Sigma sample is full of graphitic impurities and the CNT walls are not clear. Also TGA results confirm that the produced CNT is free of metallic impurities.

2. Separation and characterization of CNT

In our method, sophisticated purification procedure was not used as this does not contain any metal catalysts and also the purity of graphite used was 99.9%. The characterization was done with SEM to compare the quality of the CNT and the yield was measured by TGA.

3. Parameter optimization for

- Quality improvement : quality of the CNTs were compared with SEM images
- Yield improvement: Yield comparisons were done using TGA analysis.

5.1 Recommendations

Recommended optimized parameters for the arc discharge cnt production using Sri Lankan vein graphite are given below.


1. Arc current : around 90A~100A
2. Arcing voltage : 12-25V (constant current mode)
3. Arcing time : around 60s
4. Arcing pressure : around 700~900 torr
5. Arcing environment : He environment
6. Anode and cathode : flat surfaced Vein graphite cathode
and pointed vein graphite anode

5.1 Future works

1. The arc discharge setup needs to be modified to have a mechanism to collect the arc soot automatically
2. Manual arcing mechanism needs to be automated
3. Need to test with a suitable catalyst to produce SWCNT
4. Need to find out a method to separate the CNT from graphitic particles. Selective thermal oxidation can be used.

References

1. Endo, Moribu. Grow Carbon fibers in the vapor phase. *CHEMTECH*. Oberlin : s.n., 1988, pp. 568-576.
2. *Helical Microtubules of graphitic carbon*. Iijima, Sumio. 1991, Nature.
3. Eklund, Rinser, et al., et al. *Carbon Nanotube manufacturing & application*. s.l. : Wexford press, 2008.
4. WTEC Carbon Nanotube Study panel. *Scaling up cnt production, seperation & purification*. USA : Harper international, Nov 2006.
5. M. Daenen (N), R.D. de Fouw (ST), B. Hamers (ST, Treasurer), V. *The wondrous world of Carbon Nanotubes*. Eindhoven, Netherlands : Eindhoven University Technology, 2003.
6. Gina_Peschel. www.physik.fu-berlin.de/.../ag/ag.../Gina_Peschel-Handout.pdf. [Online] 2009. www.physik.fu-berlin.de/.../ag/ag.../Gina_Peschel-Handout.pdf.
7. ww.diss.fu-berlin.de/diss/servlets/.../derivate.../05_Chapter5.pdf; [Online] [Cited: 07 23, 2012.] ww.diss.fu-berlin.de/diss/servlets/.../derivate.../05_Chapter5.pdf;
8. Daaenen, M., et al., et al. *The wondrous world of carbon nanotubes*. s.l. : Eindhoven University of technology., 2003.
9. Ajayan, M., P. and Ebbesen. *Rep.Prog.Phy. Rep.Prog.Phy*. 2003.
10. *Carbon Nanotube manufacturing 2006*. Eklund, Peter C. National Science Foundation, Stafford II : s.n., Nov 2006. work shop on international R & D of carbon Nanotube Manufacturing and applications.
11. *Collapse and stability of single- and multi wall carbon nanotubes*. Xiao, J, et al., et al. 2007, *Nanotechnology* 18 (2007) 395703 (7pp), Vol. 18.
12. Paper, Seminar. seminar paper. [Online] [Cited: 07 20, 2011.] <http://www.seminarpaper.com/2011/12/seminar-report-on-diamond-chip.html>.
13. *Superhard phase composed of single-wall carbon nanotubes*. Popov, M. 2002.
14. slideshare. [Online] [Cited: 6 22, 2012.] www.slideshare.net/Zenblade/carbon-nanotube.
15. Lu, X.; "Curved Pi-Conjugation, Aromaticity, and the Related Chemistry of Small Fullerenes (<C60) and Single-Walled Carbon Nanotubes". Lu, X. and Chen, Z. 2005.

16. "Nanotube Electronics: A flexible approach to mobility". . Hong, Seunghun and Myung, S. 2007, Nature Nanotechnology, pp. 207-208.
17. "Thermal conductance of an individual single-wall carbon nanotube above room temperature". Pop, Eric, et al., et al. Pop, Eric et al.; Mann, David; Wang, Qian; Goodson, Kenneth; Dai, Hongjie (2005-12-22). "Thermal conductance of 2005 Dec 22, Nano Letters 6.
18. "Nanocomposites in context". Hostenson, Erik, Li, C and Chou, T. 2005, Composites Science and Technology 65, pp. 491–516.
19. The European chemical Industry council.
www.cefic.org/Documents/Other/Benefits%20of%20Carbon%20Nanotubes.pdf.
www.cefic.org. [Online] [Cited: 3 2, 2011.]
www.cefic.org/Documents/Other/Benefits%20of%20Carbon%20Nanotubes.pdf.
20. *Carbon Nanotubes - A scientometric study*. Marx, Werner and Barth, Andreas. 2004.
21. Bogala Graphite. Bogala Graphite. *Carbon*. [Online] [Cited: 05 12, 2012.]
<http://www.gk-graphite.lk/graphit.html>.
22. Kopeliovich and Dmitri. Applications of graphite. [Online] 2012. [Cited: June 30, 2012.]

http://www.substech.com/dokuwiki/doku.php?id=applications_of_graphite.
23. *Thermal behavior of purified multiwalled carbon nanotubes*. Rike Yudianti, Lucia Indarti , Holia onngo. 2010, Journal of Applied science, pp. 1978-1982.
24. *Thermogravimetric Analysis of*. Caoimhe de Fréin, Andrew R. Barron. 2009, Connexions module: m22972.
25. *Structural characterization and diameter dependant oxidative stability of single wall carbon nanotubes synthesized by catalytic decomposition of CO*. Zhou, w, et al., et al. 2001, ELSEVIER- ChemicalPphysics Letters, p. 9.
26. Samaranayake, Lilantha, et al., et al. *Process for preperation of carbon nanotube from vein graphite*. US2011/062341 A1 USPTO, 2011.
27. Asbury Carbin Inc. Introduction to Graphite. *Asbury Carbon- The worlds Graphite Source*. [Online] [Cited: May 05, 2012.]
<http://www.asbury.com/Introduction.html>.

28. *Optimisation of the arc-discharge production of multi-walled.* Cadeka, M, et al., et al. 2002, Carbon, pp. 923-928.
29. *Characterization of carbon nanotubes produced by arc discharge:.* Waldorff, Erik, et al., et al. 2004, Journal of Applied Physics by American Institute of Physics.
30. Thermal conductivity of mono atomic elements. *Journal of Physical Chemistry, Vol 19.* 1990, p. no 6.
31. www.engineeringtoolbox.com. [Online] [Cited: July 23, 2012.]
www.engineeringtoolbox.com/thermal-conductivity-d_429.html.
32. www.tainstruments.com. [Online] [Cited: March 12, 2012.]
www.tainstruments.com.
33. *Nanotechnology- Enabled Sensors.* Zadeh, K.K. & Fry, B. . 2008, New York. Springer.
34. Hitachi High Technologies Inc. *Instruction Manual on E1010 Ion Sputtering unit.* s.l. : Hitachi.
35. *Thermal Behaviour of MWCNT.* Yudiyanthi, Rike. 2010.
36. *Growth of CNT in electric discharge in Ar.* D. N Borisenko, N.N Kolesinkov, M.P Kulakov, V.V Kvender. Institute of Solid State Physics, Russian Academy of Science.
37. *"Strength and Breaking Mechanism of Multiwalled Carbon Nanotubes Under Tensile Load"* . Yu, Min-Feng, et al., et al. 28 January 2000) , Science , pp. 637–640. .
38. The engineering tool box. [Online] [Cited: June 30, 2012.]
http://www.engineeringtoolbox.com/thermal-conductivity-d_429.html.